Ecology and life history traits of Chondrichthyes: how cartilaginous fishes live and move through their environment.

Kayla C. Hall

A dissertation

submitted in partial fulfillment of the

requirements for the degree of

Doctor of Philosophy

University of Washington

2023

Reading Committee:

Adam Summers, Chair

Greg Wilson-Mantilla

Karen Petersen

Program Authorized to Offer Degree:

Biology

University of Washington

Abstract

Ecology and life history traits of Chondrichthyes: how cartilaginous fishes live and move through their environment.

Kayla C. Hall

Chair of the Supervisory Committee:

Adam Summers

Department of Biology

Chondrichthyes (chimaeras, sharks, skates and rays) are a lineage of vertebrates with skeletons composed entirely of cartilage, that have existed for over 400 million years. This long evolutionary history has allowed them to diversify their life-history traits, ecology, and biogeography as they are found throughout the world's marine and freshwater waterways. Two critical aspects of an organism's life are reproduction and locomotion. Chondrichthyans exhibit most forms of sexual reproduction, from egg-laying to live birth: oviparity, multiple types of aplacental viviparity, and placental viviparity. They also evolved many modes of locomotion, from axial-swimming (tail undulations), undulating or oscillating pectoral fins, to walking (or 'punting') along the substrate with pelvic fins. Some species use a combination of these methods to locomote, depending on their habitat. Aside from using cartilaginous fishes as my model, the tie between all of my chapters are the principles of form and function. How does the change in skeletal morphology influence how an animal moves and how is that driven by where it lives; habitat structuring encompasses what an organism encounters, to eat or avoid

being eaten, it can also be reflective of where they reproduce and how long it takes to develop. Each chapter plays off these principles and flows into the next. First, I consider chondrichthyan evolution and life-history traits, what came before and has shaped what remains today; what characteristics don't evolve in specific regions and ranges, and why might this be? Next, I consider the hydrodynamics of egg cases from multiple species of skates (Rajiformes) to determine how species-specific traits, specifically macro-morphology and microstructure, contribute to the variation where these eggs occur in order to aid in protective policies to avoid disturbing nursery grounds. Lastly, I characterize the swimming kinematics of the spotted ratfish (*Hydrolagus colliei*, Holocephali). Chimaeras are thought to move via pectoral fin-based swimming, flapping and fluttering their large fins in order to propel themselves through their deep dark world. But, chimaeras also have prominent pelvic fins, which allows us to compare the relationship between these two sets of fins, and the reliance of both sets during variable swimming conditions. In summary, I use Chondrichthyes as my system to understand how an ancient lineage of fishes live and move through their environments.

TABLE OF CONTENTS

Dedication

To my father.

I grew up fishing the freshwater lakes and rivers of Michigan with him. I never would've thought our hobby would turn into my career, or that I'd end up getting to study such fascinating and strange creatures from the depths of the ocean.

This degree and my accomplishments are all achievable because of the undying support and belief he has in me and whatever I decide to put my mind to. He taught me I could do anything. This is for him.

To my forever-partner, family, and friends thank you for all of the love and support throughout this phase of my life. For helping me, mentally & physically, make it through a global pandemic and two long battles against Covid, on top of getting me through the travail of grad-school.

To my mentors thank you for your continuous wisdom and guidance throughout the past 5 years. Thank you for helping mold me into a better teacher, communicator, scientist and person.

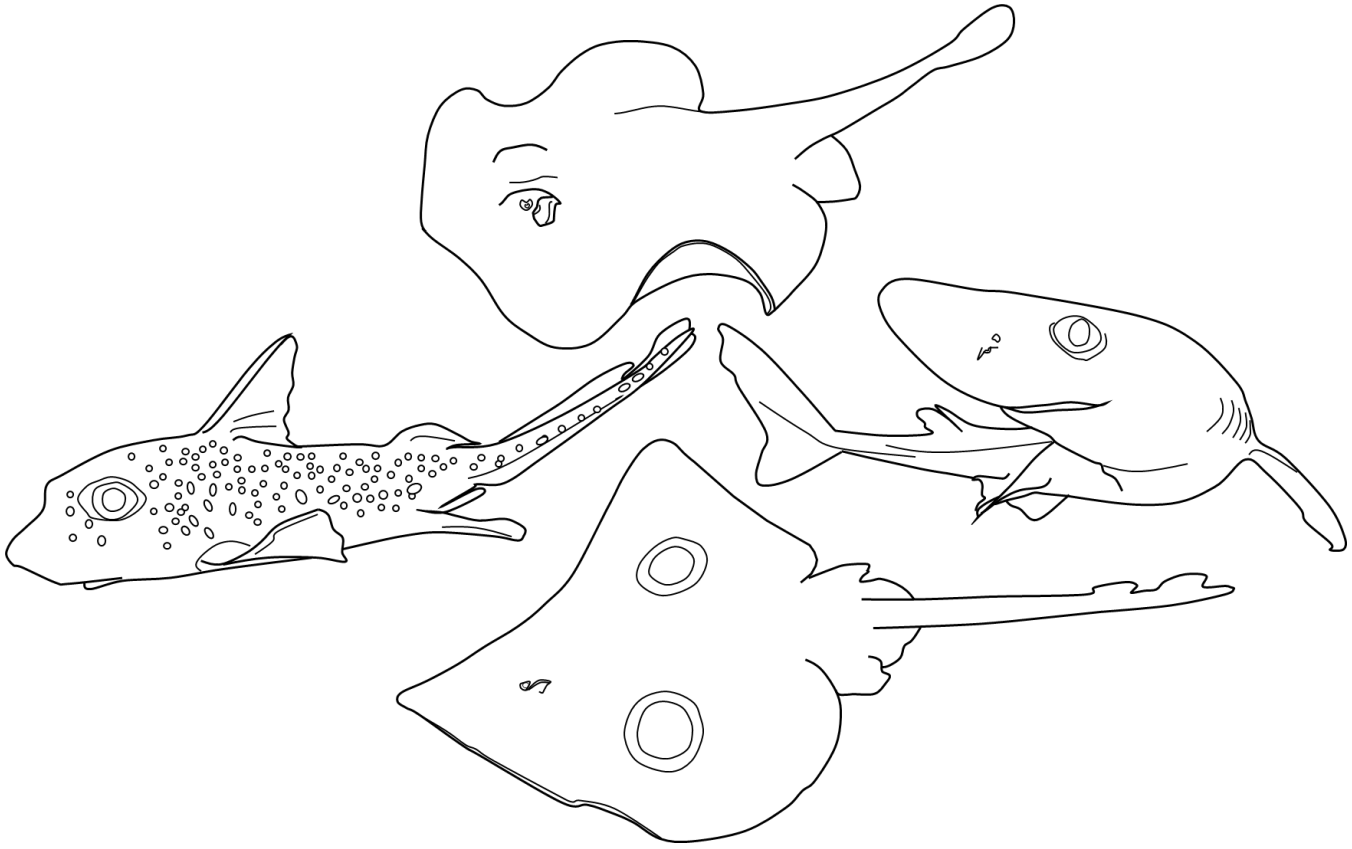

Life in the slow lane: Ecological structuring and evolutionary life-history traits of chondrichthyans.

Kayla C. Hall[1, 2], Peter J. Hundt[3], Mathew Kolmann[4], Adam P. Summers[1,2], Allison Bronson[5].

1) Friday Harbor Labs, University of Washington, 620 University Rd., Friday Harbor, WA 98250

2) University of Washington, Department of Biology, Life Sciences Building. W Stevens Way NE, Seattle, WA 98195

3) University of Minnesota, Department of Fisheries, Wildlife and Conservation Biology, 2003 Upper Buford Circle, St. Paul, MN 55108

4) University of Louisville, Department of Biology, 2301 S 3rd St, Louisville, KY 40292

5) Humboldt State University, Department of Biological Sciences, 1 Harpst St, Arcata, CA 95521

*Author for Correspondence: kchall8@uw.edu

Keywords: Biogeography, Community: structure, Ecology: evolutionary, Life history: evolution, Locomotion, Methods: meta-analysis, Phylogeny, Reproduction: strategies

Abstract

Chondrichthyes (chimaeras, sharks, skates and rays) are a 400+ million-year-old vertebrate lineage with endoskeletons composed entirely of cartilage. Throughout their long evolutionary history, cartilaginous fishes have diversified into a variety of freshwater and marine habitats, distinctive ecological roles, and evolved an array of life-history traits. We described the ecological structuring of extant chondrichthyan communities over time, with the aim of exploring correlates and mechanisms that have shaped modern assemblages. We used body size, trophic level, reproductive mode, and locomotor mode to establish the ecospace occupation of extant species from all aquatic ecosystems. This synthesis of information allowed us to run meta-analyses to view ecosystem and community structures in 3D ecospace and contrast the functional

traits and ecological roles across species. The relevant ecospace these communities fill is limited compared to the theoretical ecospace available throughout the world's waterways, especially in the deep-sea. We simulated ancestral states of reproduction on a complete modern phylogeny, which supports the evolution of viviparity much earlier in chondrichthyan history than previously suspected. Overall, these results corroborate what has been found in the paleontological record, and allows us to reinterpret the evolution of vertebrate reproductive modes and cartilaginous fish communities in deep time.

Introduction

Imagine the high-speed pursuit of a mako shark swimming down a billfish, marlin, or swordfish: sustained swimming at 75 kilometers per hour through an endless blue desert, with quick turns and a violent end. Contrast this scenario to one you might observe outside a deepwater submersible: ghost sharks and anglerfishes float by with little to no effort, undulating their body or oscillating their fins at a seemingly slow-motion pace. These novellas describe the stark differences between fast-paced life in the shallow, light-filled regions of the ocean's surface and life in the slow lane: the depths of the sea. Life in the photic zone, or upper aquatic region, offers considerably different prey options, in addition to the most light. Once you get past the 200 meter mark or into the Mesopelagic, there is little to no light. And even further, past 1000 meters, in the Bathypelagic, there is an ever-increasing force of pressure and decreasing amount of oxygen. Various abiotic factors of the deep-sea render a myriad of physiological constraints for its inhabitants. For instance, try to visualize life in the deep-sea. The first image that pops up is likely a blob-like, lethargic fish with huge eyes. Although the deep is mysterious to most, this imagery is easily conjured by many different people, because we can instinctively envision what a world would look like with no light, little food, and pressures that would crush us.

A primary driver of spatial distributions and habitat structuring of fishes is the depth at which they live, comparable to the elevational diversity gradients of mountainous terrestrial ecosystems. Akin to how elevational constraints have imposed physiological selection on adaptations that facilitate high-altitude migrations in Himalayan geese (Hawkes et al. 2011; Bishop et al. 2015; Scott et al. 2015), many deep-sea fishes have adapted to the low levels of light and oxygen. These physiological adaptations can become physiological constraints, as living near biological extremes place limits on possible phenotypic variation (Collar et al. 2009;

Cohen et al. 2012). Some of the extreme adaptations tied to living in the deep sea are seen reflected in their disproportionate body size to head and gill ratios (Hughes and Iwai 1978; Friedman et al. 2012; Wootton et al. 2015), large eyes (Marshall 1954; Douglas et al. 1995; Warrant and Locket 2004; Musilova et al. 2019), skeletal reductions (Bone and Robert 1969; Tont et al. 1977; Gerringer et al. 2017), and lack of a swim bladder (Denton and Marshall 1958; Eastman and DeVries 1981; Davenport and Kjørsvik 1986). These extreme habitats influence not just one or two traits, but entire suites of characters that alter the total organismal phenotype and by proxy, their interaction with their habitat.

A holistic approach towards encapsulating an organism's life is to consider their life-history traits and what drives them. Life-history theory was conceptualized from the notion that finite energy is available in the environment and thereby imposes constraints or trade-offs in the allocation of this energy to specific traits, like age, growth, size at maturity (standard for reproductive age), and adult mortality rate (Beverton and Holt 1959; Dulvy and Forrest 2010). Growth and body size are key functional traits within and among species that influences population abundance, geographic distribution, physiological performance and more (Peters and Wassenberg 1983; Pauly 1998; Hildrew et al. 2007; Fisher et al. 2010). Depending on life stage, an organism might invest differentially in growth, reproductive effort, and basic metabolic maintenance depending on the habitat and their neighbors. For instance, juveniles in habitats where predators are small but plentiful might prioritize growth, over maturation, and escape vulnerable small size classes (Fisher et al. 2013). However, the maximum body size an animal can achieve is ever entwined with the energetic budget it has available, which is reliant first and foremost on the food it can find. One way chondrichthyans (chimaeras, sharks, skates and rays) keep their cost of growth low is to build their endoskeleton with only cartilage. Compared to the high metabolic activity required for vascularized tissues like bone, which remodel and regenerate, cartilage can be constructed even on a sluggish metabolism (Currey 2002). Thereby, the cartilage cells provide a metabolically economical, load-bearing material to sustain chondrichthyans (Stockwell 1983; Dean 2009). An advantageous byproduct of this cheap building material is that cartilaginous fishes can attain large body sizes while paying relatively low physiological dividends.

Two critical aspects of an organism's life are locomotion and reproduction. Chondrichthyans have evolved many modes of locomotion, from axial-swimming (tail undulations), undulating or oscillating pectoral fins, to walking (or 'punting') along the substrate with pelvic fins, and some even alternate their pectoral and pelvic fins to walk. These fishes have also evolved nearly all types of known vertebrate reproductive modes, ranging from egg-laying to live-birth: oviparity, multiple types of aplacental viviparity, and placental viviparity (Castro, 2013). They have even evolved reproductive strategies that don't exist in other vertebrates, in-utero cannibalism via functional embryonic dentition (Gilmore et al. 1983; Gilmore 1993). While we are quite familiar with the vast diversity of reproductive modes in chondrichthyans, there is still a great debate as to what the ancestral state would have been. The main source of contention is whether oviparity (egg-laying) or live-bearing viviparity (yolk-only) is the plesiomorphic state in chondrichthyans. Musick and Ellis (2005) hypothesize that yolk-sac viviparity, not egg-laying, is the ancestral mode of reproduction in the sharks, skates and rays, and perhaps more importantly for chondrichthyans as a whole. This is the opposite conclusion of Dulvy and Reynolds (1997) which has oviparity as the sole reproductive mode from stem-chondrichthyans back to the beginning of the phylogenetic reconstruction with jawless fishes.

Chondrichthyes provide the opportunity to identify how the abiotic environment structures patterns of biodiversity on a large scale, as they are an ancient lineage that spans the globe. They also serve as an aquatic ectothermic scale, with a size range close to the extremities of mammals, considering a mouse to a whale: compare a small-eye pygmy shark (*Squaliolus*) smaller than a grapefruit to a whale shark (*Rhincodon*) larger than a school bus. A common test used to indicate trends of size between species, on a global scale, is Bergmann's Rule. Specifically, this is an ecogeographical rule that describes a negative relationship between body size and temperature (Hendges 2021) or that body size increases with increasing latitude (Bergmann 1847). In general, many endothermic species and most mammals conform to this rule (Ashton et al. 2000; Blackburn et al. 1999), while ectotherms, specifically fishes, have been found to both follow and break this rule (Ray 1960; Belk and Houston 2002; Fisher et al. 2010). Our aim here is to examine whether chondrichthyans, as a whole, follow Bergmann's Rule. In other words, are the largest body sizes found at increasing latitude and decreasing temperatures? There are related notions about deepwater gigantism: deep-sea creatures will be larger than their nearshore, shallow-water relatives (McClain et al. 2006), and here we seek to identify if chondrichthyans

follow this trend as well. Another strategy used to tease apart abiotic and biotic relationships, and where individuals overlap in their ecology, is the ecospace concept. This concept refers to the possible combinations of important ecological parameters without reference to limiting conditions, resources or competition among species (Bambach 1983). It describes which roles are utilized (or not utilized) and does not evaluate competition among modes of life or within modes. It serves to evaluate how many of the potential modes of life that could exist were actually present in a particular regional or temporal framework, and which were not present (Bambach 1983; 2007). This will allow us to untangle the evolution of chondrichthyans and their ecological preferences through time. From this, we can look at how chondrichthyan ecosystems have been structured at different times and scales, locally to globally.

Locomotion and reproduction may seem to have little in common; however, fishes like ratfish, sharks, and batoids operate at physiological extremes which may shape both traits. These include marathon-level migrations to natal breeding grounds (Mourier and Planes 2013; Marie et al. 2019), the longest gestation period known for all vertebrates, lasting up to three years (Tanaka 1990; López-Romero et al. 2020), vertical migrations of several hundreds to a thousand meters per day (Sims et al. 2003; Tyminski et al. 2015), and a deep, benthic assemblage that lives on sparse rations in an unchanging landscape. The aims of this study are four-fold: (a) tabulate locomotor and reproductive modes across extant chondrichthyans in space in an evolutionary framework; (b) reveal correlations between these strategies with biogeographical and depth zonation; (c) reconstruct ancestral conditions for locomotion and reproduction and quantify the number of transitions; (d) use an ecospace framework to explore the locomotor and reproductive modes of modern cartilaginous fishes to reveal absent trait pairings. We predict Bergmann's Rule will not apply to chondrichthyans across latitude and depth (as a proxy for temperature), because some of the largest elasmobranchs (mantas, whale sharks) are found in tropical waters. We also predict that reproductive modes like egg-laying are not solely the result of phylogenetic conservatism, but reflect alternate strategies for dealing with physiological constraints at depth. This hypothesis would be supported if we find multiple independent transitions to egg-laying as different lineages invade the depths.

Methods

Chondrichthyan Life-History Meta-Dataset

A meta-dataset for 1,188 chondrichthyans was compiled to include the geographical distributions of where they're found, their maximum body size, and depth range (via Weigmann 2016 and sources within), coupled with their reproductive mode, locomotor mode, and trophic level. See Supplemental Table 1.

Abundance

We analyzed the meta-data from 1,188 extant Chondrichthyan species: Chimaeras exhibit one living order with 49 species, Selachians (sharks) have eight orders with 511 species, Skates are the most diverse of all chondrichthyans, being one order with 285 species, and Rays are comprised of six orders with 343 species.

Depth Categories

Depth ranges were pulled from Weigmann (2016) and Last et al. (2016), then categorized following NOAA oceanic zonation, as this is relevant for fisheries management. We then characterized the NOAA depth zonations into two major categories, those where species are restricted, or remain within one zone, and into combined zones where species are known to migrate between various zones. Restricted Zones: are those that fall within: E: Epipelagic [0 - 200m] range of 200m, M: Mesopelagic [200 - 1,000m] range of 800m, and B: Bathypelagic [1,000 – 4,000m] range of 3,000m. Combined Zones: are those that travel between zones: EM: Epi-Meso [0 – 1,000m] range of 1,000m, MB: Meso-Bathy [200 – 4,000m] range of 3,800m, and EMB: Epi-Meso-Bathy [0 – 4,000m] range of 4,000m.

There is only one species of extant chondrichthyan known to be able to reach the Abyssal region, *Rajella bigelowi* from the depths of 625 - 4156m. Because it is a single taxon, we have grouped it with the other MB species for the analyses.

Body Size (BS)

An animal's body size correlates strongly with many physiological, ecological, and life-history traits (McMahon and Bonner 1983; McKinney and McNamara 1990; West et al. 1997). Body size can have an important influence on the organization of ecological communities and assemblages (Lawton 1990), therefore we categorized species based on their maximum length. Body size for all taxa was pulled from Weigmann (2016), then categorized by max body size,

total length or wingspan; as follows: 1) Small, size is ≤ .3m (n= 103), 2) Medium, size is between .3m - 3m (n= 1,035), 3) Large, size is from 3m - 30m (n= 50).

Reproductive Mode (RM)

1) Oviparous (Ovi) is when the fertilized embryo plus its yolk are encapsulated within an egg and then deposited into the environment where it will develop, then hatch, here "Egg laying" (n= 526). The following reproductive methods all happen via live-birth where the young are delivered by the mother: 2) Lecithotrophy (Yol) is when the embryos are supplied with "Yolk-only" (n= 257), 3) Histotrophy (His) embryos are supplemented throughout development from yolk supplies, plus maternal lipid secretions, known as "Uterine milk" (n= 280), 4) Oophagy (Oop) is when embryos are supplied with yolk to develop, and additional ova (unfertilized eggs) to ingest, known as egg eating (n= 13), 5) Adelphophagy & Oophagy (Aop) egg-eating + cannibalism of additional developing embryos in utero, or siblings that have not fully developed and died (n= 3), 6) Oophagy & Histotrophy (Ohi) egg-eating + uterine milk (n= 5), and lastly, 7) Placental (Pla) where mothers form a placental connection and directly exchange nutrients with the embryo, who is still supplied with yolk (n= 104).

Reproductive modes were pulled from Dulvy and Reynolds (1997), Kyne and Bennett (2002), McEachran and Aschliman (2004), Hamlett (2005), Musick and Ellis (2005), Castro (2013), Rocha and Gadig (2013), and (Burgos-Vázquez et al. 2017). Reproductive rank order follows increasing amount of energetic maternal investment and anatomical modifications occurring to the maternal uterus in order to produce offspring; similar to the order in Dulvy and Reynolds (1997). But, here we have consolidated their reproductive scheme to focus on the final output of the reproductive process, i.e. egg-laying here exemplifies specimens that deposit egg cases onto the seafloor, where the embryos then develop for an extended period of time before hatching. Moreover, we have collapsed their numbering scheme of 2 & 3 into one output, now number 2 being lecithotrophic viviparity: where embryos solely feed off of yolk throughout development, and mothers give birth to full-grown precocial young. See Dulvy & Reynolds (1997) and Supplemental Table 1 for further descriptions of reproductive classifications.

This scheme better allows us to make inferences into extinct taxa with regards to fossils, whether it be egg-cases or full-body preserved taxa with reproductive features (Long et al. 2008). This scheme will allow us to place extinct taxa into the hypothetical ecospace and compare them

to the extant taxa we see today, allowing us to make further inferences about the evolutionary ecology and life-history traits that have persisted or disappeared throughout time.

Locomotor Mode (LM)

1) Anguilliform (Ang) swimming is when the entire trunk and tail participate in lateral undulations where more than one wave is present (n= 248), 2) Carangiform (Car) swimming is when undulations, of the axial skeleton (in this case their tail), are mostly confined to the posterior half of the body with less than one wave present (n= 228), 3) Thunniform (Thu) swimming is when only the tail and caudal peduncle undulate; a distinguishing feature of fast swimming lamniforms (n= 16), 4) Anguilliform + Undulatory (Aun) swimming is the continuous lateral undulations of the axial skeleton, plus undulating of pectoral fins (n= 131), 5) Undulatory (Und) swimming is having more than one wave present on the pectoral fins at a time (n= 161), 6) Oscillatory + Undulatory (Osu) swimming is when the pectoral fins have 0.5-1 wave present at any time (n= 61), 7) Oscillatory (Osc) swimming is when the pectoral fins move up and down with less than half a wave on the fins (n= 41), 8) Undulatory + Punting (Upu) is when the pelvic fins are planted into the substrate and then retracted caudally, which thrusts the body forward, plus undulating of pectoral fins (n= 285), and lastly, 9) Walking + Anguilliform (Wan) is when synchronous pectoral and pelvic fins alternate diagonally to 'walk' along the substrate, plus anguilliform/axial swimming (explained above, n= 17).

Swimming mode for taxa was pulled from Pridmore (1994), Webb (1994), Goto et al. (1999), Rosenberger (2001), Koester and Spirito (2003), Maia et al. (2012, and references within), Allen et al. (2016), Travis (2020). Here we've broken down the distinct swimming or locomotor modes for all Classes and most Orders. Due to the lack of kinematic data for many species, swimming mode here has been generalized to the Order level. While there has been a distinction in the literature of carangiform swimming to sub-carangiform swimming mode, there are not enough kinematic studies to differentiate them on this great a scale. Therefore, we have considered any species or orders in the literature that fall within either of those two categories to be carangiform swimmers for the analyses done here.

Similar to the rank ordering of the maternal investment, here we consider the mechanical and physiological investments needed for the animal to navigate through its different environments. Starting with axial motions, or a singular plane of movement, we then move onto axial +

undulatory movement which goes from body caudal movements to now employing a secondary plane, being the pectoral fins. This progression transitions to a more modified mode of swimming seen in rays, where they propel themselves via only their pectoral fins. We then have pectoral fin based swimming coupled with the pushing off/activation of the pelvic fins, found in skates. Finally, we have a single family of sharks (Hemiscylliidae) that are known to employ axial swimming when submerged, but are also known to employ synchronous switching of the pectoral and pelvic fins to walk through the subtidal coral environments off the Australian coast where they're found.

Trophic Level (TL)

The trophic level, for all available 1,089 species, was pulled and calculated from FishBase using the dietr package in R, following the FishBasePreyVals & FoodTroph functions. dietr provides trophic levels from the conglomerate datasets, composed of diet data and prey trophic level data (Borstein 2020).

For species with unknown TL's, where FishBase and dietr couldn't calculate the TL, we imposed two TL values. If there was more than 1 species within the Genus with a dietr TL, we 1) copied the TL of the species with the highest prey sample, in order to minimize skew from prey abundance, and 2) the average dietr TL, across the available species within Genus, was taken and applied to the unknown specimens, in order to avoid inconsistent prey biases. These steps were completed for 633 species, across 109 Genera. Similar to the categorization of rank order used with BS, LM, and RM, for TL, we used the rank category from the dietr value or our average value imposed from the related species within a genera. For the ranking, raw trophic levels were rounded up to the trophic categories of 3: secondary consumers, 4: tertiary consumers, 5: apex predators. For example, the great white shark (*Carcharodon carcharias*) TL = 4.7, and rank = 5.

Biogeographical Distribution of Chondrichthyans.

Geographic distributions from the 10 major ocean areas and the subsequent combinations of those areas were used to visualize the majority of extant species. In fig. 1, 30 distinct locations are shown, out of the 127 total aquatic combinations, following NOAA, IHO (1953) and Weigmann (2016). The labeling of aquatic areas here follows the third edition of the Limits of Oceans and Seas (IHO, 1953). The 10 major ocean areas include the Western Indian Ocean

(WIO), Eastern Indian Ocean (EIO), South West Pacific Ocean (SWP), North West Pacific (NWP), North East Pacific (NEP), South East Pacific (SEP), South West Atlantic Ocean (SWA), North West Atlantic (NWA), North East Atlantic including the Mediterranean and Black Seas (NEA) and South East Atlantic (SEA).

Using aquatic area and species richness from our meta-dataset we were able to visualize these geographical distributions in fig. 1 by using the following R packages: dplyr, ggplot2, ggmap, ggspatial, ggthemes, mapdata, mapproj, maps, marmap, MASS, vegan (R Core Team 2020; RStudio Team 2020).

Body Size by Depth

Max body size and depth range data were taken for 1,151 of the 1,188 species from Weigmann (2016). A handful of unknown depth ranges for rays were supplemented from Last et al. (2016). Body size (BS) of each species was characterized as being 1) small, 2) medium, or 3) large. The total number of species (or species richness) for each body size was then categorized by depth zone. The BS breakdown for the 6 depth zones were visualized using the Doughnut plot in Excel, where the ring width of each plot represents the total % of chondrichthyans found in that zone. The BS data was standardized, dividing the total number of species of each size within a depth zone by the total number of species that have depth data (1,151 sp.), this allowed us to change the scale of the plots without altering the information conveyed to the viewer. The 6 plots were then combined into two main plots, and adjusted in InkScape to create fig. 2. The 3 zones grouped into the left-side plot are those with species that are Stenobathic or having a small depth range which they are able to live, those being the Epipelagic, Mesopelagic, and those two regions combined (EM); and the right-side plot being the more Eurybathic zones where species are able to live and move through a greater depth of water, being the Bathypelagic, Meso-Bathypelagic, and those three regions combined (EMB).

To test if Bergmann's Rule applies to chondrichthyans we compared body size to both latitudinal zone and depth zone we ran multiple ANOVA's and Tukey tests (Table S1).

Species Richness by Depth

Species richness for each depth zone in fig. 3 was visualized using the 100% stacked column plot in Excel. Where each band represents the number of Orders present and band length is the

percentage of species within the Order. A visual of the community structuring throughout the depths, with an increasing depth range along the Stenobathic-Eurybathic continuum, zone order being: E, M, EM, B, MB, EMB.

Reproductive Phylogeny of Modern Chondrichthyans

We used the Stein et al. (2018) phylogeny consisting of 1,192 chondrichthyans, 10,000 fully resolved trees with 10 fossil calibration scenarios "10.cal.tree.nex", downloaded via http://vertlife.org/sharktree/downloads/. We then dropped the missing tips between our dataset and the Stein et al. (2018) 10.cal.tree phylogenies and then combined our character trait datasets with those trees. These data were then run through the make.simmap function for 1,000 simulations to create the stochastic character maps. Additionally, we chose the 95% confidence consensus tree to map the ancestral state reconstructions, via the ace function, onto our chosen topology. The final simmap trait tree was chosen to visualize the state changes over chondrichthyan history, with precedence given to the deep nodes, branch lengths, and order of major classes. We recognize that species-specific relations may be considerably plastic across this abundance of trees, but the major general trends hold true, and for this manuscript are our focus.

Further, it's worth noting that the conditions and simulations are solely considering modern extant species of chondrichthyans. We are interpreting modern chondrichthyans, sans outgroup, as the reproductive history for the closest sister group (Acanthodians) is seemingly non-existent in the fossil record. To test for phylogenetic signal of reproductive modes, across modern chondrichthyans, we used two packages (phylosig and phyloSignal) to analyze and compare results between the K and Lambda methods under a Brownian Motion model. R packages for ancestral states and to create fig. 4 include: ape, caper, geiger, nlme, mvtnorm, phangorn, phytools, tidyverse (R Core Team 2020; RStudio Team 2020).

Reproductive Mode by Depth

The proportion of reproductive modes that are present in each depth zone was visualized in R using a waterfall chart. The R packages used to create the waterfall chart in fig. 5 were dplyr and ggplot2 (R Core Team 2020; RStudio Team 2020). Where each band represents the reproductive mode(s) found within a depth category, and the length of each band is the percentage of species

that exhibit that specific mode. The total bar length indicates the range in meters for each depth category.

Ecospace + Ecological Disparity

Three general factors are generally used when assigning species to assemblages/guilds: food source (diet), space utilization (locomotion), and bauplan (size). The bauplan of an organism includes all aspects of its physiology, reproductive strategy, growth, and other such intrinsic features that influence the presence or success of the organism in the habitat of the community (Bambach 1983; Bush et al. 2007). But because chondrichthyans exhibit the most variation in reproductive modes of all vertebrates, we have incorporated this variable as a category for ecospace visualization.

Following Bambach (1983; Bambach et al. 2007) who formulated the ecospace method, and Chen et al. (2019) who re-envisioned fossil mammals using this 3D space and framework, we used similar methods to revamp how extant chondrichthyans are analyzed. Eco-physiological parameters (body size, reproductive mode, and locomotor mode) were used to form a three-dimensional theoretical ecospace of 189 ecological-parameter-value combinations (~"niches," or eco-cells, *sensu* Chen et al. 2019; with 3 body-size ranks × 7 reproductive mode ranks × 9 locomotor ranks). The R packages used to create fig. 6 and 7,were rgl and scatter3d; using the type = "p" and "h" separately to get the vertical lines to correspond to the symbols, as to create a "lollipop" effect for viewing the 3D space (R Core Team 2020; RStudio Team 2020), illustrator was then used to align and clean up the overlaid ecospace images for each depth zone and latitude group (see Supplemental figures 3 and 4).

Using these parameters, we can quantify the magnitude of the filled ecospace of each community using two indices: ecological richness (ERich) and ecological disparity (EDisp). Ecological richness measures the number of eco-cells occupied by a community in the theoretical ecospace. ERich is expected to be highly correlated with species richness: the higher the number of species, the higher the ERich in a community. Ecological disparity is how morphologically different species in the same ecosystem are from each other and measures the magnitude of ecological differences among species in a given ecospace. Following Chen et al. (2019) and Dr. Meng Chen's code, found here https://github.com/biomchen/mammal-community

we were able to calculate these indices. EDisp is calculated as the mean pairwise distance of all species pairs in the same community. The calculation for one pair of species (i, j) is:

$$EDisp(i,j) = | BSi - BSj | + | LMi - LMj | + | RMi - RMj |$$

where BS is the Body Size rank, RM is the Reproductive Mode rank, and LM is the Locomotor Mode rank for species i and j. Example: $EDisp(i, j) = | 2 - 3 | + | 2 - 8 | + | 3 - 3 | = 7$

We compared the EDisp for all species and communities, using both BS and LM, then the third factor was RM: BS + LM + RM. Because RM may fall more within the physiological realm, we ran a separate analysis of EDisp, RM was replaced with the Trophic Level (TL): BS + LM + TL. This was done to simulate a more traditional ecological scheme where diet preference, such as herbivore vs. carnivore, is taken into account.

Results

Biogeographical Diversity of Chondrichthyans

These fishes have thrived for hundreds of millions of years, in varying environments, thus it might come as no surprise that they are widely geographically distributed. And similar to Weigmann (2016) and Stein et al. (2018), we find that some bodies of water do exhibit a higher species richness than others. In fig. 1, we show 30 distinct locations out of the 127 total combinations, found in Weigmann 2016; while these locations make up 24% of the known biogeography of chondrichthyans, they account for 78% of all chondrichthyans or 932 species. There are certain distinct locations that exhibit hot spots; we find that most hot spots are larger, or have more species, in endemic regions, versus in cosmopolitan regions.

Endemic Regions: The largest hotspot is the North West Pacific (NWP) Ocean with 128 endemic species. The second largest hotspot is found in the West Pacific, being the South West Pacific (SWP) with 120 species. The Western Indian Ocean (WIO) hosts 86 species, and the Eastern Indian Ocean (EIO) has 74. The North West Atlantic (NWA) has 78, and the South West Atlantic (SWA) has 34. The North East Pacific (NEP) has 29, and the South East Pacific (SEP) has 32. The North East Atlantic (NEA) has 35, while the South East Atlantic (SEA) has only 2 endemic species.

Cosmopolitan Regions: The largest hotspot of cosmopolitan regions is the EIO+SWP region southwest of Australia, with 68 species. The NEP+SEP region is the only cosmopolitan region that outcompetes its endemic sister regions, with 42 species present. We primarily find this due to the high rates of latitudinal migrations of these species. The SEA+WIO region south of Cape Town, South Africa has many more species than its sister SEA region, with 34 species.

When comparing the "Polar" and "Equatorial" groups of species (Table S1), we found no significant difference ($p = 0.0593729$) between them, indicating that maximum body length is not biased towards increasing latitudinal zones or decreasing temperatures. Therefore, chondrichthyans do not follow Bergmann's Rule.

Body Size & Species Richness by Depth

Partitioning species maximum body size by depth allowed us to identify and quantify patterns found across chondrichthyans. In fig. 2 we visualize the major trends in chondrichthyan body size with relation to the depth at which they're found. Interestingly, we find that the Mesopelagic, Meso-Bathypelagic, and Bathypelagic zones do not exhibit the large body size class. In other words, all chondrichthyans that live below 200 meters are under 3 meters long/wide.

Stenobathic Zones: The Epipelagic (E) ring width represents 34% of all Chondrichthyans. The 434 species restricted to the top zone exhibit all body size categories; Max length is the Longcomb sawfish (*Pristis zijsron*) at 730cm. The Mesopelagic (M) ring width represents 15% of all Chondrichthyans. The 187 species restricted to the middle zone do not exhibit large body sizes; Max length is the Japanese velvet dogfish (*Scymnodon ichiharai*) at 151cm. The Epi-Meso (EM) ring width represents 22% of all Chondrichthyans. The 285 species that can swim through the top two zones exhibit all body sizes; Max length is the Giant oceanic manta ray (*Mobula birostris*) at 700cm.

Eurybathic Zones: The Bathypelagic (B) ring width represents 2% of all Chondrichthyans. The 21 species restricted to the deep do not exhibit large body sizes. Max length and the deepest swimming species is the Pallid skate (*Bathyraja pallida*) at 162cm and 3,280m, respectively. The Meso-Bathypelagic (MB) ring width represents 10% of all Chondrichthyans. The 123 species that can swim through the bottom zones do not exhibit large body sizes; Maximum length is the Pacific white skate (*Bathyraja spinosissima*) at 203cm. The Epi-Meso-Bathypelagic (EMB) ring

width represents 8% of all Chondrichthyans. The 101 species that can swim throughout all zones exhibit all body sizes; Maximum length is the Whale shark (*Rhincodon typus*) at 1,700cm, the deepest swimming species being the Cookiecutter shark (*Isistius brasiliensis*) to 3,700m.

When comparing body size across the 6 depth zones via ANOVA we found a significant difference ($p = 1.47e\text{-}15$), indicating that body sizes do vary between species across the depths, but not that body sizes increase as depths increase. Upon further inspection, the Tukey test indicated that the only depth combinations that did show significant differences between each other were Meso:Epi $p = 0.0000004$, EMB:Epi $p = 0.0000047$, Epi-Meso:Meso $p = 0.0000000$, EMB:Meso $p = 0.0000000$, MesoBathy:Meso $p = 0.0010229$, EMB:Epi-Meso $p = 0.0007405$, and MesoBathy:EMB $p = 0.0003163$. Overall, chondrichthyans do not follow Bergmann's Rule, where increasing depth is an indicator for decreasing temperature.

Species Richness & Community Structuring Throughout the Depths

The distribution of extant species with respect to specific depth zonation's they inhabit are visualized in fig. 3 using a stacked barplot. This shows the community structuring throughout the depths, as it has zones in order of increasing depth range along the Stenobathic-Eurybathic continuum: E, M, EM, B, MB, EMB. Where N= species richness for each zone. The highest species richness is found in the upper 0-200 meters of the photic zone with 434 species, and is heavily dominated by the myliobatiform rays. The next most speciose zone is the EM zone from 0-1000m with 285 species, followed by the Mesopelagic or 200-1000m zone with 187 species. The first 1000 meters of aquatic environments contain 79% of all chondrichthyans for which we have depth data. Aside from species richness trends, we can see clear trends in Order coverage throughout the various zones. The predominant ones being: there are no Chimaeriformes that solely inhabit the top 200 meters, but they're found in increasing abundance with depth. Similarly, while skates are present in the Epipelagic, they increase in abundance with depth and make up the majority of species found from 1000-3000 meters. Lastly, the Carcharhiniformes have been highly successful in conquering all depth zones, as they're found relatively ubiquitous in number in each zone.

Phylogenetic Distribution of Locomotor and Reproductive Modes

When considering the ancestral states of locomotor mode across modern chondrichthyans, we found that across the 1000 stochastic character maps, we find an average of 15.825 transitions between locomotor modes. The percentage of time spent in each state, from longest to shortest period: Anguilliform (22.44%) → Carangiform (19.58%) → Undulatory + Punting (15.27%) → Anguilliform + Undulatory (14.92%) → Undulatory (13.05) → Undulatory + Oscillatory (7.12%) → Oscillatory (3.554%) → Thunniform (2.904%) → Walking + Anguilliform (1.158%). Of these transitions the highest occurring were from Anguilliform (Ang) to Carangiform (Car) 4.279 times, from Anguilliform + Undulatory (Aun) to Undulatory (Und) 1.962 times, and from Undulatory (Und) to Undulatory + Oscillatory (Osu) 1.887 times (see Table S1). The most basal node of modern chondrichthyans was reconstructed as Ang being 41%, Osu = 36.9%, Car =18.5%, Upu = 11% the stochastic character reconstructions, reflecting the older Orders and their locomotor mode, Chimaeras (Osu), Selachi (Ang), and the batoids: Skates (Upu) and Rays (Aun); see Figure S1.

While we did not include extinct taxa as outgroups, many who were viviparous, our simulations of the reproductive traits support viviparity via yolk to being ~25% of the total reproductive modes possible on the most basal chondrichthyans node. This is the major difference between the original Dulvy and Reynolds (1997) paper that found oviparity ancestrally, going all the way back to agnathans.

Across the 1000 stochastic character maps, we find an average of 23.36 transitions between reproductive modes. The percentage of time spent in each state, from longest to shortest period: Oviparity (37.72%) → Yolk-only (27.36%) → Uterine Milk (23.56%) → Placental (7.920%) → Oophagy (2.697) → Oophagy + Uterine Milk (0.5519%) → Oophagy + Adelphophagy (0.191%). Of these transitions, 7.4 are from Oviparous to Yolk-only Viviparity and 0.998 rate of transitions *vice versa* (see Figure S2), indicating that the majority of transitions have occurred between these two reproductive modes throughout modern chondrichthyan history. The most basal node of modern chondrichthyans was reconstructed as Oviparity being 75% and Yolk-only being 25% of the stochastic character reconstructions, indicating that while oviparity is still the predominantly predicted reproductive mode near the base of the chondrichthyan tree, viviparity should not be counted out.

Phylogenetic signal of reproductive mode via K method equates to 2.76545, which corresponds to Blomberg's K, a Brownian motion model where there is more "phylogenetic signal" than expected under BM. Similarly, Lambda = 0.999934/1.012448 corresponds to a Brownian motion model; and all analyses exhibit significant p-values indicating that reproductive modes of close relatives are more similar than random pairs of species.

Species Reproductive Mode by Depth

Previous studies broadly define "deepwater" species as those at depths > 200 meters (Rigby 2015; Treberg and Speers-Roesch 2016); they miss the major trends we were able to distinguish by parsing out the life-history traits of chondrichthyans by each specific depth zone. Each band represents the reproductive mode(s) found within a depth category, and the length of each band is the percentage of species that exhibit that specific mode; the total bar length indicates how many meters are contained within each depth range. In the top photic zones or the zone to the right where species are known to travel throughout all zones, we see multiple modes, or almost all modes of reproduction present, while the only one we see utilized in those restricted to the deepest zone is egg-laying. All species inhabiting the Bathypelagic or 1000-4000 meters are solely egg-layers. These data reflect physiological restraints of reproductive modes in the deep for cartilaginous species living today.

Ecospace of All Chondrichthyans + Ecological Disparity

We visualized the entire meta-dataset using a 3D projection of ecospace of 189 eco-cells. Of the 189 theoretical eco-cells, 39 of them are filled which amounts to 23% of all possible life-history trait combinations or niches across the globe and throughout the depths of all available aquatic systems. This is the ecospace occupation of Chondrichthyes across all depth zones, with body size, reproductive mode, and swimming mode serving as the main axes on the left, we have the different levels which follow various modes of locomotion, and a representative taxon to visualize body shape.

We can see that sharks come in all body sizes and exhibit most of the reproductive modes, as they cover the bottom region of this ecospace. Sharks evolved all reproductive modes but only swim using few variations of axial locomotion, this may be due to their fast paced life, compared to that of batoids and chimaeras, or may be purely phylogenetically driven. Either way the

Galeomorphii sharks sustain all seven different reproductive modes while only swimming via anguilliform, carangiform, thunniform, and walking. In contrast, Batoids are more diverse in the appendages used to propel themselves, having various pectoral fin morphologies and amplitudes and some using their pelvic fins to punt along the bottom; but batoids more constrained when it comes to reproductive modes. The chimaeras are even more constrained to only a few options on all three axes, being two body sizes, one swimming category, and one reproductive mode. The ecospace for all depth zonation's and latitude groups are featured in the supplemental figures S3 and S4, respectively.

Ecological disparity (EDisp) within each depth zone, for both treatments, are listed here in decreasing order, where the first zones have the highest magnitude of ecological differences or the greatest morpho-physio-functional variation between the species in each zone. The Epi-Mesopelagic zone has 285 species and is the host to the highest ecological disparity with 2.39 (RM) and 2.02 (TL). The EDisp of the Mesopelagic is a close second with 187 species and 2.07 (RM) and 2.23 (TL). While the Epipelagic has the highest species richness with 434 species, it is not the highest region with respect to morphological variation for both ecological disparity schemes, coming out to 1.92 (RM) and 1.54 (TL). Next, is the Epi-Meso-Bathypelagic zone which hosts 101 species capable of spanning all 3 zones, with EDisp values of 1.83 (RM) and 1.57 (TL). The Meso-Bathypelagic has 123 species and EDisp values of 1.52 (RM) and 1.58 (TL). The Bathypelagic has the lowest species richness with 21 species, in addition to the least ecological disparity when considering both the comparisons of the more physiological basis (BS, LM, RM) being 0.78 and the more ecological combination (BS, LM, TL) at 1.01.

Bathypelagic Ecospace

In the deepest zone there are three groups, the chimaeras, catsharks, and skates, each of which utilizes a different mode of swimming. Although differing in phylogeny and morphology, all deep sea species share similar body sizes, in that all species that inhabit the deepest zone are under 3 meters and all lay eggs. The eggs themselves have distinct morphologies but share a similar function of having to persist in the depths long enough to be able hatch and be self-sufficient.

Discussion

All of the 21 species of cartilaginous fishes that live exclusively in the deep-sea, lay eggs - it seems a requirement for living in this hostile environment. Egg-laying arose independently three times in deep-sea chondrichthyans; spanning each major superorder: the chimaeras, sharks, and skates. Life-history strategies are generally shaped by the allocation of available energy for survival and reproduction (Roff 1994). An advantage of egg-laying over live-bearing in the deep is that the mother need only provide a pair of ova, with no additional maternal investment. The ova can be provisioned as resources are located, and a temporary lean time simply slows yolk production (Gilmore et al. 2005). When food is plentiful again the yolking up process can continue until there is enough to provision and encapsulate the fertilized eggs. In contrast, live-bearing requires continuously supporting the developing embryo, and a food shortage must be made up for with maternal stores or diapause; and too long a diapause can result in embryo death (Lessa 1982; Simpfendorfer 1992; Morris 1999; Waltrick et al. 2012). Chondrichthyans opportunistically store sperm for months to years (Castro et al. 1988; Storrie et al. 2008). This is an advantage, especially in the deep-sea where mates are rarely encountered (Moura et al. 2011; Finucci et al. 2017). Sperm storage decouples the timing between mating and ovulation (Storrie et al. 2008; Holt and Lloyd 2010; Awruch 2013; Dutilloy and Dunn 2020). We propose that egg-laying works well when food resources are patchy, mating is unpredictable, and the potential for higher reproductive output can stave off extinction (García et al. 2008; Simpfendorfer and Kyne 2009).

At deeper depths and higher latitudes, the water is colder; so our dataset represents two opportunities, albeit somewhat confounded, for testing whether cartilaginous fishes follow Bergmann's rule: that bigger organisms are found in colder climates. The deep-sea is rife with gigantism in the invertebrate world, from giant squid, to giant, and even supergiant isopods. As for poleward body size increase, there are the iconic examples from tetrapods (Bergmann 1847), and in a diversity of marine organisms, including squid (Rosa et al. 2012), fiddler crabs (Johnson et al. 2019), echinoderms (Dahm 1996), many gastropods and some bivalves. However, for cartilaginous fishes, Bergmann's rule does not apply - there is no increase in size with latitude, and there is a decrease in size with depth. Those species confined to deeper water are smaller

than average, with a maximum length of 1.6m. Though several of the largest species, the planktivorous Whale Shark, Basking Shark, and Manta Ray, are found in temperate and tropical waters they are not biasing against an underlying relationship - when these large outliers are removed there is still no latitudinal increase in length. Furthermore, while these ocean giants are capable of covering all depth zones, they only dive deep for short periods to feed. These large species are incapable of rolling in the deep.

We have no comprehensive explanation for the differences between other ectotherms that show a size increase with decreasing temperature and cartilaginous fishes that do not. In both groups there are deep species that mature later than shallow water species (Wourms 1977; García et al. 2008; Rosa and Seibel 2010). This leads to a longer period where all food resources are converted into becoming a larger animal rather than split between growth and reproduction. In neither case is large size being driven by a thermal surface area to volume ratio effect, as they are ectothermic. With large size comes a lower mass specific metabolic rate, which should favor larger size in nutrient poor depths, and while that may be driving gigantism in some invertebrates, it is not governing the cartilaginous fishes. Our only explanation harkens back to our observation that for cartilaginous fishes, egg-laying is required for continuous habitation. Each of the three lineages found at depth first evolved in shallow water as egg-laying clades (Haedrich 1996; Siverson and Cappetta 2001; McEachran and Aschliman 2004; Priede et al. 2020). The chimeras, skates, and catsharks share another quality -- they are all small bodied (less than 1.6m in size). We know of no causal link between these facts, but it is clear that all three lineages carried their small size into the deep-sea - it is possible that this is a phylogenetic artefact rather than a physiological or ecological one.

Our analysis of chondrichthyan presence by depth did not include the abyssal zone (>4000m) because sharks, rays and chimeras are all but absent from this habitat. We propose the abyss is a forbidden zone for life-history reasons. Abyssal invertebrates and bony fishes are R-selected strategists that produce hundreds to thousands of buoyant eggs. In contrast, although egg-laying chondrichthyans out reproduce their live-bearing and ovoviviparous kin (Ebert and Davis 2007; Simpfendorfer and Kyne 2009), they still have a low intrinsic rate of increase. Chondrichthyans lay two eggs at a time, and they take some care to deposit these in places that will maximize the likelihood of hatching. Contrary to deep-sea bony fishes that produce buoyant eggs, egg-laying

chondrichthyan species deposit their embryo into a capsule, which remains stationary throughout development, a period of months to years (Wourms 1977; Ebert and Winton 2010; Hoff 2008). The deeper the species lives, or deposits eggs, the less oxygen the embryos secure and the more inhospitable the environmental temperatures become. These two factors greatly exacerbate the developmental timing of embryos. One stratagem employed by the Pacific white skate (*Bathyraja spinosissima*) is to deposit their eggs near hydrothermal vents in order to incubate the embryos and speed up the developmental process, which still takes years (Salinas-de-León et al. 2018). The abyssal ocean is unstable with variable and high speed currents, sediment falls, seismically driven rearrangement of the bottom, and fluctuation in suspended particles (Thistle et al. 1985; Aller 1989; Aller and Stupakoff 1996; Deflandre et al. 2002). None of these are conducive to hatching success in species with years-long development times in egg capsules fixed to the substrate.

Alternatively, or in addition, physiological constraints could keep cartilaginous fishes from the deepest sea. They maintain neutral buoyancy with oils in the liver, and these are dietarily expensive to maintain, perhaps too expensive for the food limited abyss. Also, cartilaginous fishes require a good deal of dietary nitrogen because they osmoregulate with a combination of urea and Trimethylamine N-oxide (TMAO, Priede et al. 2006; Treberg and Speers-Roesch 2016). All marine fishes lose nitrogen through the gills, so it must be replenished, but for cartilaginous fishes the problem is more extreme because they lose nitrogen dense molecules that may not be replaceable in the abyss. Lastly, it has been argued that TMAO itself is toxic at very high pressures, but since bony fishes survive with concentrations higher than those of sharks, rays and chimeras (Priede 2006; Treberg and Speers-Roesch 2016; Priede et al. 2021), this is not a likely explanation for the lack of cartilaginous fishes in the abyssal deeps.

Characterizing the ecospaces of modern chondrichthyans has allowed us to parse out what traits have evolved, and more importantly what traits haven't evolved (or were lost). For instance, thunniform and oscillatory locomotor modes are found in the upper pelagic zone (0-1000m), although they are sometimes used to invade deeper waters for brief feeding bouts (Gleiss et al. 2011; Coffey et al. 2020; Vedor et al. 2021). So either there is a biomechanical/physiological explanation for their absence in the deep sea, or as in small, deep cartilaginous fishes, the explanation lies in phylogeny. Or, consider the wide range of locomotor

modes employed by cartilaginous fishes that migrate through all three depth zones - every mode save undulation and walking. Our data suggest that undulation is not conducive, either energetically or hydrodynamically, to sustained vertical dives from the surface into the deep. In this case the biomechanical explanation appears likely, as undulatory rays have a circular body shape, a whip-like tail, and propel themselves exclusively with the margin of the disk. Adding in the tail as a propulsor allows the similarly shaped electric rays, which use anguilliform + undulatory swimming, to occupy the entire water column. Electric rays have been observed to pitch their rostrum down, or nosedive, in a steep, fast descent as their large caudal fin acts as a motor.

We address whether the ecospace trends we see in extant cartilaginous fishes apply to what we know of the fossil record. Do fossils reveal a different set of constraints and opportunities, or do they fall within the scope of Recent fishes? It is difficult to assess the ecospace parameters we selected without good skeletal material, which is rare in the fossil record. But there are some entire or partially articulated skeletons that allow us to dive through deep time to better understand what the world was like when the majority of life was aquatic. In some cases the fossil record reveals clades of chondrichthyans that occupied different ecospaces than they do now. For example, the Jurassic chimaeroid *Squaloraja* (Dean 1895), has guitarfish-like pectoral fins, rather than the flexible flapping fins of modern species. The flattened body plan and exaggerated cranial/rostral morphology, alter the fluid dynamics of this specimen compared to their modern streamlined counterparts. An elongate triangular body plan tends to be more energetically efficient with pectoral fin based steering and anguilliform caudal fin propulsion, similar to today's guitarfishes. A Mississippian chimaerid, *Chondrenchelys* (Lund 1982), was very eel-like in morphology, with a long tapered body to caudal fin implying anguilliform swimming -- another locomotor niche not seen in chimaeras today. Similar patterns of ecospace expansion relative to Recent clades is seen in reproduction, feeding, and locomotor morphology (see supplemental figure S5).

There are examples of entirely new ecospaces occupied by extinct forms; for example the Xenacanthine and Hybodontid sharks, both Carboniferous lineages, were found exclusively in freshwater. There are no extant, obligate freshwater species of shark, so this would be a new ecospace niche. In addition to the environmental niche these taxa filled, they included

morphological roles not found today; some possessed a diphycercal caudal fin or leaf-shaped tail, similar to the modern Chimaeridae, a character non-existent in modern sharks. Another extinct example, the hybodont *Onychoselache's* tail was straight and tapered, unlike the heterocercal tails in all modern sharks. This taxon is thought to represent an early elasmobranch body plan in which the paired fins and girdles were adapted for station holding and, perhaps, submerged walking (Coates et al. 2007). These theories of morphology have been supported by Soler-Gijón et al. (2001) where a morpho-functional analysis of the fossil traces point to the anguilliform locomotor mode of Xenacanthine sharks.

The fossil record provides us with many examples of extinct stem-chondrichthyan reproductive modes that are no longer found today, many of which were viviparous. For instance, although all modern Holocephalans are oviparous, fossil evidence supports multiple other reproductive modes, in addition to egg-laying seen in *Crookallia* (Helodontidae, Patterson 1965; Fischer et al. 2014). For instance, some Holocephalan species gave live-birth, as in *Delphyodontos dacriformes* which were oophagic and potentially adelphophagic (Lund 1980), while others like *Harpagofututor volsellorhinus* were histotrophic (Grogan and Lund 2011). Despite excluding extinct outgroups, with distinct reproductive modes, from our ancestral states reconstruction, the story of viviparity at the basal nodes of chondrichthyan reproductive evolution is evident. It is important to note that although we didn't include these taxa in our analyses, our results are more reflective of what the fossil record supports: there were many extinct viviparous taxa that would now belong to egg-laying only clades, and also *vice versa* with many extinct egg-laying sharks whose only living relatives are viviparous (see Figure S6. Kriwet et al. 2009; Fischer et al. 2014). While it is still not conclusive as to whether the ancestral state was oviparity or viviparity, this modern phylogeny has gotten us closer to the answer. We currently find the reproductive likelihood of modern chondrichthyans to have stemmed from egg-laying ancestors; but we note that with the addition of extinct taxa to this phylogeny the percentage of viviparity being supported as the ancestral state in chondrichthyans would likely dramatically increase.

Although we have a general understanding of vertebrate reproduction throughout time, the key for making grand scale interpretations, with respect to chondrichthyans, lie in understanding the acanthodians. Acanthodians are supported as sister to chondrichthyans (Woodward 1891;

Brazeau 2009; Davis et al. 2012; Zhu et al. 2013; Burrow et al. 2016; Qiao et al. 2016; Zhu et al. 2016); therefore, they were internal fertilizers would shed new light on trends of vertebrate evolution as a whole. It is assumed that internal fertilization was not a likely mode of reproduction in acanthodians due to their large pelvic fin spines (Watson 1937; Maisey 1984; Maisey et al. 2017; Johanson et al. 2019), coupled by the lack of fossilized embryos within any adult female described thus far. Although this missing link delays a conclusion if this paraphyletic stem group of chondrichthyans was oviparous, viviparous, or was an external spawner similar to bony fishes (Zhu et al. 2013; Giles et al. 2015; Long et al. 2015; Coates et al., 2017; Johanson et al. 2019).

We can refer to fossilized stem-gnathostomes, the placoderms, and their reproductive modes to infer large scale trends across vertebrate evolution. Placoderms are the ancestral jawed and paired finned vertebrates, and similar to chondrichthyans, some possessed clasper-like pelvic structures used to facilitate internal fertilization (Long et al., 2015). Fossil placoderms and prehistoric nursery site structures support placoderms as being both oviparous and viviparous (Long et al. 2008; Long et al. 2009; Johanson et al. 2014; Olive 2016). The presence of both yolk-sac viviparity and egg-case oviparity in placoderms and basal chondrichthyans suggests that the derived and variable reproductive biology is actually a basal condition among gnathostomes with both approaches representing early and successful strategies (Carr and Jackson 2018; Bernard Mottequin et al. 2021). Overall, we find that the reproductive evolution of vertebrates is less black and white than once proposed, and that further renditions and refinements of the vertebrate tree of life will allow us to tease a part this notion of what came first, the chicken (viviparity) or the egg (oviparity).

Acknowledgments

Thank you to Meng Chen for the code to calculate ecological disparity (EDisp) and Jonathan Huie for assistance in modifying the code for this study. To Greg Wilson-Mantilla for the many foundational discussions we had on community structuring, and the push to consider doing this work on my study system.

FIGURES

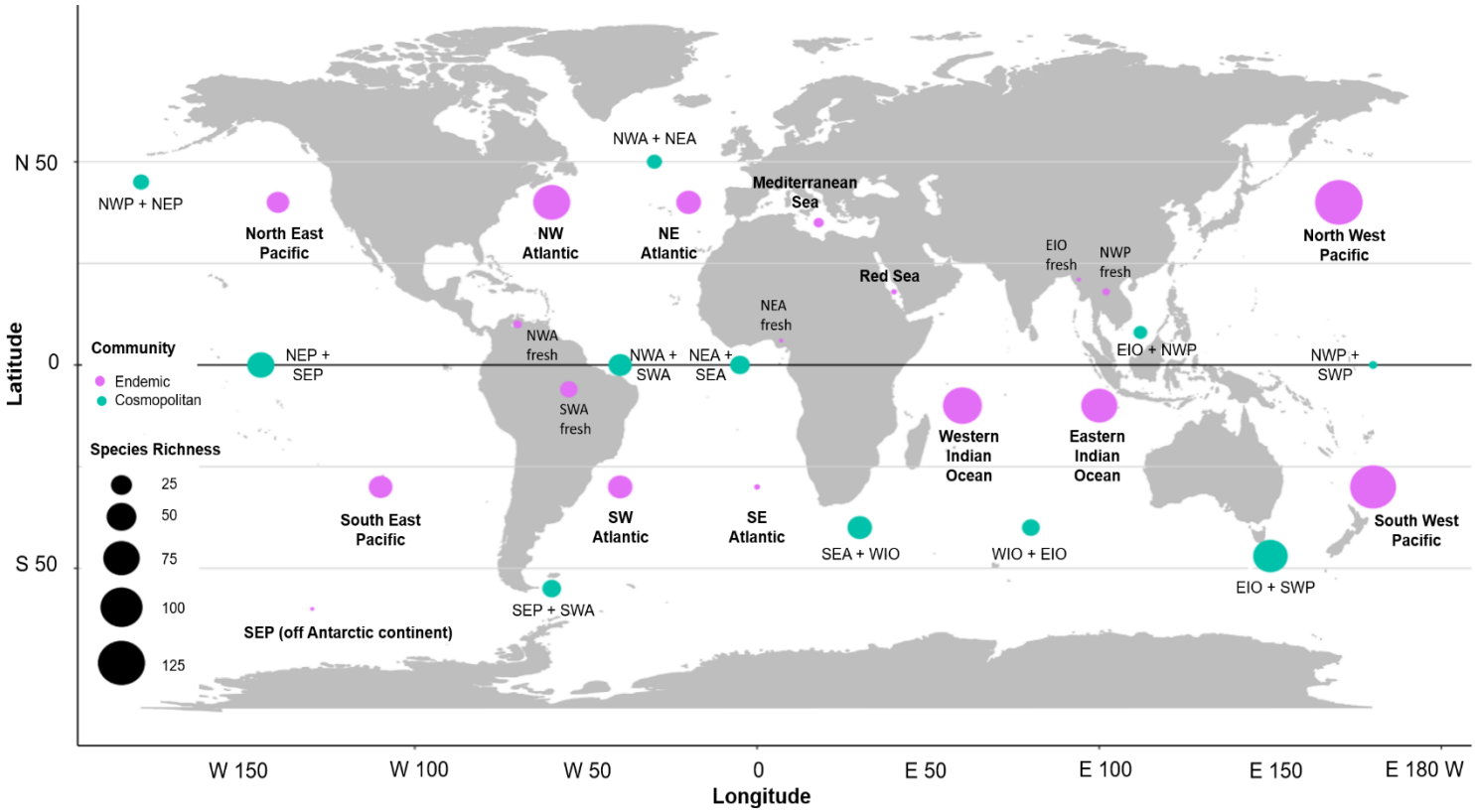

Figure 1: Biogeographical diversity of Chondrichthyans. 30 distinct geographical locations, 932 species or 78% of all extant Chondrichthyans. The species richness is indicated by circle size, where pink indicates species that are endemic to one aquatic area, and turquoise indicates species that move between two regions or cosmopolitan (See online version for color). Bolded locations are ones where species are endemic to an exclusive region, all other locations are identified by the +, in which species move between specified locations. The + between two areas indicates that species move between the two; when this symbol is horizontal between two labels this means that species travel either East or West between them, and when it is vertical between two labels it indicates that species travel either North or South between these areas.

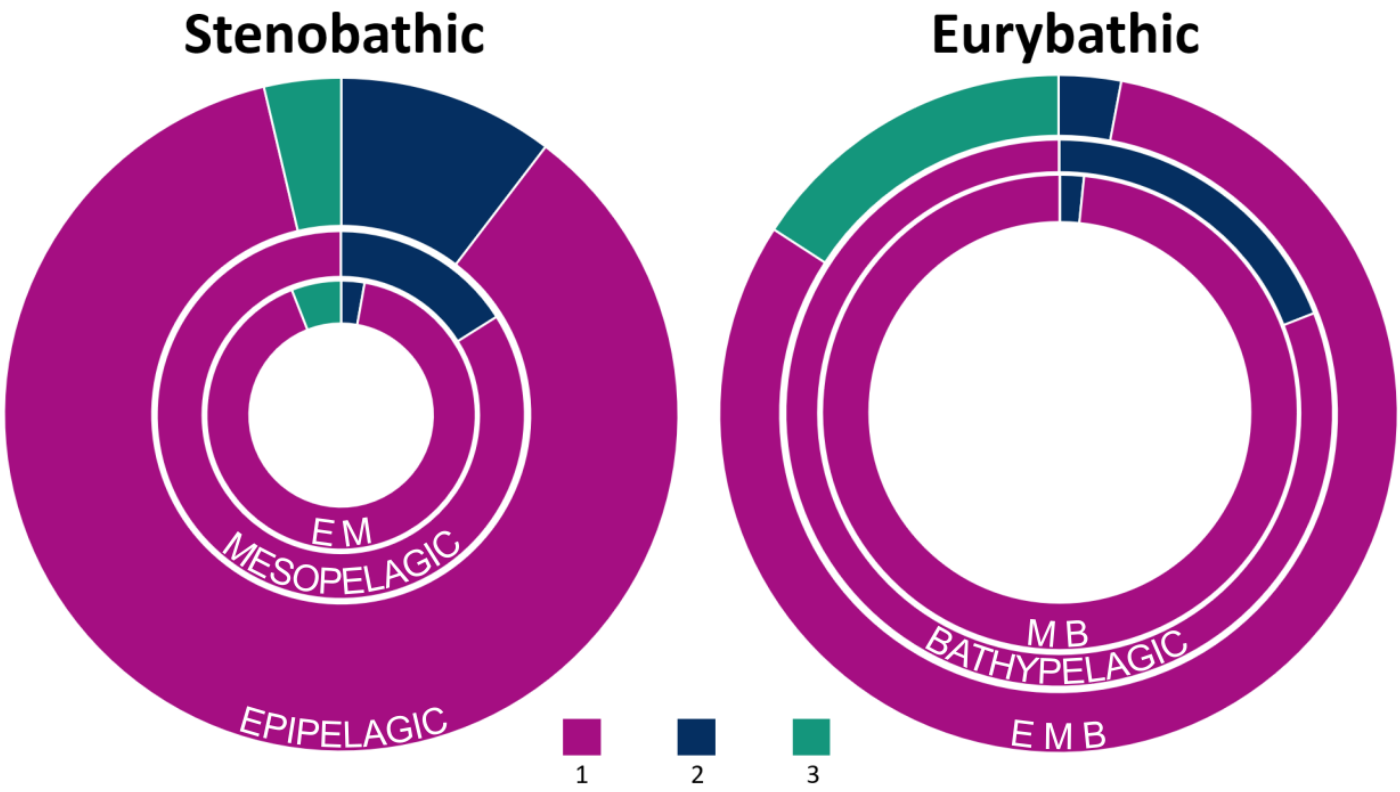

Figure 2: Body size by depth zone. Abundance of each body size category per depth zone is conveyed by ring proportion and the width of each plot represents the total % of chondrichthyans found in that zone 1) Small, size is ≤ .3m, 2) Medium, size is between .3m - 3m, 3) Large, size is from 3m - 30m. Species that belong to Stenobathic are those that fall within: E: Epipelagic [0 - 200m], M: Mesopelagic [200 - 1,000m], and B: Bathypelagic [1,000 – 4,000m]. Those that are Eurybathic fall within EM: Epi-Meso [0 – 1,000m], MB: Meso-Bathy [200 – 4,000m], and EMB: Epi-Meso-Bathy [0 – 4,000m].

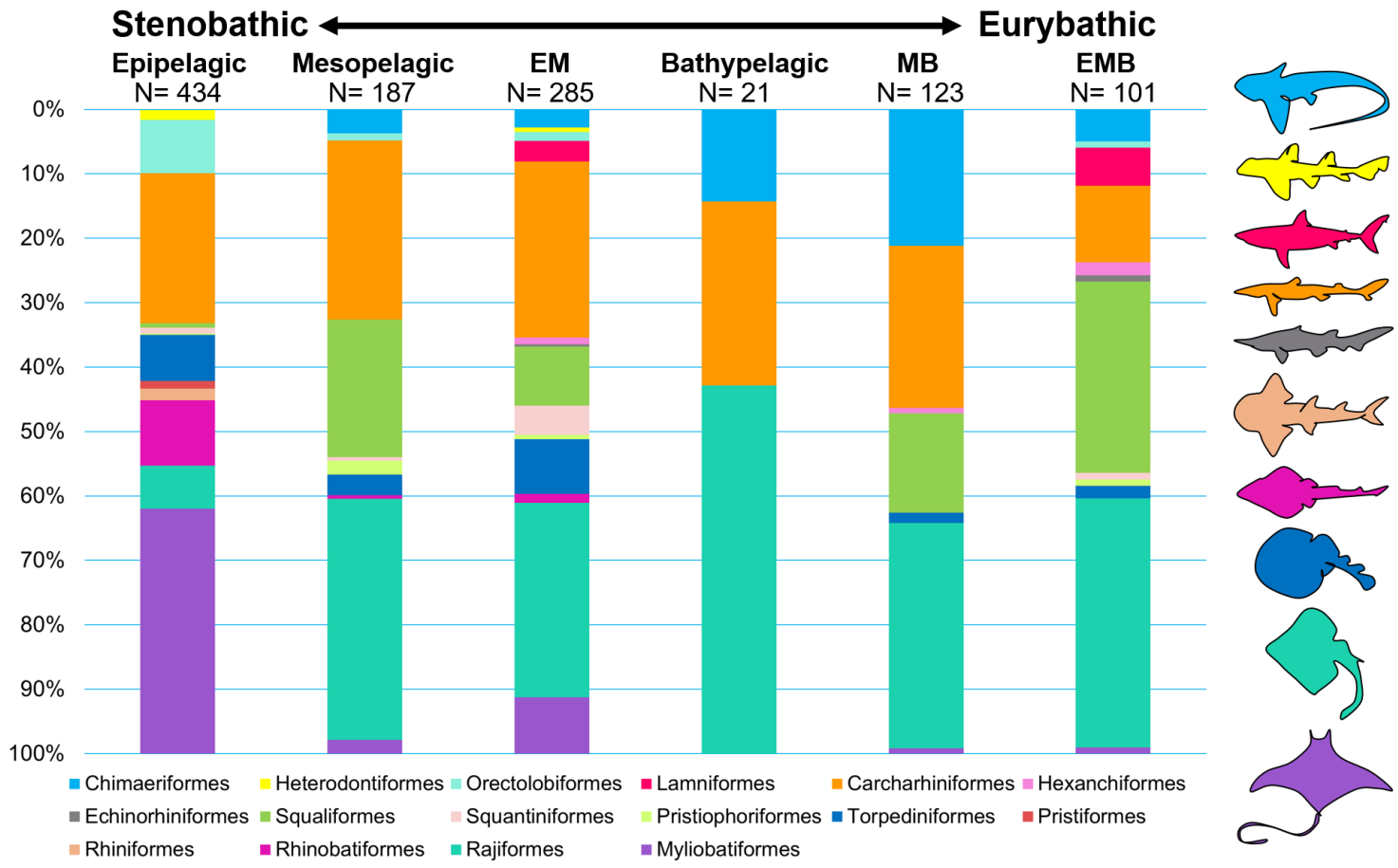

Figure 3: Community structuring throughout the depths. The 16 Orders of Chondrichthyes are shown. Each band represents the Orders found within a depth category; color band length is the percentage of species for a given Order, relating presence of specific taxa to reproductive modes. See online version for color breakdown.

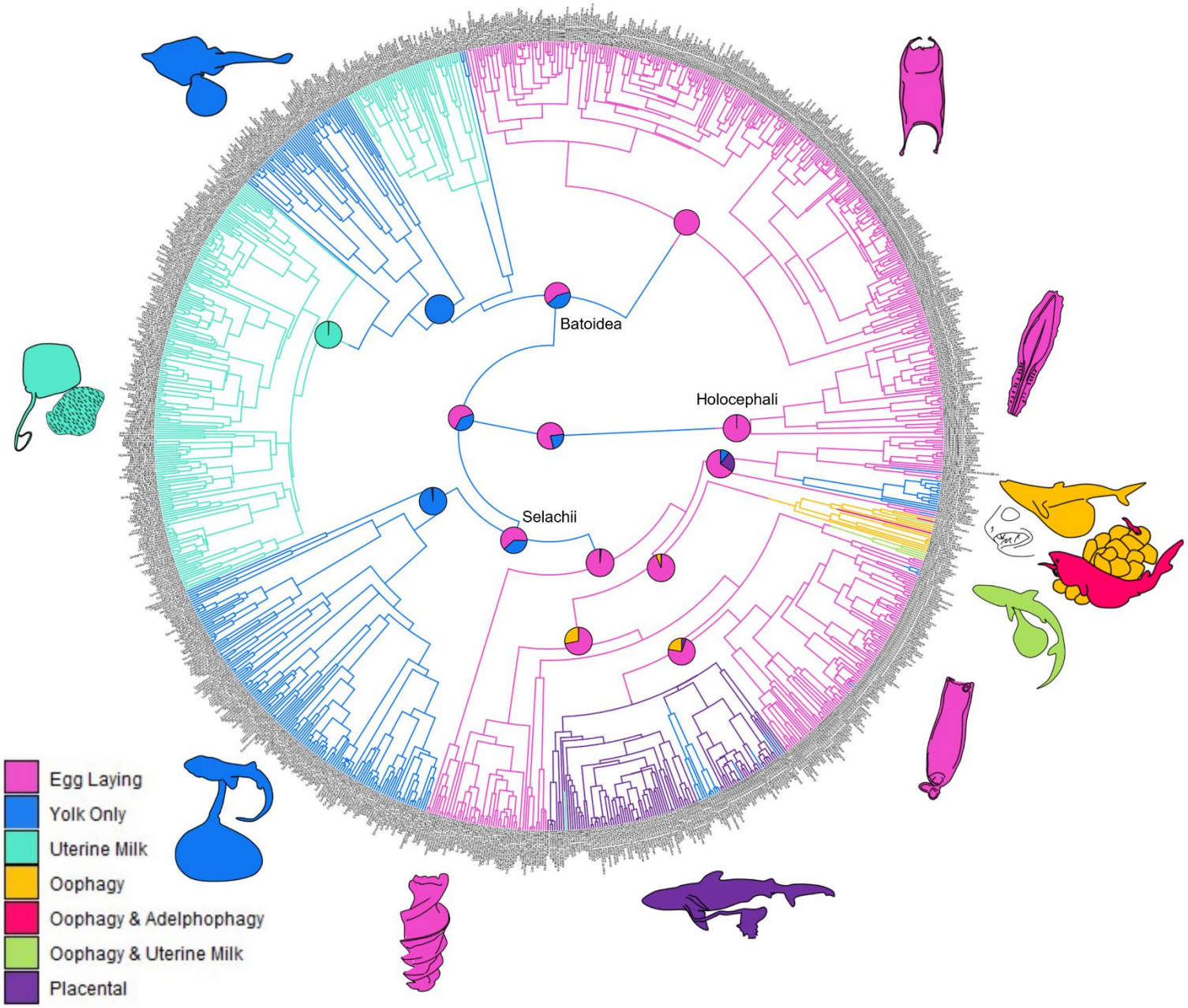

Figure 4: Reproductive phylogeny of modern chondrichthyans. Ancestral state reconstructions of reproductive modes across 1,181 species. 1) Oviparous, 2) Lecithotrophy, 3) Histotrophy, 4) Oophagy, 5) Adelphophagy & Oophagy, 6) Oophagy & Histotrophy, 7) Placental. See online version for color breakdown.

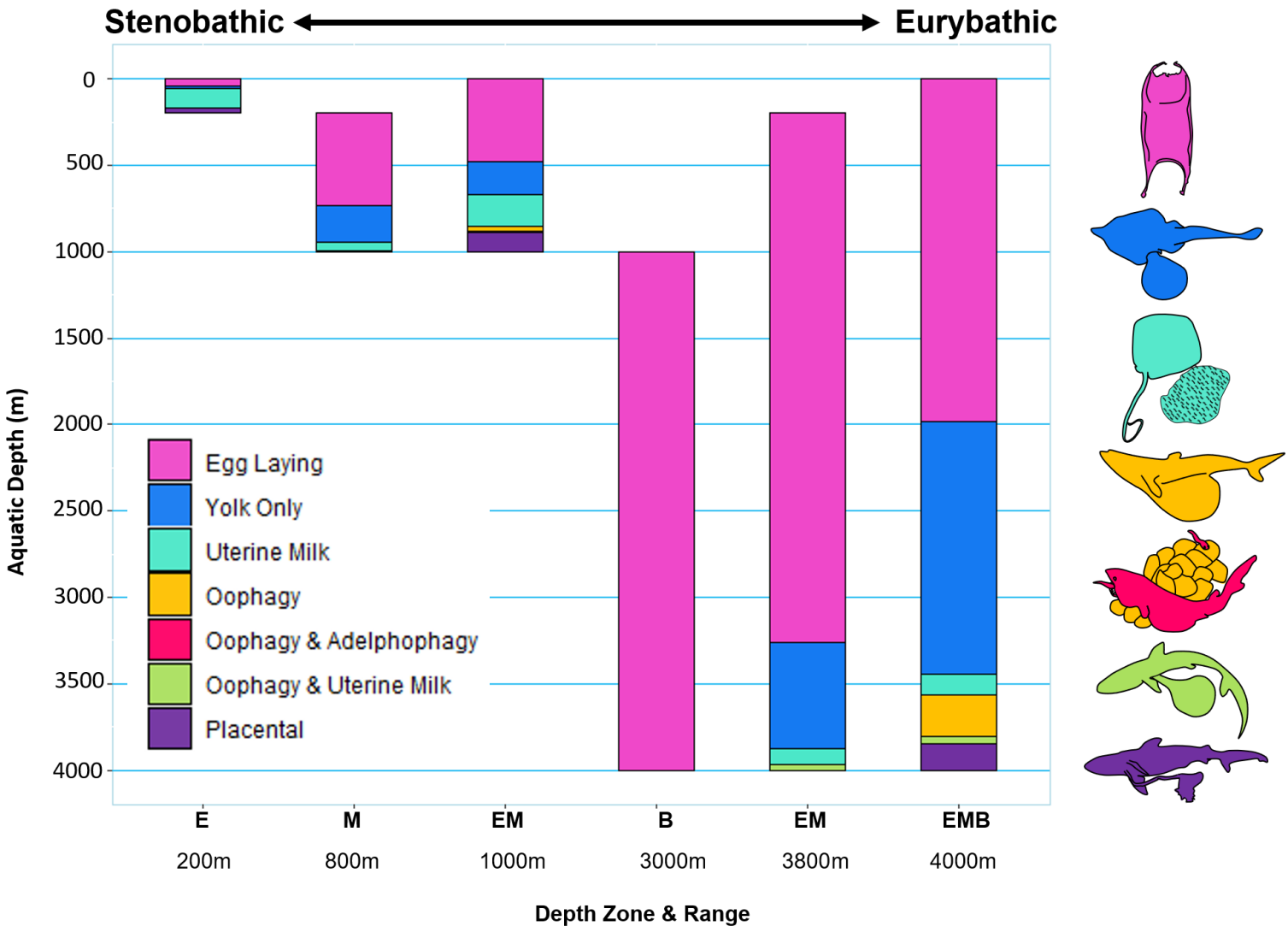

Figure 5: Reproductive mode by depth. Each band represents the reproductive mode(s) found within a depth category; color band length is the percentage of species. Bar length indicates how many meters each depth range is. 1) Oviparous, 2) Lecithotrophy, 3) Histotrophy, 4) Oophagy, 5) Adelphophagy & Oophagy, 6) Oophagy & Histotrophy, 7) Placental. See online version for color breakdown.

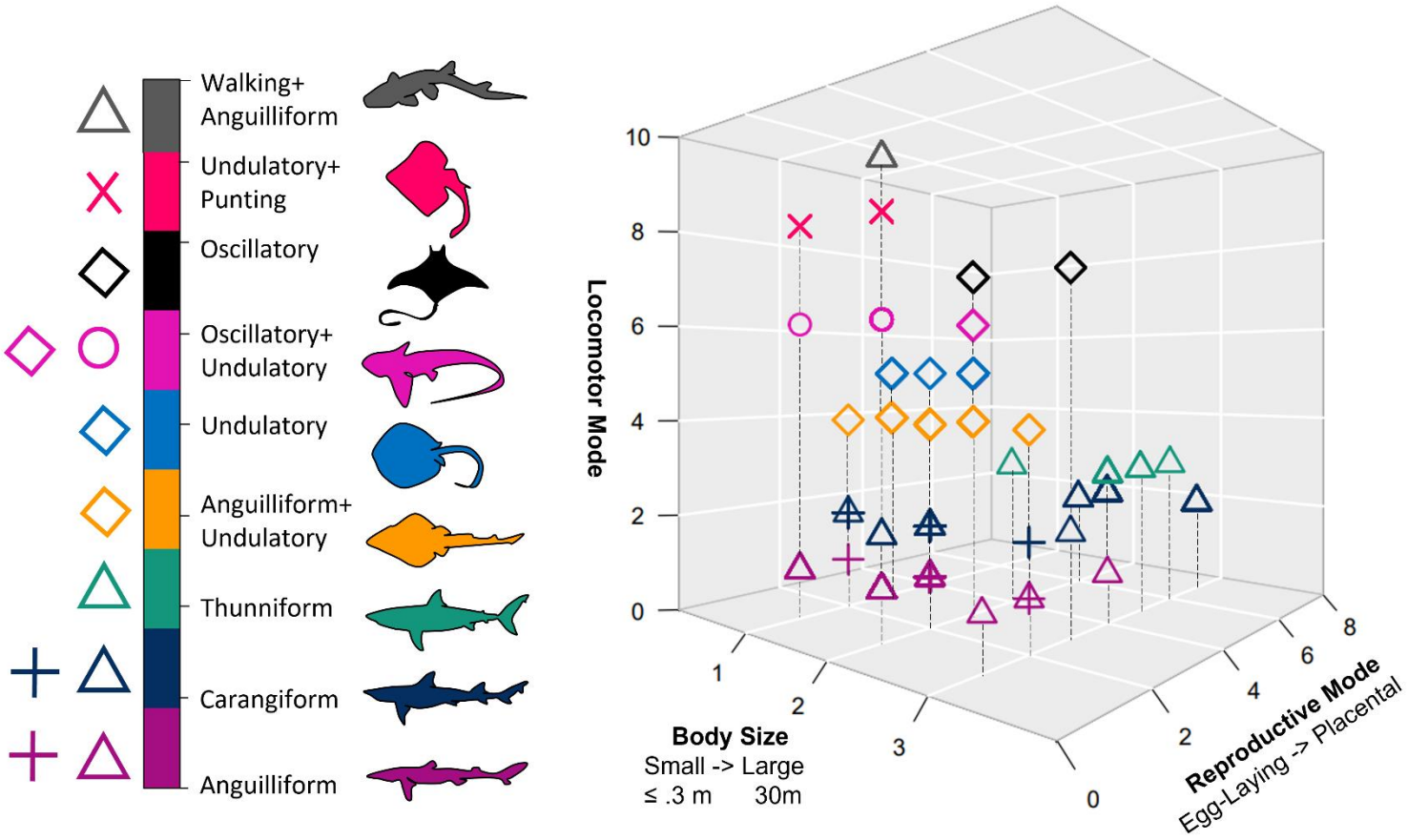

Figure 6: Ecospace of all depth zones. Here were looking at the ecospace of chondrichthyes across all depth zones, the ecospace occupation of 1,149 extant chondrichthyan communities from various aquatic systems around the world. The symbols, on the left-most side of figure, indicate the 5 major classes of Chondrichthyes: Chimaeriformes [○], Galeomorphii [▲], Squalomorphii [┼], Rajiformes [X], and the remaining Batoids [guitarfishes, electric rays, myliobatiformes, ♦]. On the right side we see the Total Ecospace plot, where all depth categories and species traits are represented. The axes of the ecospace are described by Height: Locomotor Mode, Width: Body Size, Depth: Reproductive Mode. The symbols follow the locomotor scale color-code, where each different swimming mode is a new level. Shown by the 3 variable levels of axial swimming, pectoral fin based swimming, pectoral and pelvic fin combination, and the

extreme locomotor mode of the “walking” Epaulette sharks. See online version for color breakdown.

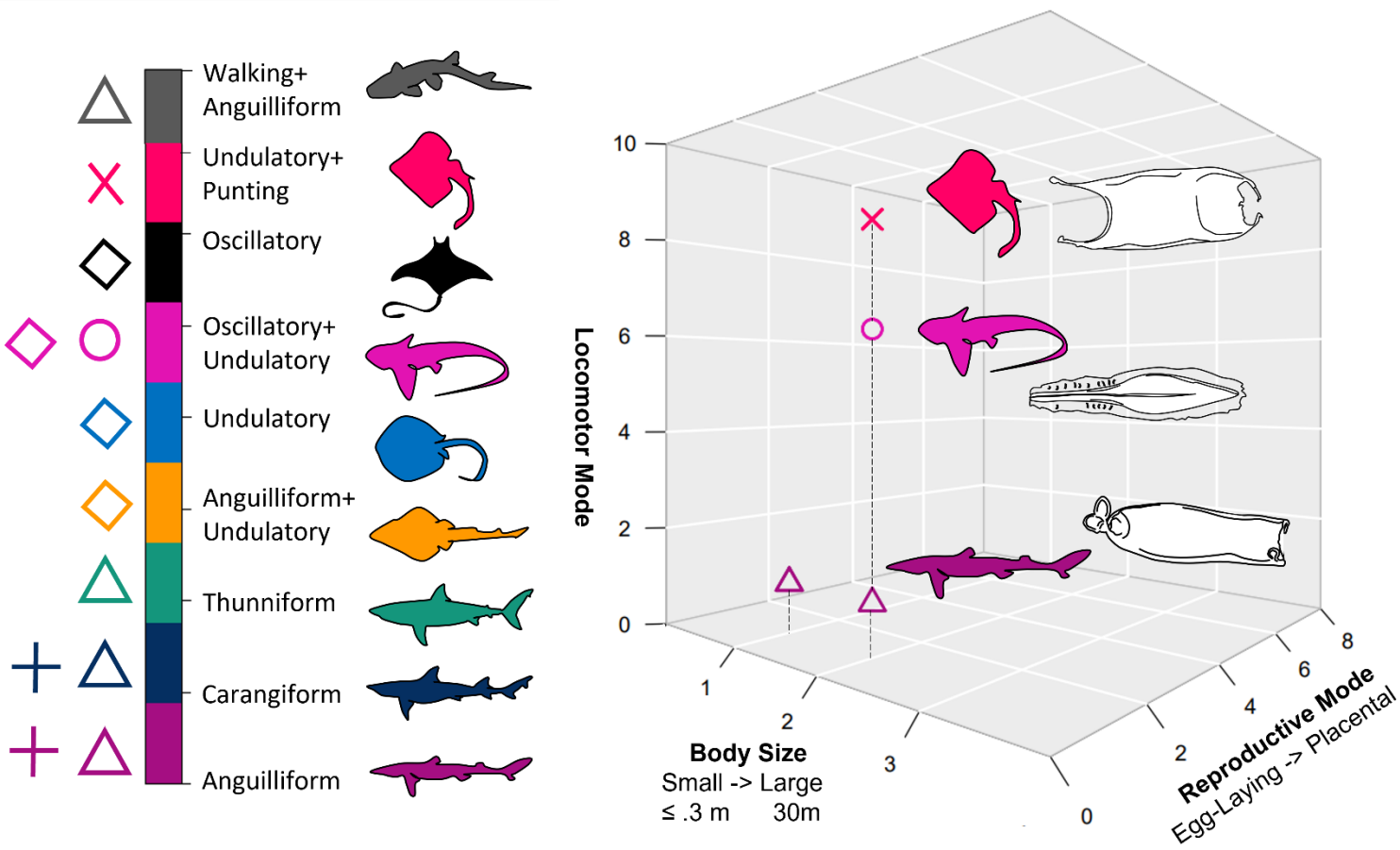

Figure 7: Ecospace of just the Bathypelagic zone **[**1000 – 4000m**]**. This ecospace is represented by 21 species, and 4 character trait combinations. Same information of Fig. 6 axes and symbols applies here.

Supplemental Figures:

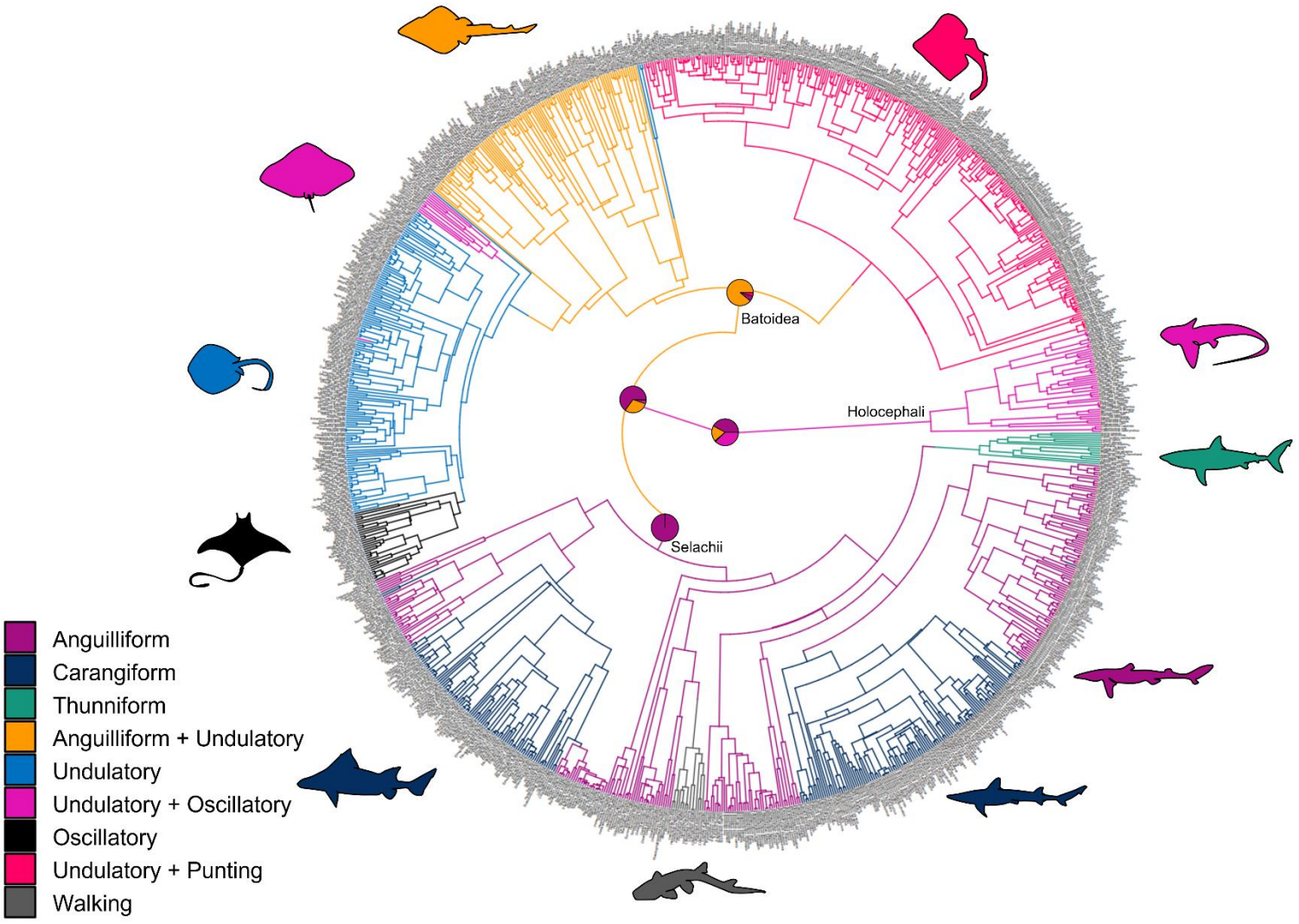

Figure S1: Locomotor phylogeny of modern chondrichthyans. Ancestral state reconstructions of locomotor modes across 1,181 species. 1) Anguilliform, 2) Carangiform, 3) Thunniform, 4) Anguilliform + Undulatory, 5) Undulatory, 6) Oscillatory + Undulatory, 7) Oscillatory, 8) Undulatory + Punting, 9) Walking + Anguilliform.

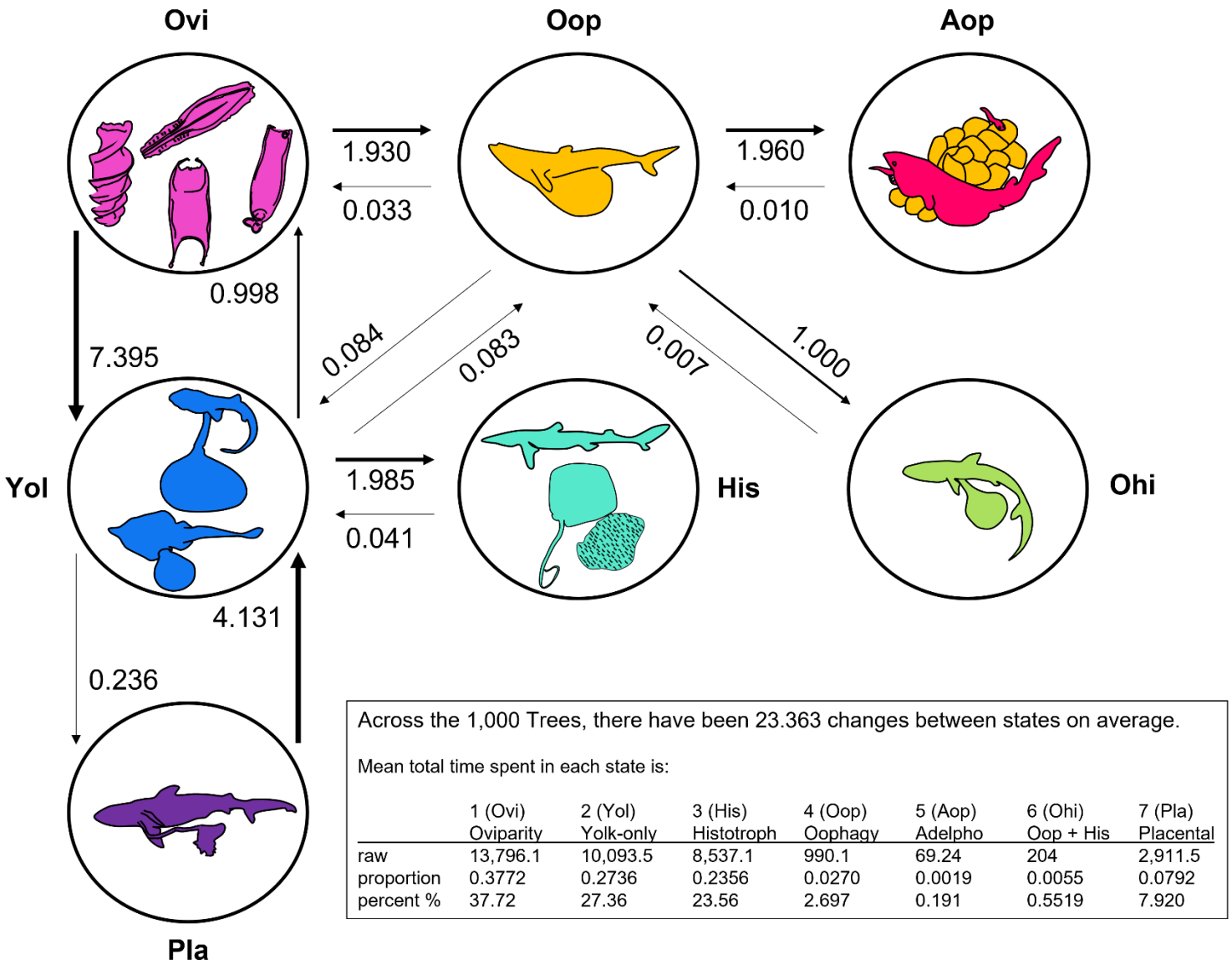

Across the 1,000 Trees, there have been 23.363 changes between states on average.

Mean total time spent in each state is:

	1 (Ovi) Oviparity	2 (Yol) Yolk-only	3 (His) Histotroph	4 (Oop) Oophagy	5 (Aop) Adelpho	6 (Ohi) Oop + His	7 (Pla) Placental
raw	13,796.1	10,093.5	8,537.1	990.1	69.24	204	2,911.5
proportion	0.3772	0.2736	0.2356	0.0270	0.0019	0.0055	0.0792
percent %	37.72	27.36	23.56	2.697	0.191	0.5519	7.920

Figure S2: Ancestral state reconstruction of reproductive modes across 1,000 simulations of chondrichthyan evolution. Oviparity has the highest percentage of time spent in that reproductive mode throughout time and has the most changes between states to yolk-only reproduction, the second biggest state change from egg-laying is then to oophagy (a modified version of yolk-only). The reproductive mode of Yolk-only has the second-highest percentage of time spent throughout chondrichthyan evolution, with only a 10% difference from Oviparity, but as seen in Figure 4 Yolk-only occurred more than expected (~25%) as a reproductive mode at the root node of Chondrichthyes.

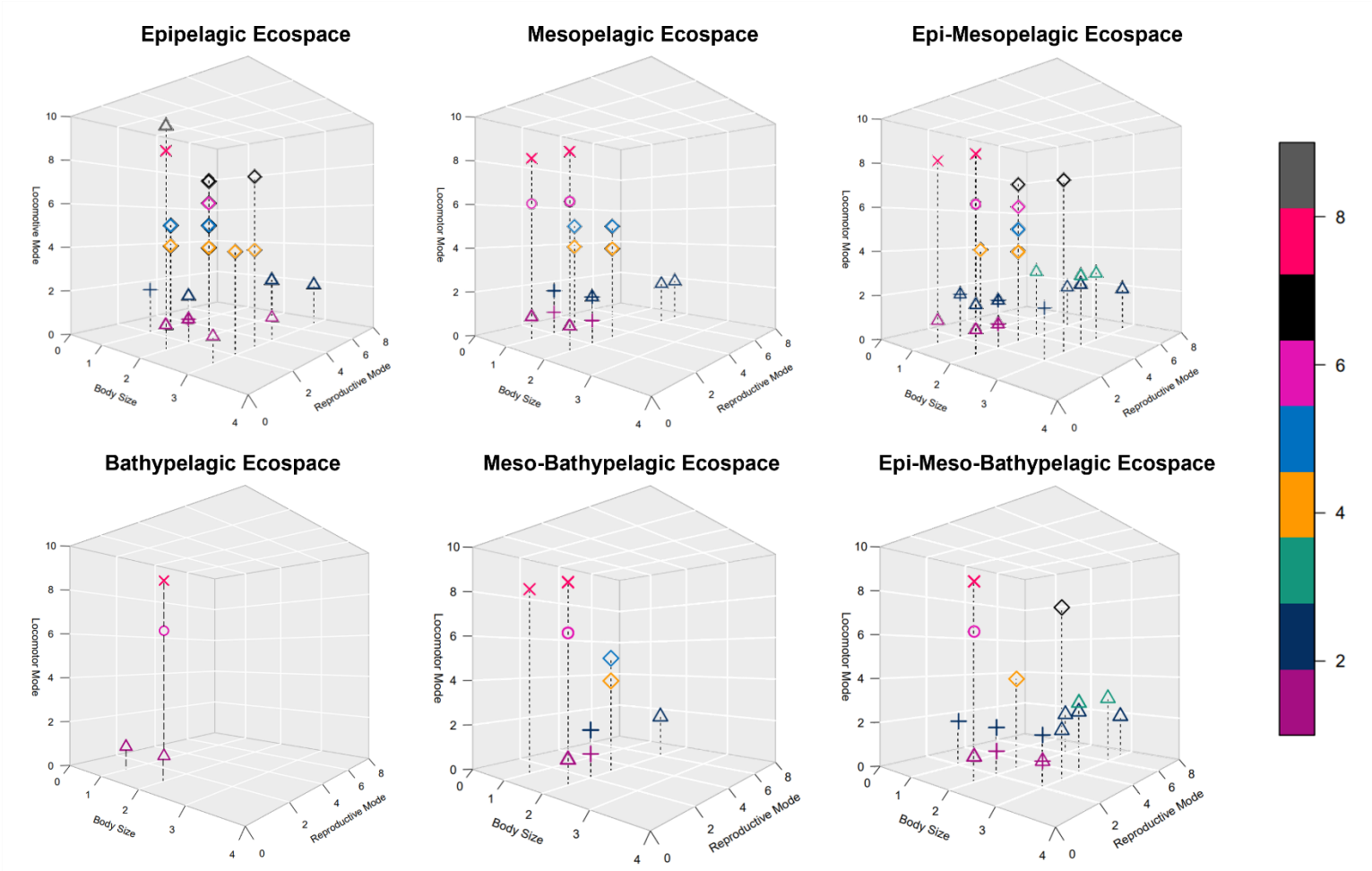

Figure S3: Ecospace of extant species by each depth zone.

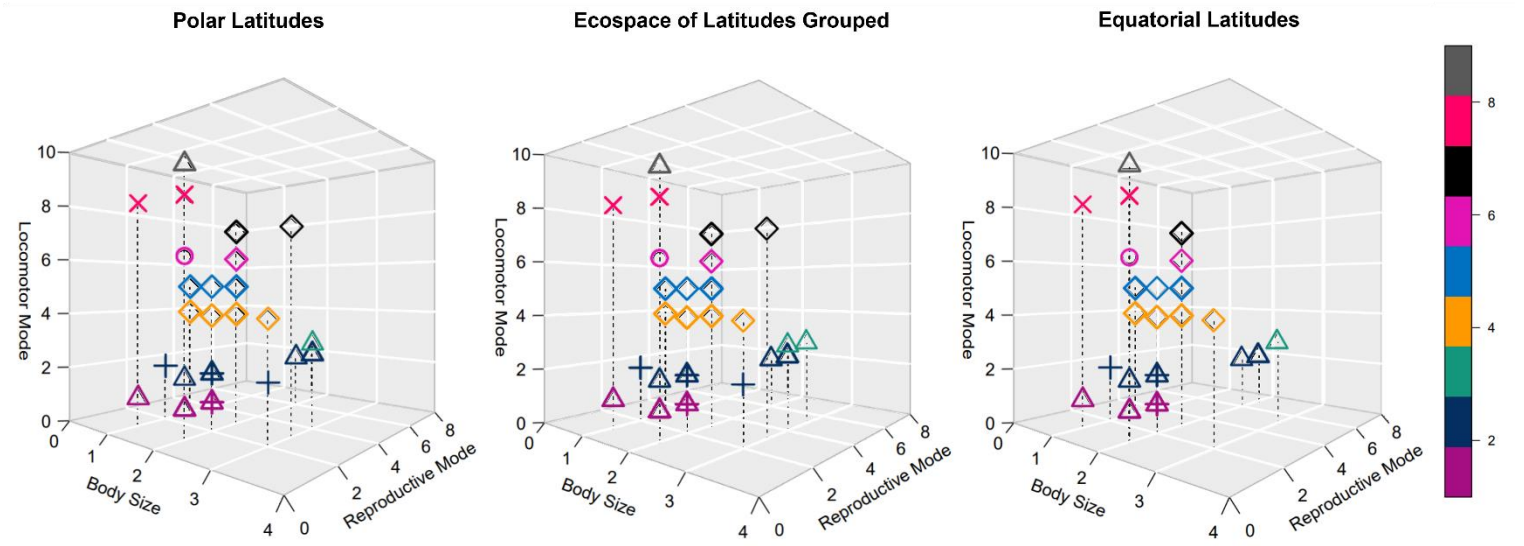

Figure S4: Ecospace of extant species by latitude group.

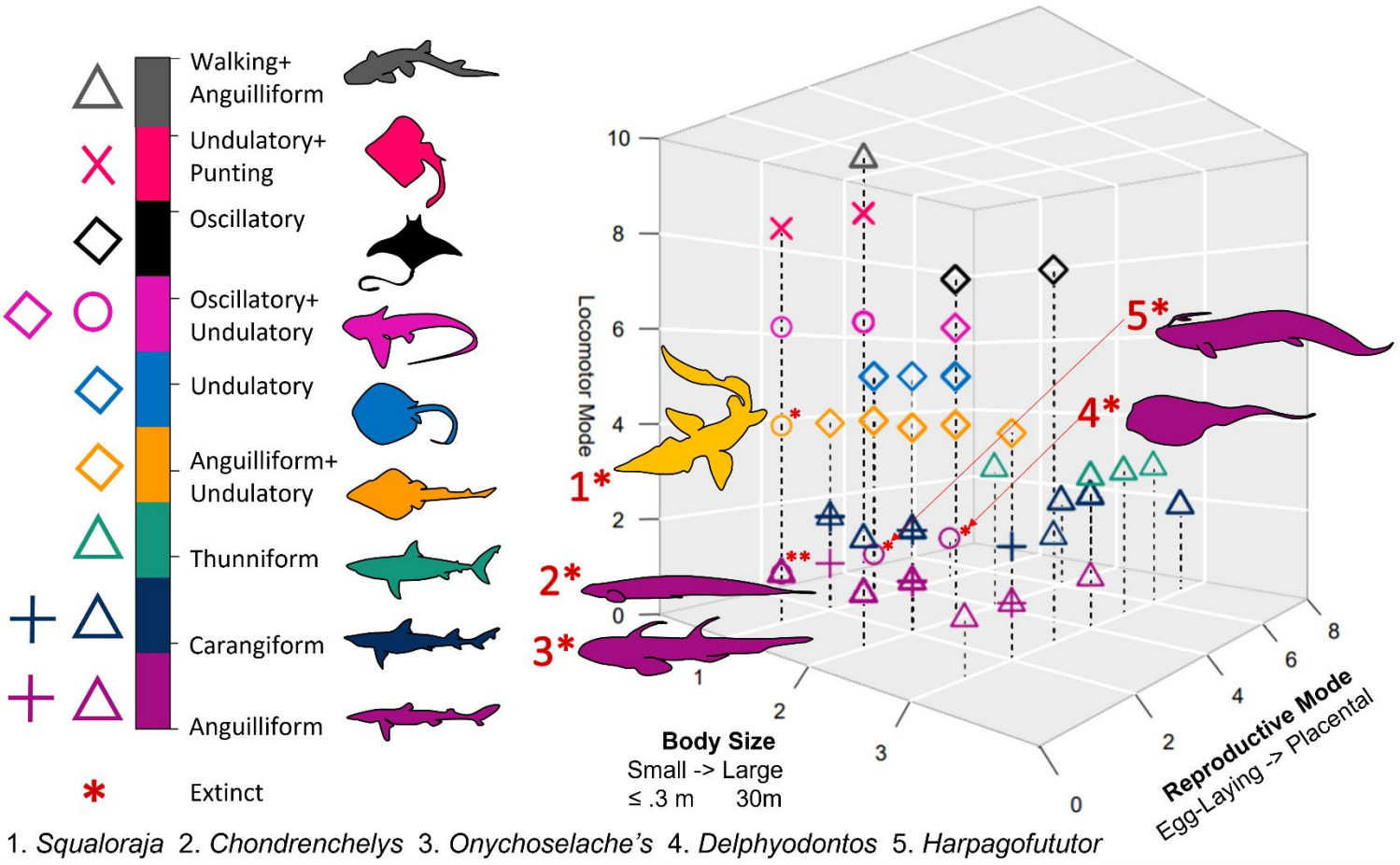

Figure S5: Ecospace of extinct and extant chondrichthyans. Silhouettes featured on the ecospace graph display the species-specific morphology of extinct individuals, based on the literature.

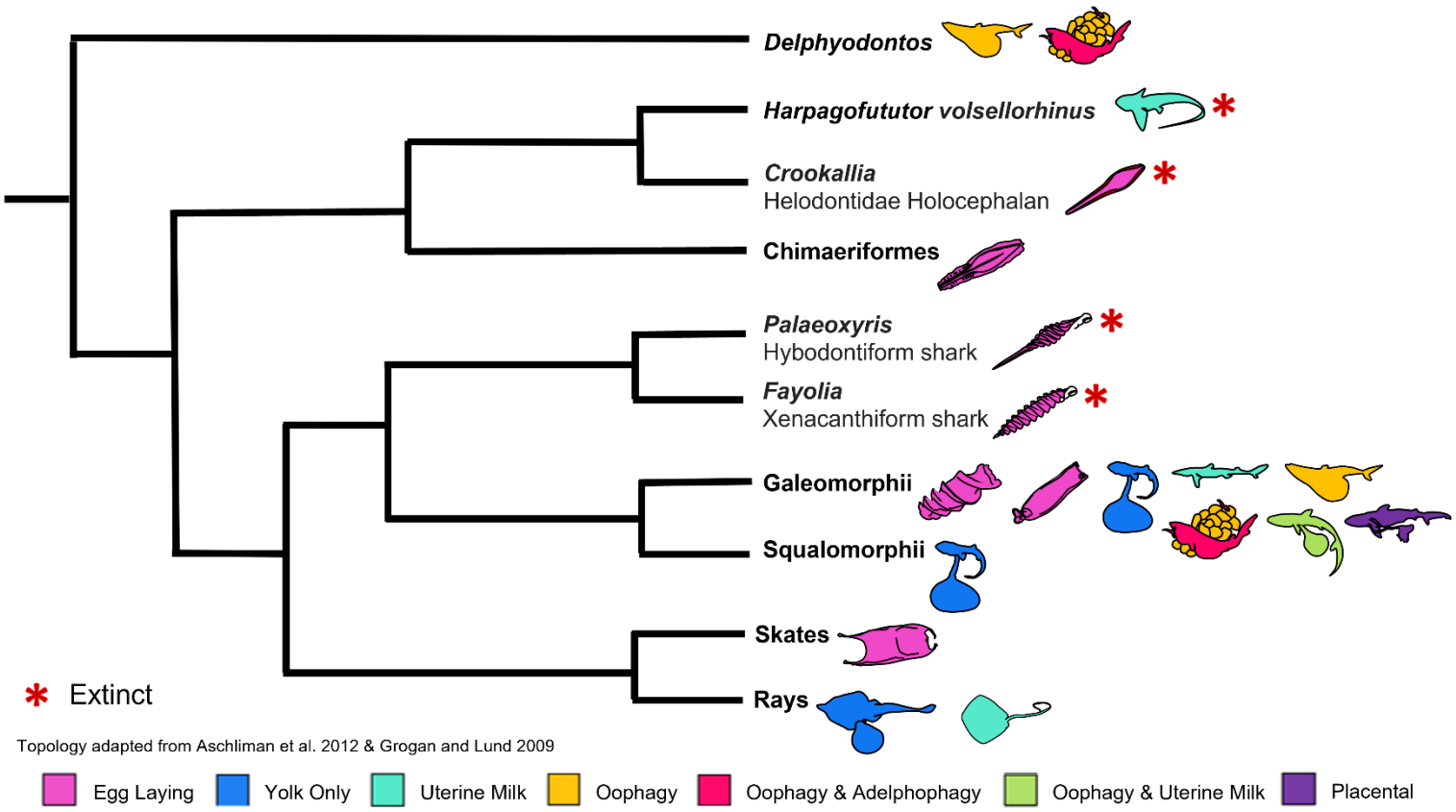

Figure S6: Extinct and Extant representative topology of Chondrichthyes. With character traits of each reproductive mode exhibited next to each group.

References

Allen, G.R., M.V. Erdmann, W.T. White, and C.L. Dudgeon. 2016. Review of the bamboo shark genus *Hemiscyllium* (Orectolobiformes: Hemiscyllidae). Journal of the Ocean Science Foundation, 23, pp.51-97.

Aller, J.Y. 1989. Quantifying sediment disturbance by bottom currents and its effect on benthic communities in a deep-sea western boundary zone. Deep Sea Research Part A. Oceanographic Research Papers, 36(6), pp.901-934.

Aller, J.Y., and Stupakoff, I. 1996. The distribution and seasonal characteristics of benthic communities on the Amazon shelf as indicators of physical processes. Continental Shelf Research, 16 (5-6), pp.717-751.

Ashton, K.G., Tracy, M.C., Queiroz, A.D. 2000. Is Bergmann's rule valid for mammals? The American Naturalist, 156(4), pp.390-415.

Awruch, C.A. 2013. Reproductive endocrinology in chondrichthyans: the present and the future. General and comparative endocrinology, 192, pp.60-70.

Bambach, R.K. 1983. Ecospace utilization and guilds in marine communities through the Phanerozoic. In Biotic interactions in recent and fossil benthic communities (pp. 719-746). Springer, Boston, MA.

Bambach, R.K., Bush, A.M., and Erwin, D.H. 2007. Autecology and the filling of ecospace: key metazoan radiations. Palaeontology, 50(1), pp.1-22.

Belk, M.C., and Houston, D.D. 2002. Bergmann's rule in ectotherms: a test using freshwater fishes. The American Naturalist, 160 (6), pp.803-808.

Bergmann, C. 1847. Uber die verhaltnisse der warmeokonomie der thiere zu ihrer grosse. Göttinger Studien. Pt. 1, pages 595–708.

Beverton, R.J.H., and Holt, S.J. 1959. A review of the lifespans and mortality rates of fish in nature, and their relation to growth and other physiological characteristics. In Ciba

Foundation Symposium-The Lifespan of Animals (Colloquia on Ageing) (Vol. 5, pp. 142-180). Chichester, UK: John Wiley & Sons, Ltd.

Bishop, C.M., Spivey, R.J., Hawkes, L.A., Batbayar, N., Chua, B., Frappell, P.B., Milsom, W.K., Natsagdorj, T., Newman, S.H., Scott, G.R., and Takekawa, J.Y. 2015. The roller coaster flight strategy of bar-headed geese conserves energy during Himalayan migrations. Science, 347(6219), pp.250-254.

Blackburn, T.M., Gaston, K.J., and Loder, N. 1999. Geographic gradients in body size: a clarification of Bergmann's rule. Diversity and distributions, 5(4), pp.165-174.

Bone, Q., and Roberts, B.L. 1969. The density of elasmobranchs. Journal of the Marine Biological Association of the United Kingdom, 49(4), pp.913-937.

Borstein, S.R. 2020. dietr: an R package for calculating fractional trophic levels from quantitative and qualitative diet data. Hydrobiologia, 847(20), pp.4285-4294.

Brazeau, M.D. 2009. The braincase and jaws of a Devonian ‘acanthodian’ and modern gnathostome origins. Nature, 457(7227), pp.305-308.

Burgos-Vázquez, M.I., Mejía-Falla, P.A., Cruz-Escalona, V.H., and Brown-Peterson, N.J. 2017. Reproductive strategy of the giant electric ray in the southern gulf of California. Marine and Coastal Fisheries, 9(1), pp.577-596.

Burrow, C.J., and Murphy, M.A. 2016. Early Devonian (Pragian) vertebrates from the northern Roberts Mountains, Nevada. Journal of Paleontology, 90(4), pp.734-740.

Bush, A.M., Kowalewski, M., Hoffmeister, A.P., Bambach, R.K., and Daley, G.M. 2007. Potential paleoecologic biases from size-filtering of fossils: Strategies for sieving. Palaios, 22(6), pp.612-622.

Carr, R.K., and Jackson, G. 2018. A preliminary note of egg-case oviparity in a Devonian placoderm fish. Acta Geologica Polonica, 68(3).

Castro, J.I. 2013. A primer on shark reproduction for aquarists. Reproduction of marine life, birth of new life, pp.52-69.

Castro, J.I., Bubucis, P.M., and Overstrom, N.A.. 1988. The reproductive biology of the chain dogfish, *Scyliorhinus retifer*. Copeia, pp.740-746.

Chen, M., Strömberg, C.A., and Wilson, G.P. 2019. Assembly of modern mammal community structure driven by Late Cretaceous dental evolution, rise of flowering plants, and dinosaur demise. Proceedings of the National Academy of Sciences, 116(20), pp.9931-9940.

Coates, M.I., and Gess, R.W. 2007. A new reconstruction of *Onychoselache traquairi*, comments on early chondrichthyan pectoral girdles and hybodontiform phylogeny. Palaeontology, 50(6), pp.1421-1446.

Coates, M.I., Gess, R.W., Finarelli, J.A., Criswell, K.E., and Tietjen, K. 2017. A symmoriiform chondrichthyan braincase and the origin of chimaeroid fishes. Nature, 541(7636), pp.208-211.

Coffey, D.M., Royer, M.A., Meyer, C.G., and Holland, K.N. 2020. Diel patterns in swimming behavior of a vertically migrating deepwater shark, the bluntnose sixgill (*Hexanchus griseus*). PLoS ONE 15(1): e0228253.

Cohen, A.A., Martin, L.B., Wingfield, J.C., McWilliams, S.R., and Dunne, J.A. 2012. Physiological regulatory networks: ecological roles and evolutionary constraints. Trends in Ecology & Evolution, 27(8), 428–435.

Collar, D.C., O'Meara, B.C., Wainwright, P.C., and Near, T.J. 2009. Piscivory limits diversification of feeding morphology in centrarchid fishes. Evolution: International Journal of Organic Evolution, 63(6), pp.1557-1573.

Currey, J.D. 2002. Bones. Princeton University Press, Princeton.

Dahm, C. 1996. Okologie und Populationsdynamik antarktischer Ophiuroiden (Echinodermata). Ber Polarforsch, 194, pp.1-289.

Davenport, J., and Kjørsvik, E. 1986. Buoyancy in the lumpsucker *Cyclopterus lumpus*. Journal of the Marine Biological Association of the United Kingdom, 66(1), pp.159-174.

Davis, S.P., Finarelli, J.A., and Coates, M.I. 2012. Acanthodes and shark-like conditions in the last common ancestor of modern gnathostomes. Nature, 486(7402), pp.247-250.

Dean, B. 1895. Fishes, living and fossil: an outline of their forms and probable relationships (Vol. 3). Macmillan and Company.

Dean, M.N., Mull, C.G., Gorb, S.N., and Summers, A.P. 2009. Ontogeny of the tessellated skeleton: insight from the skeletal growth of the round stingray *Urobatis halleri*. Journal of Anatomy, 215(3), pp.227-239.

Deflandre, B., Mucci, A., Gagné, J.P., Guignard, C., and jørn Sundby, B. 2002. Early diagenetic processes in coastal marine sediments disturbed by a catastrophic sedimentation event. Geochimica et Cosmochimica Acta, 66(14), pp.2547-2558.

Denton, E.J., and Marshall, N.B. 1958. The buoyancy of bathypelagic fishes without a gas-filled swimbladder. Journal of the Marine Biological Association of the United Kingdom, 37(3), pp.753-767.

Douglas, R.H., Partridge, J.C., and Hope, A.J. 1995. Visual and lenticular pigments in the eyes of demersal deep-sea fishes. Journal of Comparative Physiology A, 177(1), pp.111-122.

Dulvy, N.K., and Forrest, R.E. 2010. Life histories, population dynamics, and extinction risks in chondrichthyans. In Sharks and their relatives II (pp. 655-696). CRC Press.

Dulvy, N.K., and Reynolds, J.D. 1997. Evolutionary transitions among egg–laying, live–bearing and maternal inputs in sharks and rays. Proceedings of the Royal Society of London. Series B: Biological Sciences, 264(1386), pp.1309-1315.

Dutilloy, A., and Dunn, M.R. 2020. Observations of sperm storage in some deep-sea elasmobranchs. Deep Sea Research Part I: Oceanographic Research Papers, 166, p.103405.

Eastman, J.T., and DeVries, A.L. 1981. Buoyancy adaptations in a swim-bladderless Antarctic fish. Journal of Morphology, 167(1), pp.91-102.

Ebert, D.A., and Davis, C.D. 2007. Descriptions of skate egg cases (Chondrichthyes: Rajiformes: Rajoidei) from the eastern North Pacific. Zootaxa, 1393(1), pp.1-18.

Ebert, D.A., and Winton, M.V. 2010. Chondrichthyans of high latitude seas. In Sharks and their relatives II (pp. 131-174). CRC Press.

Finucci, B., Dunn, M.R., Jones, E.G., and Anderson, J. 2017. Reproductive biology of the two deep-sea chimaerids, longnose spookfish (*Harriotta raleighana*) and Pacific spookfish

(*Rhinochimaera pacifica*). Deep Sea Research Part I: Oceanographic Research Papers, 120, pp.76-87.

Fischer, J., Licht, M., Kriwet, J., Schneider, J.W., Buchwitz, M., and Bartsch, P. 2014. Egg capsule morphology provides new information about the interrelationships of chondrichthyan fishes. Journal of Systematic Palaeontology, 12(3), pp.389-399.

Fisher, J.A., Frank, K.T., and Leggett, W.C. 2010. Global variation in marine fish body size and its role in biodiversity–ecosystem functioning. Marine ecology progress series, 405, pp.1-13.

Fisher, R.A., Call, G.C., and Grubbs, R.D. 2013. Age, growth, and reproductive biology of cownose rays in Chesapeake Bay. Marine and Coastal Fisheries, 5(1), pp.224-235.

Friedman, J.R., Condon, N.E., and Drazen, J.C. 2012. Gill surface area and metabolic enzyme activities of demersal fishes associated with the oxygen minimum zone off California. Limnology and Oceanography, 57(6), pp.1701-1710.

García, V.B., Lucifora, L.O., and Myers, R.A. 2008. The importance of habitat and life history to extinction risk in sharks, skates, rays and chimaeras. Proceedings of the Royal Society B: Biological Sciences, 275(1630), pp.83-89.

Gerringer, M.E., Drazen, J.C., Linley, T.D., Summers, A.P., Jamieson, A.J., and Yancey, P.H. 2017. Distribution, composition and functions of gelatinous tissues in deep-sea fishes. Royal Society open science, 4(12), p.171063.

Giles, S., Friedman, M., and Brazeau, M.D. 2015. Osteichthyan-like cranial conditions in an Early Devonian stem gnathostome. Nature, 520(7545), pp.82-85.

Gilmore, R.G. 1993. Reproductive biology of lamnoid sharks. Environmental Biology of Fishes, 38(1), pp.95-114.

Gilmore, R.G., Dodrill, J., and Unley, P. 1983. Reproduction and embryonic development of the sand tiger shark, *Odontaspis taurus* (Rafinesque). U.S. Fish. Bull. 81: 201-225.

Gilmore, R.G., and Dodrill, J.W. 2005. Oophagy, intrauterine cannibalism and reproductive strategy in lamnoid sharks. Reproductive biology and phylogeny of chondrichthyes: sharks, batoids and chimaeras, 3, pp.435-62.

Gleiss, A.C., Norman, B., and Wilson, R.P. 2011. Moved by that sinking feeling: variable diving geometry underlies movement strategies in whale sharks. Functional Ecology, 25(3), pp.595-607.

Goto, T., Nishida, K., and Nakaya, K. 1999. Internal morphology and function of paired fins in the epaulette shark, *Hemiscyllium ocellatum*. Ichthyological Research, 46(3), pp.281-287.

Grogan, E.D., and Lund, R. 2011. Superfoetative viviparity in a Carboniferous chondrichthyan and reproduction in early gnathostomes. Zoological Journal of the Linnean Society, 161(3), pp.587-594.

Haedrich, R.L. 1996. Deep-water fishes: evolution and adaptation in the earth's largest living spaces. Journal of Fish Biology, 49, pp.40-53.

Hawkes, L.A., Balachandran, S., Batbayar, N., Butler, P.J., Frappell, P.B., Milsom, W.K., Tseveenmyadag, N., Newman, S.H., Scott, G.R., Sathiyaselvam, P., and Takekawa, J.Y. 2011. The trans-Himalayan flights of bar-headed geese (*Anser indicus*). Proceedings of the National Academy of Sciences, 108(23), pp.9516-9519.

Hendges, C.D., Patterson, B.D., and Cáceres, N.C. 2021. Big in the tropics: Ecogeographical clines in peccary size reveal the converse of Bergmann's rule. Journal of Biogeography, 48(5), pp.1228-1239.

Hildrew, A.G., Raffaelli, D.G., and Edmonds-Brown, R. 2007. Body size: the structure and function of aquatic ecosystems. Cambridge University Press.

Hoff, G.R. 2008. A nursery site of the Alaska skate (*Bathyraja parmifera*) in the eastern Bering Sea. Fishery Bulletin, 106(3), pp.233-244.

Holt, W.V., and Lloyd, R.E. 2010. Sperm storage in the vertebrate female reproductive tract: how does it work so well?. Theriogenology, 73(6), pp.713-722.

Hughes, G.M., and Iwai, T. 1978. A morphometric study of the gills in some Pacific deep-sea fishes. Journal of Zoology, 184(2), pp.155-170.

IHO (1953). Report of the International Hydrographic Organization. Working Paper No. 57. 20th Session of the United Nations Group of Experts on Geographical Names, New York, 17–28 January 2000.

Johanson, Z., and Trinajstic, K. 2014. Fossilized ontogenies: the contribution of placoderm ontogeny to our understanding of the evolution of early gnathostomes. Palaeontology, 57(3), pp.505-516.

Johanson, Z., Manzanares, E., Underwood, C., Clark, B., Fernandez, V., and Smith, M. 2020. Evolution of the dentition in holocephalans (Chondrichthyes) through tissue disparity. Integrative and Comparative Biology, 60(3), pp.630-643.

Johnson, D.S., Crowley, C., Longmire, K., Nelson, J., Williams, B., and Wittyngham, S. 2019. The fiddler crab, *Minuca pugnax,* follows Bergmann's rule. Ecology and evolution, 9(24), pp.14489-14497.

Koester, D.M., and Spirito, C.P. 2003. Punting: an unusual mode of locomotion in the little skate, *Leucoraja erinacea* (Chondrichthyes: Rajidae). Copeia, 2003(3), pp.553-561.

Kriwet, J., Kiessling, W., and Klug, S. 2009. Diversification trajectories and evolutionary life-history traits in early sharks and batoids. Proceedings of the Royal Society B: Biological Sciences, 276(1658), pp.945-951.

Kyne, P.M., and Bennett, M.B. 2002. Reproductive biology of the eastern shovelnose ray, *Aptychotrema rostrata* (Shaw & Nodder, 1794), from Moreton Bay, Queensland, Australia. Marine and Freshwater Research, 53(2), pp.583-589.

Last, P., Naylor, G., Séret, B., White, W., de Carvalho, M., and Stehmann, M. 2016. Rays of the World. CSIRO publishing

Lawton, J.H. 1990. Species richness and population dynamics of animal assemblages. Patterns in body size: abundance space. Philosophical Transactions of the Royal Society of London. Series B: Biological Sciences, 330(1257), pp.283-291.

Lessa, R.P. 1982. Biologie et dynamique des populations de *Rhinobatos horkelii* (Muller and Henle, 1841) du Plateau continental due Rio Grande so Sul (Brésil). Ph. D. diss. Oceanography, Univ. Bretagne Occidentale.

Long, J., Trinajstic, K., Young, G.C., and Senden, T. 2008. Live birth in the Devonian period. Nature, 453, 650–652.

Long, J.A., Trinajstic, K., and Johanson, Z. 2009. Devonian arthrodire embryos and the origin of internal fertilization in vertebrates. Nature, 457(7233), pp.1124-1127.

Long, J.A., Burrow, C.J., Ginter, M., Maisey, J.G., Trinajstic, K.M., Coates, M.I., Young, G.C., and Senden, T.J. 2015. First shark from the Late Devonian (Frasnian) Gogo Formation, Western Australia sheds new light on the development of tessellated calcified cartilage. PLoS One, 10(5), p.e0126066.

López-Romero, F.A., Klimpfinger, C., Tanaka, S., and Kriwet, J. 2020. Growth trajectories of prenatal embryos of the deep-sea shark *Chlamydoselachus anguineus* (Chondrichthyes). Journal of fish biology, 97(1), pp.212-224.

Lund, R. 1980. Viviparity and intrauterine feeding in a new holocephalan fish from the Lower Carboniferous of Montana. Science, 209(4457), pp.697-699.

Lund, R. 1982. *Harpagofututor volsellorhinus* new genus and species (Chondrichthyes, Chondrenchelyiformes) from the Namurian Bear Gulch Limestone, *Chondrenchelys problematica* Traquair (Visean), and their sexual dimorphism. Journal of Paleontology, pp.938-958.

Maia, A.M., Wilga, C.A., and Lauder, G.V. 2012. Biomechanics of Locomotion in Sharks, Rays, and Chimaeras. Biology of Sharks and Their Relatives, p.125.

Maisey, J.G. 1984. Chondrichthyan phylogeny: a look at the evidence. Journal of Vertebrate Paleontology, 4(3), pp.359-371.

Maisey, J.G., Miller, R., Pradel, A., Denton, J.S., Bronson, A., and Janvier, P. 2017. Pectoral morphology in *Doliodus*: bridging the 'acanthodian'-chondrichthyan divide. American Museum Novitates, 2017(3875), pp.1-15.

Marie, A.D., Herbinger, C., Fullsack, P., and Rico, C. 2019. First reconstruction of kinship in a scalloped hammerhead shark aggregation reveals the mating patterns and breeding sex ratio. Frontiers in Marine Science, 6, p.676.

Marshall, N.B. 1954. Aspects of deep-sea biology. Philosophical Library.

McClain, C.R., Boyer, A.G., and Rosenberg, G. 2006. The island rule and the evolution of body size in the deep sea. Journal of Biogeography, 33(9), pp.1578-1584.

McEachran, J.D., and Aschliman, N. 2004. Phylogeny of batoidea. Biology of sharks and their relatives, (Boca Raton (FL), pp.79-113.

McKinney, M.L., and McNamara, K.J. 1990. Trends in body-size evolution. Evolutionary trends, pp.75-118.

McMahon, B.K., and Bonner, J.T.. 1983 On size and life. Freeman, New York.

Morris, J.A. 1999. Aspects of the reproductive biology of the Bluntnose stingray, *Dasyatis say*, in the Indian River lagoon system. University of Central Florida, Orlando, Florida.

Mottequin, B., Goolaerts, S., Hunt, A.P., and Olive, S. 2021. The erroneous chondrichthyan egg case assignments from the Devonian: implications for the knowledge on the evolution of the reproductive strategy within chondrichthyans. The Science of Nature, 108(5), pp.1-16.

Moura, T., Serra-Pereira, B., Gordo, L.S., and Figueiredo, I. 2011. Sperm storage in males and females of the deepwater shark Portuguese dogfish with notes on oviducal gland microscopic organization. Journal of Zoology, 283(3), pp.210-219.

Mourier, J., and Planes, S. 2013. Direct genetic evidence for reproductive philopatry and associated fine-scale migrations in female blacktip reef sharks (*Carcharhinus melanopterus*) in French Polynesia. Molecular Ecology, 22(1), pp.201-214.

Musick, J.A., Ellis, J.K., and Hamlett, W.C. 2005. Reproductive evolution of chondrichthyans. *Hamlett, WC, Reproductive biology and phylogeny of Chondrichthyes, sharks, batoids and chimaeras, pp.45-71.*

Musilova, Z., Cortesi, F., Matschiner, M., Davies, W.I., Patel, J.S., Stieb, S.M., de Busserolles, F., Malmstrøm, M., Tørresen, O.K., Brown, C.J., and Mountford, J.K. 2019. Vision using multiple distinct rod opsins in deep-sea fishes. Science, 364(6440), pp.588-592.

Olive, S., Clément, G., Daeschler, E.B., and Dupret, V. 2016. Placoderm assemblage from the tetrapod-bearing locality of Strud (Belgium, Upper Famennian) provides evidence for a fish nursery. Plos One, 11(8), p.e0161540.

Patterson, C. 1965. The phylogeny of the chimaeroids. Philosophical Transactions of the Royal Society of London, Series B, 249, 101–219.

Pauly, D. 1998. Tropical fishes: patterns and propensities. Journal of fish Biology, 53, pp.1-17.

Peters, R.H., and Wassenberg, K. 1983. The effect of body size on animal abundance. Oecologia, 60(1), pp.89-96.

Pridmore, P.A. 1994. Submerged walking in the epaulette shark *Hemiscyllium ocellatum* (Hemiscyllidae) and its implications for locomotion in rhipidistian fishes and early tetrapods. Zool. Anal. Complex Syst. 98, 278–297

Priede, I.G., Froese, R., Bailey, D.M., Bergstad, O.A., Collins, M.A., Dyb, J.E., Henriques, C., Jones, E.G., and King, N. 2006. The absence of sharks from abyssal regions of the world's oceans. Proceedings of the Royal Society B: Biological Sciences, 273(1592), pp.1435-1441.

Priede, I.G., Burgass, R.W., Mandalakis, M., Spyros, A., Gikas, P., Burns, F., and Drewery, J. 2020. Near-equal compressibility of liver oil and seawater minimizes buoyancy changes in deep-sea sharks and chimaeras. Journal of Experimental Biology, 223(9), p.jeb222943.

Qiao, T., King, B., Long, J.A., Ahlberg, P.E., and Zhu, M. 2016. Early gnathostome phylogeny revisited: multiple method consensus. PloS one, 11(9), p.e0163157.

R Core Team. 2021. R: A language and environment for statistical computing. R Foundation for Statistical Computing, Vienna, Austria. URL https://www.R-project.org/.

Ray, C. 1960. The application of Bergmann's and Allen's rules to poikilotherms. Journal of Morphology 106: 85–108.

Rigby, C., and Simpfendorfer, C.A. 2015. Patterns in life history traits of deep-water chondrichthyans. Deep Sea Research Part II: Topical Studies in Oceanography, 115, pp.30-40.

Rocha, F., and Gadig, O.B.F. 2013. Reproductive biology of the guitarfish *Rhinobatos percellens* (Chondrichthyes, Rhinobatidae) from the São Paulo Coast, Brazil, western South Atlantic Ocean. Journal of fish biology, 82(1), pp.306-317.

Roff, D. 1994. The evolution of life histories. Journal of Evolutionary Biology, 7(1), pp.116-118.

Rosa, R., Gonzalez, L., Dierssen, H.M., and Seibel, B.A. 2012. Environmental determinants of latitudinal size-trends in cephalopods. Marine Ecology Progress Series, 464, pp.153-165.

Rosenberger, L.J. 2001. Pectoral fin locomotion in batoid fishes: undulation versus oscillation. Journal of Experimental Biology, 204(2), pp.379-394.

RStudio Team. 2021. RStudio: Integrated Development for R. RStudio, PBC, Boston, MA URL http://www.rstudio.com/.

Salinas-de-León, P., Phillips, B., Ebert, D., Shivji, M., Cerutti-Pereyra, F., Ruck, C., Fisher, C.R., and Marsh, L. 2018. Deep-sea hydrothermal vents as natural egg-case incubators at the Galapagos Rift. Scientific reports, 8(1), pp.1-7.

Scott, G.R., Hawkes, L.A., Frappell, P.B., Butler, P.J., Bishop, C.M., and Milsom, W.K. 2015. How bar-headed geese fly over the Himalayas. Physiology, 30(2), pp.107-115.

Simpfendorfer, C.A. 1992. Reproductive strategy of the Australian sharpnose shark, *Rhizoprionodon taylori* (Elasmobranchii: Carcharhinidae), from Cleveland Bay, northern Queensland. Marine and Freshwater Research, 43(1), pp.67-75.

Simpfendorfer, C.A., and Kyne, P.M. 2009. Limited potential to recover from overfishing raises concerns for deep-sea sharks, rays and chimaeras. Environmental Conservation, 36(2), pp.97-103.

Sims, D.W., Southall, E.J., Richardson, A.J., Reid, P.C., and Metcalfe, J.D. 2003. Seasonal movements and behaviour of basking sharks from archival tagging: no evidence of winter hibernation. Marine Ecology Progress Series, 248, pp.187-196.

Siverson, M., and Cappetta, H.. 2001. A skate in the lowermost Maastrichtian of southern Sweden. Palaeontology, 44(3), pp.431-445.

Soler-Gijón, R., and Moratalla, J.J. 2001. Fish and tetrapod trace fossils from the Upper Carboniferous of Puertollano, Spain. Palaeogeography, Palaeoclimatology, Palaeoecology, 171(1-2), pp.1-28.

Stein, R.W., Mull, C.G., Kuhn, T.S., Aschliman, N.C., Davidson, L.N., Joy, J.B., Smith, G.J., Dulvy, N.K., and Mooers, A.O. 2018. Global priorities for conserving the evolutionary history of sharks, rays and chimaeras. Nature ecology & evolution, 2(2), pp.288-298.

Stockwell, R.A. 2012. Metabolism of cartilage. Cartilage, 1, pp.253-73.

Storrie, M.T., Walker, T.I., Laurenson, L.J., and Hamlett, W.C. 2008. Microscopic organization of the sperm storage tubules in the oviducal gland of the female gummy shark (*Mustelus antarcticus*), with observations on sperm distribution and storage. Journal of Morphology, 269(11), pp.1308-1324.

Tanaka, S., Shiobara, Y., Hioki, S., Abe, H., Nishi, G., Yano, K., and Suzuki, K. 1990. The reproductive biology of the frilled shark, *Chlamydoselachus anguineus*, from Suruga Bay, Japan. Japanese Journal of Ichthyology, 37(3), pp.273-291.

Thistle, D., Yingst, J.Y., and Fauchald, K.. 1985. A deep-sea benthic community exposed to strong near-bottom currents on the Scotian Rise (western Atlantic). Marine Geology, 66(1-4), pp.91-112.

Tont, S.A., Pearcy, W.G., and Arnold, J.S. 1977. Bone structure of some marine vertebrates. Marine biology, 39(2), pp.191-196.

Travis, K.G. 2020. Comparative Biomechanics of Submerged and Partially Emerged Walking in the Epaulette Shark. Thesis; California State University, Long Beach.

Treberg, J.R., and Speers-Roesch, B. 2016. Does the physiology of chondrichthyan fishes constrain their distribution in the deep sea? Journal of Experimental Biology, 219(5), pp.615-625.

Tyminski, J.P., de la Parra-Venegas, R., González Cano, J., and Hueter, R.E. 2015. Vertical movements and patterns in diving behavior of whale sharks as revealed by pop-up satellite tags in the eastern Gulf of Mexico. PloS one, 10(11), p.e0142156.

Vedor, M., Mucientes, G., Hernández-Chan, S., Rosa, R., Humphries, N., Sims, D.W., and Queiroz, N. 2021. Oceanic diel vertical movement patterns of blue sharks vary with water temperature and productivity to change vulnerability to fishing. Frontiers in Marine Science, p.891.

Waltrick, D., Awruch, C., and Simpfendorfer, C. 2012. Embryonic diapause in the elasmobranchs. Reviews in Fish Biology and Fisheries, 22(4), pp.849-859.

Warrant, E.J., and Locket, N.A. 2004. Vision in the deep sea. Biological Reviews, 79(3), pp.671-712.

Watson, D.M.S. 1937. II-The Acanthodian fishes. Philosophical Transactions of the Royal Society of London. Series B, Biological Sciences, 228(549), pp.49-146.

Webb, P.W. 1994. The biology of fish swimming. Mechanics and physiology of animal swimming, 4562.

Weigmann, S. 2016. Annotated checklist of the living sharks, batoids and chimaeras (Chondrichthyes) of the world, with a focus on biogeographical diversity. Journal of Fish Biology, 88(3), pp.837-1037.

West, G.B., Brown, J.H., and Enquist, B.J. 1997. A general model for the origin of allometric scaling laws in biology. Science, 276(5309), pp.122-126.

Woodward, A.S. 1891. Catalogue of the fossil fishes in the British Museum (Natural History). Part II. London, British Museum (Natural History): xliv and 567p.

Wootton, T.P., Sepulveda, C.A., and Wegner, N.C. 2015. Gill morphometrics of the thresher sharks (genus *Alopias*): Correlation of gill dimensions with aerobic demand and environmental oxygen. Journal of morphology, 276(5), pp.589-600.

Wourms, J.P. 1977. Reproduction and development in chondrichthyan fishes. American Zoologist, 17(2), pp.379-410.

Zhu, M., Yu, X., Ahlberg, P.E., Choo, B., Lu, J., Qiao, T., Qu, Q., Zhao, W., Jia, L., Blom, H., and Zhu, Y.A. 2013. A Silurian placoderm with osteichthyan-like marginal jaw bones. Nature, 502(7470), pp.188-193.

Zhu, M., Ahlberg, P.E., Pan, Z., Zhu, Y., Qiao, T., Zhao, W., Jia, L., and Lu, J. 2016. A Silurian maxillate placoderm illuminates jaw evolution. Science, 354(6310), pp.334-336.

Integrative and Comparative Biology

Integrative and Comparative Biology, volume 62, number 3, pp. 805–816
https://doi.org/10.1093/icb/icac108

Society for Integrative and Comparative Biology

COMPLIMENTARY/POSTER SESSION PAPER

Interspecific Differences in the Flow Regimes and Drag of North Pacific Skate Egg Cases

Kayla C. Hall[*,†,1], Jaida N. Elcock[‡,§], Gerald R. Hoff[¶], Duane E. Stevenson[¶], Adam P. Summers[*,†] and Cassandra M. Donatelli[*,||]

[*]Friday Harbor Labs, University of Washington, 620 University Road, Friday Harbor, WA 98250, USA; [†]Department of Biology, University of Washington, Life Sciences Building, W Stevens Way NE Seattle, WA 98195, USA; [‡]Department of Biology, Woods Hole Oceanographic Institution, Woods Hole Road, MS 31, Clark 223, Woods Hole, MA 02543, USA; [§]Department of Earth and Planetary Science, Massachusetts Institute of Technology, 77 Massachusetts Ave 54-918, Cambridge, MA 02139, USA; [¶]NOAA, National Marine Fisheries Service, Alaska Fisheries Science Center, 7600 Sand Point Way NE, Seattle, WA 98115, USA; [||]Fowler School of Engineering, Chapman University, 1 University Dr, Orange, CA 92866, USA

From the symposium "Integrating ecology and biomechanics to investigate patterns of phenotypic diversity: Evolution, development, and functional traits" presented at the annual meeting of the Society for Integrative and Comparative Biology virtual annual meeting, January 3–February 28, 2022.

[1]Email: kchall8@uw.edu

Synopsis Skates are a diverse group of dorso-ventrally compressed cartilaginous fish found primarily in high-latitude seas. These slow-growing oviparous fish deposit their fertilized eggs into cases, which then rest on the seafloor. Developing skates remain in their cases for 1–4 years after they are deposited, meaning the abiotic characteristics of the deposition sites, such as current and substrate type, must interact with the capsule in a way to promote long residency. Egg cases are morphologically variable and can be identified to species. Both the gross morphology and the microstructures of the egg case interact with substrate to determine how well a case stays in place on a current-swept seafloor. Our study investigated the egg case hydrodynamics of eight North Pacific skate species to understand how their morphology affects their ability to stay in place. We used a flume to measure maximum current velocity, or "break-away velocity," each egg case could withstand before being swept off the substrate and a tilt table to measure the coefficient of static friction between each case and the substrate. We also used the programing software R to calculate theoretical drag on the egg cases of each species. For all flume trials, we found the morphology of egg cases and their orientation to flow to be significantly correlated with break-away velocity. In certain species, the morphology of the egg case was correlated with flow rate required to dislodge a case from the substrate in addition to the drag experienced in both the theoretical and flume experiments. These results effectively measure how well the egg cases of different species remain stationary in a similar habitat. Parsing out attachment biases and discrepancies in flow regimes of egg cases allows us to identify where we are likely to find other elusive species nursery sites. These results will aid predictive models for locating new nursery habitats and protective policies for avoiding the destruction of these nursery sites.

Introduction

Skates (Rajiformes) are the most speciose superorder of all cartilaginous fish, comprised of roughly 280 species (Ebert and Winton 2010; Chiquillo et al. 2014), yet a great deal of their ecological preferences remain unknown. All skates are slow-growing oviparous fish that deposit their eggs in capsules onto the seafloor where they remain throughout embryonic development for a period of 1–4 years, depending on species (Wourms 1977; Hoff 2008, 2009; Ebert and Winton 2010). Some species in the North Pacific use nursery sites—locations where adults gather to deposit eggs at densities anywhere from 500 to 800,500 eggs/km^2 (Hoff 2008, 2010). There are currently 26 known nursery sites for six

Advance Access publication July 4, 2022

species of skates in the eastern Bering Sea (Rooper et al. 2019). Maximum entropy models have shown that there is a limited area of the upper continental slope where conditions would likely support nursery areas (Rooper et al. 2019), but most of these regions remain unexplored and unprotected. There are 16 species of skates known to inhabit various geographical zones throughout the eastern North Pacific, ranging from the Salish Sea in northern Washington to the Gulf of Alaska, Aleutian Islands, and Bering Sea (Stevenson et al. 2007). Though egg cases are morphologically variable and can be identified to species (Stevenson et al. 2007; Ishihara et al. 2012), they all have a similar general anatomy with a large main body and hollow "horn" structures which allow seawater to flow through the body of the case (Fig. 2; Koob and Summers 1996; Long and Koob 1997). Both the gross morphology and the microstructure of the egg case interact with substrate to determine how well a case stays in place on a current-swept seafloor (Vogel 1994). Our goal is to use computational and physical hydrodynamic tests of flow and friction, coupled with geographic information system (GIS) data, to predict the locations of undocumented nursery sites in the North Pacific. Break-away velocity, or the flow velocity which causes an egg case to lift off of the seafloor, can be incorporated into fine-scale maps of potential habitats to rule out areas as prospective nursery sites. This will inform management strategies that protect these areas and the species that use them. The ecological preferences of these skates, in part determined by specific life-history stages, make them highly susceptible to trawling and long-line fishing, as these generally take place at continental shelf depths.

Our current understanding of the hydrodynamics of egg cases is limited to one quantitative account by Koob and Summers (1996). The authors measured the relative drag vs orientation for little skate (*Leucoraja erinacea*) egg cases. Their results showed that the lowest relative drag occurred when the long axis of the case was parallel to flow (anterior–posterior orientation) due to the streamlined shape. The egg cases experienced higher relative drag when oriented perpendicular to flow in a lateral orientation. In addition to flow around the case, they found that water flows through the capsule via the horn slits, which open about $\frac{1}{3}$ into development. These hydrodynamic properties are thought to enhance survival by providing consistent oxygen to satisfy the increasing respiratory demands as development progresses (Koob and Summers 1996).

Egg cases have been found in habitats where flow is as slow as 1 cm/s (Sigler et al. 2015; Reichert 2020). Embryos are able to oxygenate their egg cases in such a low current environment by actively creating flow through the horn slits with an embryonic-stage specific transitory tail appendage (Long and Koob 1997). Long and Koob (1997) found that little skates beat their tails, producing waves of regular amplitude and axial curvature. The tail pumping generates a positive pressure in the horn occupied by the tail, which then causes a negative pressure in the unoccupied horns (Long and Koob 1997). This system causes water to exit the occupied horn and fill the three empty horns (Long and Koob 1997). The tail pump system appears to be co-adapted for ventilating the capsule, as the horns alone do not circulate enough new oxygenated water within the case. It is proposed that tail pump ventilation increases as passive flow within the capsule decreases, due to the embryos growing and taking up more volume (Long and Koob 1997).

To properly implement management strategies for a skate population we need to understand how they live and move through their environment. If we are to build upon predictive models, (i.e., Rooper et al. 2019), we need a better sense of what skates do across all life stages. For example, juvenile and adult Alaska skates (*Bathyraja parmifera*) occupy different portions of the habitat (Hoff 2008). Further, adults are known to frequent shallow depths of 30 m but are also found at depths from 145 to 380 m, which is where their nursery sites are located (Fig. 1; Hoff 2008, 2010, and Hoff pers comm). Nursery sites in canyon slope areas are heavily fished via trawls and longlines (Stevenson et al. 2019), increasing risk to crucial life stages: females laying eggs and developing embryos. Meanwhile, neonates and juvenile skates exhibit dramatic emigrations from nursery sites to avoid predators (Hoff 2010, 2016). Evaluating habitat and substrate effects are essential for pinpointing and protecting hotspots where skates are most likely to deposit eggs. For example, only a single nursery site has been found for *Beringraja binoculata,* one of two species that houses multiple embryos per capsule (Hitz 1964). The *B. binoculata* nursery site was found at a relatively shallow depth of 65 m off the Oregon coast (Fig. 1, Fig. 6, Supplementary Table 1; Hitz 1964). Thus, any new or altered environmental stress, either natural or anthropogenic, could endanger this and additional unknown nursery sites for this migrating population. In 2014, the North Pacific Fishery Management Council designated six habitat areas of particular concern (HAPC) for skate nurseries in the eastern Bering Sea, recognizing their uniqueness and importance as essential nursery sites and fish habitats, yet many remain unprotected (Melton et al. 2014; Rooper et al. 2019). A recent analysis of bycatch data indicated that fishing gear is being deployed in and near skate nursery sites, including designated HAPC locations (Stevenson et al. 2019). Therefore, it is necessary to map skate habitats more distinctly to better inform fisheries management and

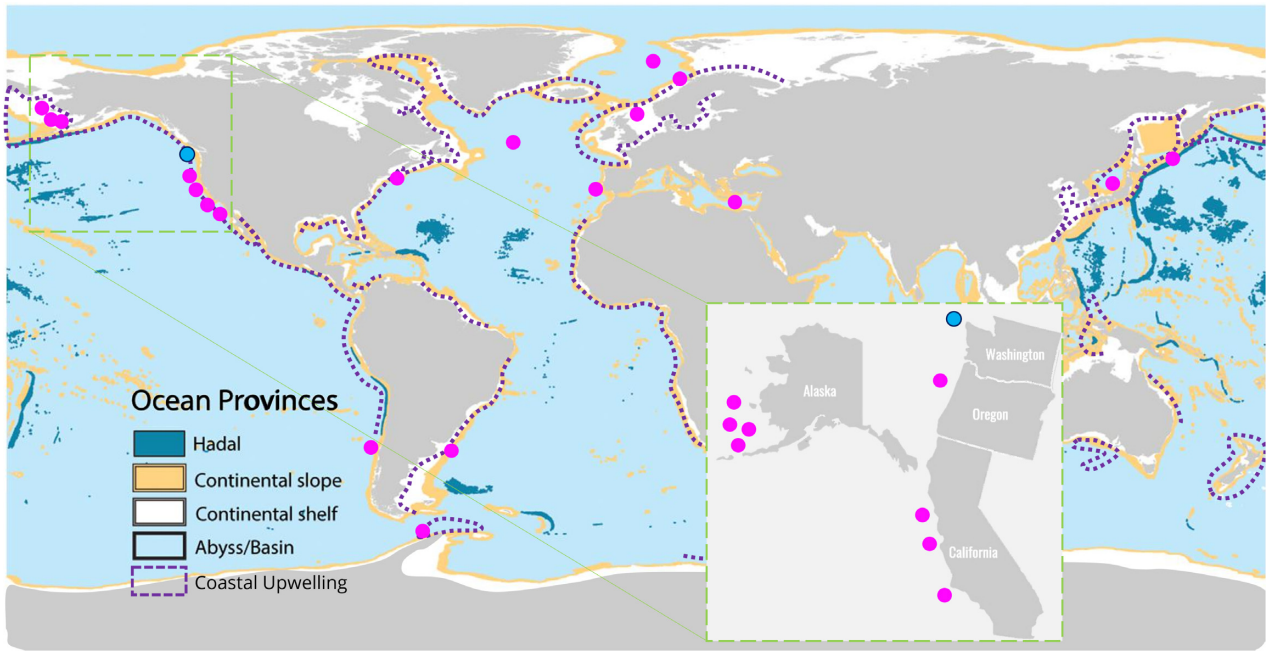

Fig. 1 Distribution of elasmobranch egg case nursery sites. Pink dots indicate the 20 sites found from literature sources (see Supplementary Table 1). The blue dot, off the coast of Washington, is the region we propose as a nursery site for *B. binoculata* and *R. rhina*. The inset indicates the nursery sites of the eight species used in this study.

implement strategies for bycatch reduction at specific life stages.

The aims of this study are three-fold: (a) to describe and compare the gross morphology of the egg cases as well as microstructures covering the surface; (b) to test the hydrodynamic and frictional forces skate egg cases are capable of withstanding, before breaking away from the substrate; (c) to use these data in conjunction with ecological and oceanographic surveys to inform predictions about potential nursery sites.

Methods

We compiled the global distribution and characteristics of elasmobranch egg case nursery sites from peer-reviewed literature sources (see Supplementary Table 1). We plotted these data on a map (Fig. 1; adapted from Atwood et al. 2020) with the addition of zones of coastal upwelling, following National Oceanic and Atmospheric Administration (NOAA) upwelling maps, and the locations of nursery sites (see Supplementary Table 1).

Morphology and morphometrics

We gathered physical data on preserved egg cases from eight North Pacific species: *Bathyraja aleutica, B. interrupta, B. minispinosa*, *B. parmifera, B. trachura*, and *B. taranetzi* are from the Aleutian Islands and eastern Bering Sea; *Beringraja binoculata* and *Raja rhina* are found throughout the northeast Pacific Ocean. All egg cases were preserved in 70% ethanol. We selected undamaged egg cases, with yolk and/or embryo, for the trials.

Prior to testing, we gathered morphometrics of each individual egg case, including the total length (TL), case length (CL), width (W), and height (H), followed by macrophotography (Fig. 2). In each image the egg case was isolated from the background in Microsoft Photos (Microsoft Corporation, Redmond, WA, USA). We transformed the image to black/white via the threshold function in Fiji (Schindelin et al. 2012) and used the Magic Wand tool to collect the projected area of dorsal, anterior/posterior, and lateral views (Fig. 2).

Friction trials

Friction between two materials can be described by the static friction coefficient (μ; Bowden and Tabor 1950). We measured the coefficient of static friction on the preserved specimens using a motorized metal tilt table, controlled by a programable circuit board Arduino (Arduino, Torino, Italy). Egg cases were placed on the tilt table in the air on wet sandpaper (60 grit), which was attached with magnets to the tilt table, to simulate sediment (Fig. 3A). The table was tilted at a rate of 0.273°/s until the egg case slid off, and the angle was recorded by a Johnson's magnetic angle locator. The coefficient of static friction (μ), can be calculated from the angle

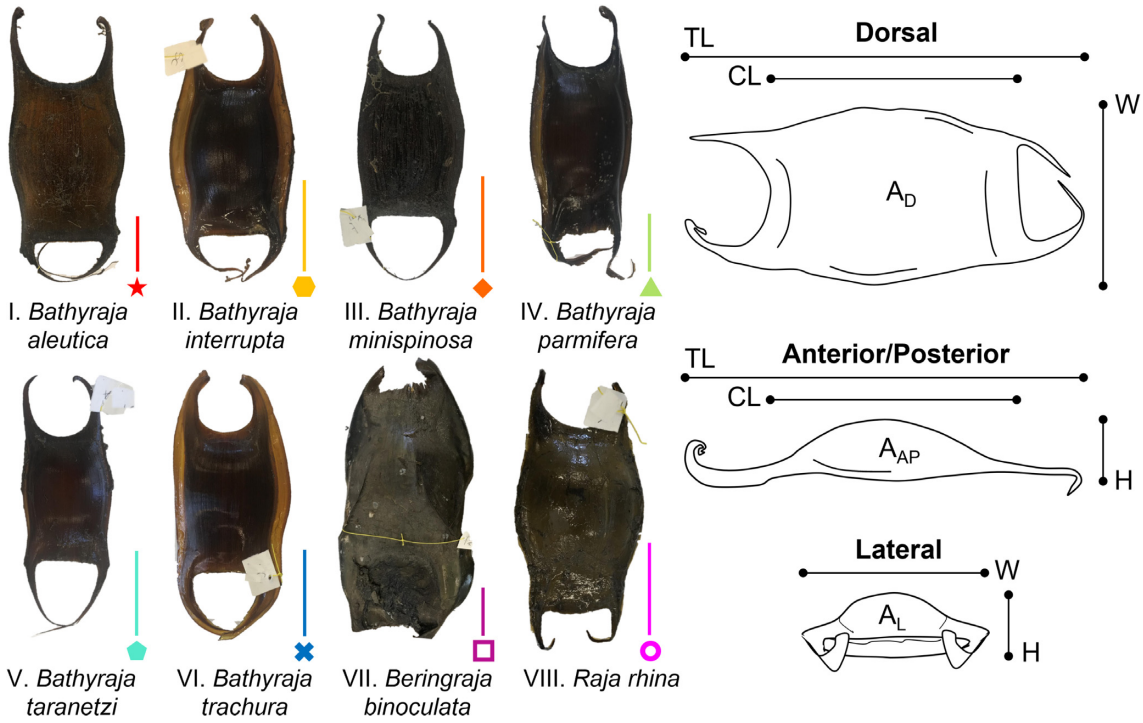

Fig. 2 Gross morphology and morphometrics of skate egg cases used in this study. The scale bar is 5 cm and color-coded specific to species, symbol is also species specific: Magenta star—**I**. *Bathyraja aleutica*, Gold hexagon—**II**. *Bathyraja interrupta*, Orange diamond—**III**. *Bathyraja minispinosa*, Lime triangle—**IV**. *Bathyraja parmifera*, Aqua pentagon—**V**. *Bathyraja trachura*, Blue X—**VI**. *Bathyraja taranetzi*, Purple square—**VII**. *Beringraja binoculata*, and Pink circle—**VIII**. *Raja rhina*. The morphometrics of each individual egg case were gathered to include the total length (TL), case length (CL), width (W), and height (H). The dorsal area (AD), anterior–posterior area (AAP), and lateral area (AL) were collected for each individual as well.

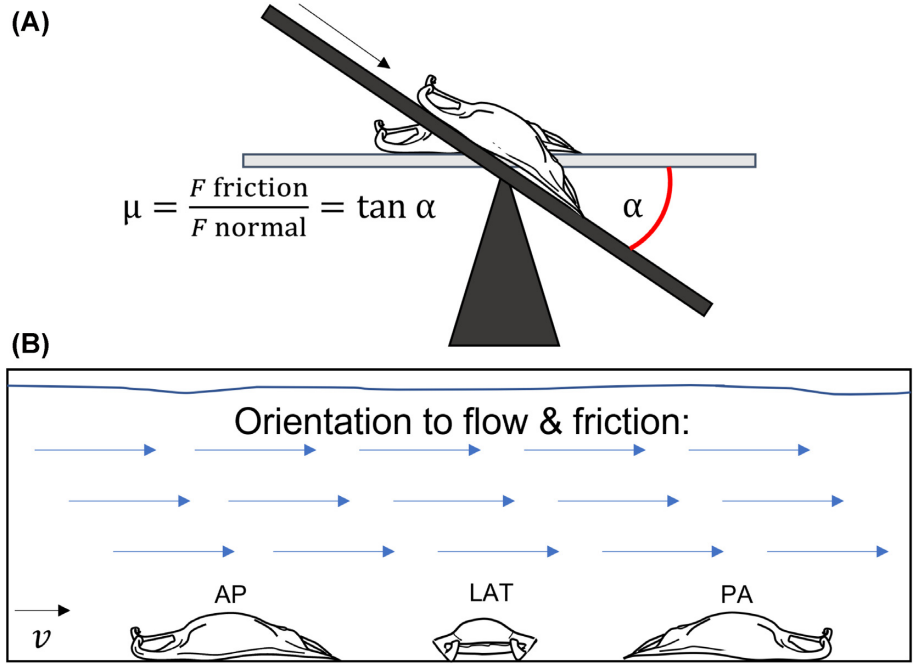

Fig. 3 Methodology to quantify friction and flow. **(A)** We measured the coefficient of friction on the specimens using a motorized metal tilt table. The coefficient of static friction (μ), can be calculated from the angle (α). Egg cases were placed on the tilt table on wet sandpaper to simulate sediment. **(B)** We used a flume to determine the water velocity (cm/s) at which an egg case breaks free of the substrate, blue arrows indicate direction of flow with reference to egg case. The egg cases were tested in three orientations in both the friction and flow trials: Anterior/Posterior (AP), Lateral (LAT), and Posterior/Anterior (PA).

(α; Ditsche and Summers 2019):

$$\mu = \frac{F_{\text{Friction}}}{F_{\text{Normal}}} = tan(\alpha).$$

We measured the coefficient of static friction for the eight species, with six different egg cases for five of the species, and three capsules for *B. taranetzi*, *B. minispinosa*, and *R. rhina*. The friction trials were repeated three times for each individual, in all three orientations (anterior/posterior, lateral, and posterior/anterior; Fig. 3B).

Break-away trials

We used a flume with a 152.4 × 38.1 × 50.8 cm working area (Rolling Hills Research Corporation, Model 1520 Water Tunnel) to determine the water velocity at which an egg capsule breaks free of the substrate (break-away velocity, cm/s). Egg cases were placed into a water depth of 35.56 cm, onto the substrate in the orientation of interest without any attachment hardware so that the only thing keeping them in place was the friction between the substrate and the contact surface of the egg case. Each egg case was tested three times, in all three orientations, and the velocity at which the egg broke contact with the substrate was recorded (Fig. 3B). We used the same 60 grit sandpaper substrate in the flume as in the friction measurements, current velocity started at 12.7 cm/s and increased by 2.54 cm/s every 10 s, until the case broke contact with the substrate.

We used R (version 4.1.3, R Core Team 2021), a free coding language for statistics and modeling, via RStudio (RStudio Team 2020), a free integrated development environment (IDE) for R, to estimate drag force for each egg case based on morphometrics. For our drag estimate, we used the equation

$$F_D = \frac{1}{2} A \rho v^2 C_D,$$

where F_D is drag force (N), A is the projected area perpendicular to flow (m^2), ρ is the density of seawater (1020 kg/m^3), v is free stream flow velocity (cm/s; Vogel 1994), and C_D is drag coefficient (unitless). We estimated C_D using the equation for drag based on thickness ratio:

$$C_D = 1 + 1.5\left(\frac{h}{w}\right)^{\frac{3}{2}} + 7\left(\frac{h}{w}\right)^3,$$

where h is the maximum height of the egg case (m) and w is the length of the egg case parallel to flow (m). This equation is derived from measurements of the drag of streamlined shapes based on wetted area from Hoerner (1965): Chapter 6 Drag of Streamline Shapes, equation (28).

Table 1 Linear model results.

	Independent variables		
	AP	**PA**	**LAT**
Predictor variables	**Species**	**Species**	**Species**
Friction coefficient	**<0.001**	0.337	0.154
Estimated drag	**<0.001**	**<0.001**	**<0.001**
Break-away velocity	**0.006**	**<0.001**	**0.027**

Values shown are *P*-values. Abbreviations are as follows: A–P-Anterior/Posterior, P–A-Posterior/Anterior, LAT-Lateral.

Table 2 Linear mixed effect model results.

	Independent variables		
Predictor variables	**Friction Coefficient**	**Break-away Velocity**	**Estimated Drag**
Orientation	**0.022**	n/a	**<0.001**
Species	**<0.001**	0.089	**<0.001**
Orientation∗species	**0.011**	n/a	0.074
Area	n/a	0.251	n/a
Area∗species	n/a	**0.007**	n/a
Friction coefficient	n/a	n/a	n/a

Values shown are *P*-values.

Scanning electron microscopy

To visualize microstructure, we collected 1 × 1 cm samples from the midline of the ventral surface and the right anterior horn of an egg case from each species (Fig. 4). We stored samples in 70% ETOH, then preserved them in 2% Glutaraldehyde with 0.1M phosphate buffer for 1 h at 22°C. The samples were then rinsed twice in 0.1M phosphate buffered saline for 10 min, we then used an acetone dehydration series before final drying in hexamethyldisilazane (Laforsch and Tollrian 2000; Heiden et al. 2005). We coated samples in gold palladium and imaged them with a NeoScope JCM-5000 scanning electron microscope.

Calculations and statistics

We performed one-way ANOVAs to determine if the coefficient of static friction, break-away velocity, and estimated drag (20 cm/s) (independent variables) were different between species (predictor variable). For these models, data were subset by orientation resulting in nine total models (Table 1). To determine the overall relationship between break-away velocity, coefficient of static friction, and estimated drag (20 cm/s), we created linear mixed effect models using the "lme4" package and ANOVAs using the "car" package in R (Table 2; Bates et al. 2015; Fox and Weisberg 2019). The "lme4" package is designed to fit linear and mixed effect models using Eigen and S4. Please see Bates et al. 2015for more

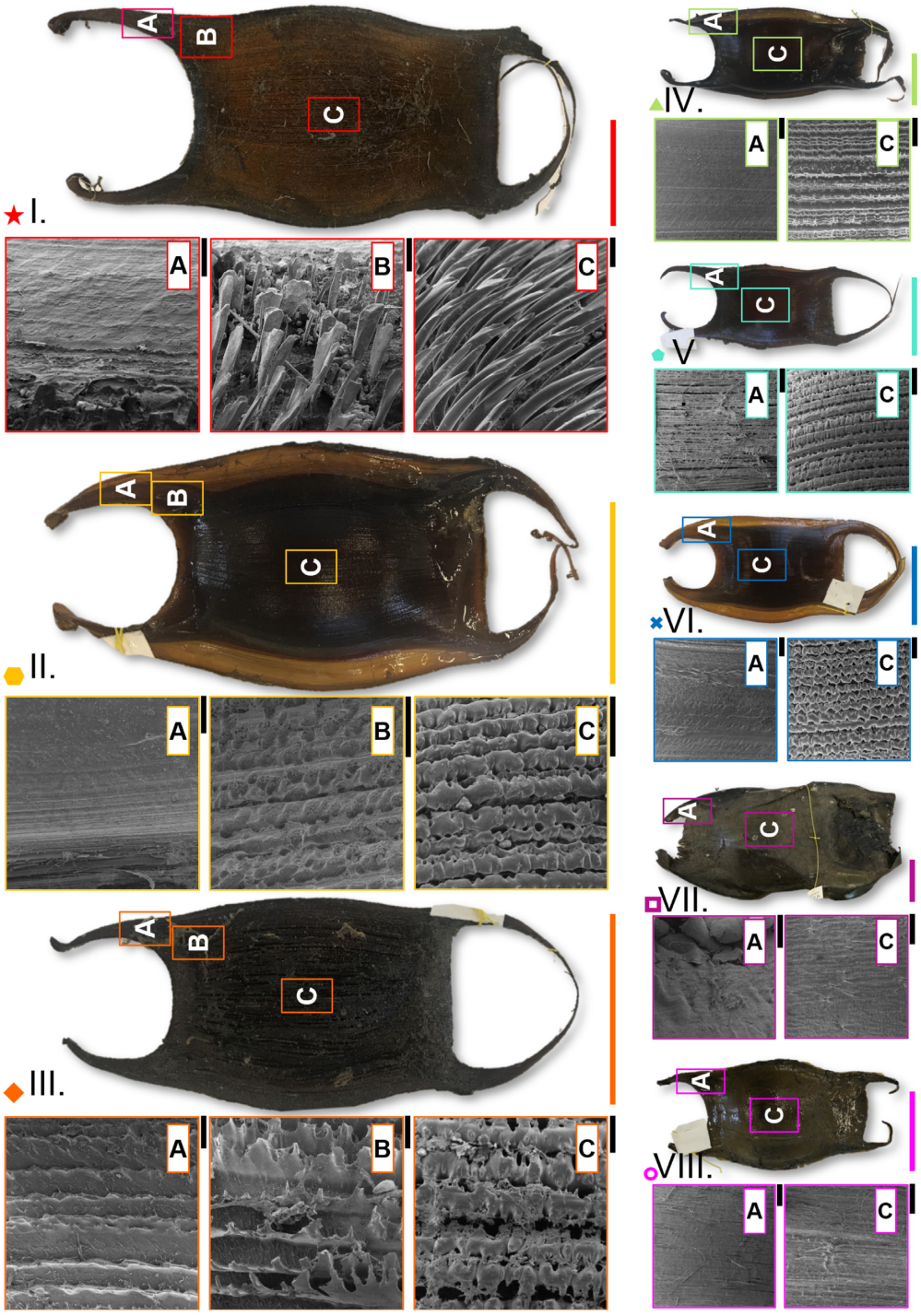

Fig. 4 SEM showing the variation within and among species of egg case microstructure. The samples of 1 × 1 cm from **(A)** the right anterior horn, **(B)** the transitional region between the body capsule to horn, and **(C)** the midline of the ventral surface. The black SEM scale bar is 500 μm. The colorcoded scale bars for gross morphology are 5 cm. Magenta star—**I**. *Bathyraja aleutica*, Gold hexagon—**II**. *Bathyraja interrupta*, Orange diamond—**III**. *Bathyraja minispinosa*, Lime triangle—**IV**. *Bathyraja parmifera*, Aqua pentagon—**V**. *Bathyraja trachura*, Blue **X**—**VI**. *Bathyraja taranetzi*, Purple square—**VII**. *Beringraja binoculata*, and Pink circle—**VIII**. *Raja rhina*.

information about the implementation of the mixed effect models. For the break-away velocity and the coefficient of static friction models, we used the averages of each independent variable per individual over 2–3 trials. We created three models. In the first, the coefficient of static friction was the dependent variable, and orientation and species were predictor variables. In the second, break-away velocity was the dependent

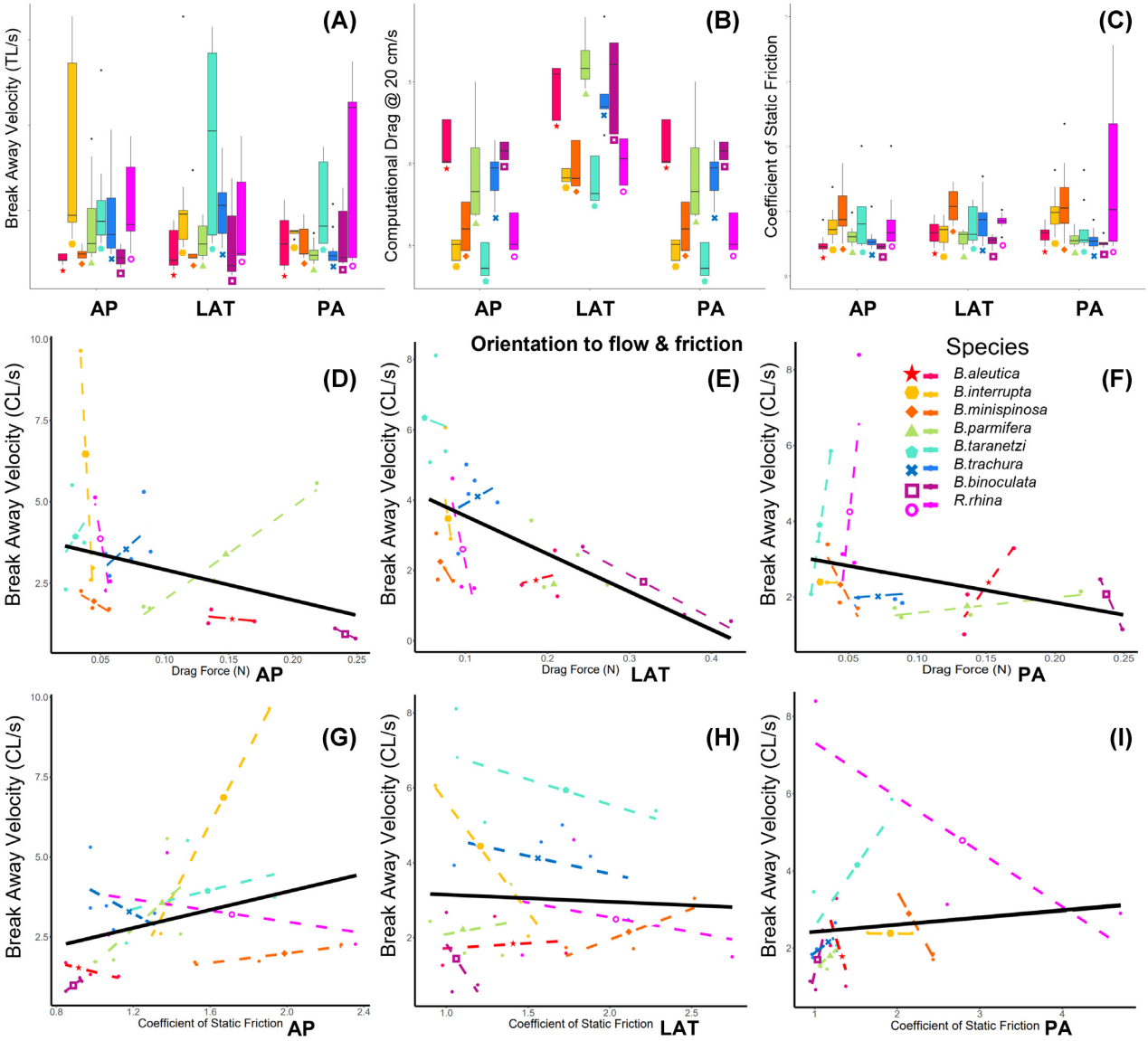

Fig. 5 Friction and flow experimental and computational results. The top panel compares the orientation of egg cases to: **(A)** Break-Away Velocity (cm/s), **(B)** Computational Drag at 20 cm/s, and **(C)** Coefficient of Static Friction. The middle panel compares the relationship between Drag Force (N) and Break-Away Velocity in case length per second (CL/s), in order to standardize for size variation across species in each orientation: **(D)** AP, **(E)** LAT, and **(F)** PA. And the bottom panel compares the relationship between the Coefficient of Static Friction and Break-Away Velocity in case length per second (CL/s), in order to standardize for size variation across species in each orientation: **(G)** AP, **(H)** LAT, and **(I)** PA. The orientation abbreviations are as follows: Anterior/Posterior (AP), Lateral (LAT), and Posterior/Anterior (PA). The black line on **(D–I)** shows the overall trend, which is significant (see Table 2); the dashed lines represent the specific trend of each species. Genus species are color-coded as follows: Magenta star—**I**. *Bathyraja aleutica*, Gold hexagon—**II**. *Bathyraja interrupta*, Orange diamond—**III**. *Bathyraja minispinosa*, Lime triangle—**IV**. *Bathyraja parmifera*, Aqua pentagon—**V**. *Bathyraja trachura*, Blue **X**—**VI**. *Bathyraja taranetzi*, Purple square—**VII**. *Beringraja binoculata*, and Pink circle—**VIII**. *Raja rhina*.

variable, and area to flow and species were predictor variables. In the third, estimated drag (20 cm/s) was the dependent variable and orientation and species were predictor variables. In all three models, individual ID was included as a random factor. Figures 5 (experimental data) and 6 (environmental data) plots were generated using ggplot2 (Wickham 2016). A subset of data from Supplementary Table 1 was visualized via ggplot2 (Wickham 2016), to show the relationship between depth and current velocity from elasmobranchs found *in situ* in various nursery sites across the globe (Fig. 6).

Results

We found 20 documented egg case nursery sites across 10 bodies of water in the literature, all of which

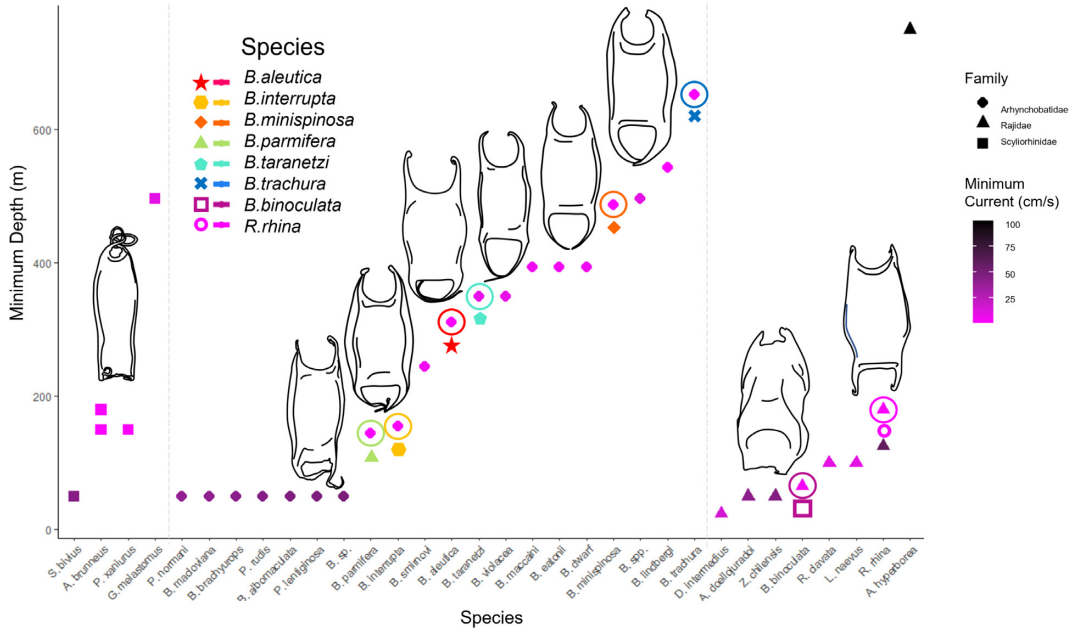

Fig. 6 Range in depth and current velocity that egg cases of each species can withstand. On the graph, from left to right, are the egg cases found at various depths (m), from species of catsharks (Scyliorhinidae) shown as squares, softnose skates (Arhynchobatidae) shown as circles, and egg cases from the hardnose skate (Rajidae) shown as triangles. The data points range in color from pink to black, indicating the minimum current (cm/s) they have been found in. Egg case schematics are scaled to each other, not to true size. Circled data points are the color-symbol-coded skate species from this study. These data and literature sources can be found in Supplementary Table 1.

are in regions where coastal upwelling occurs near continental slopes (Fig. 1). Water temperatures at laying sites ranged from 0.25 to 13°C, and depths ranged from 25 to over 1000 m (see Supplementary Table 1). In some places where water was particularly cold, such as the Lofoten–Vesterålen continental margin in Norway, egg cases are laid in cold seeps where the water is warmer than the surroundings (Sen et al. 2019). Sediment type was not consistent across nursery location, rather there is a strong association of nursery sites at the heads of undersea canyons near continental slopes (see Supplementary Table 1).

All nursery sites are deeper than 25 m, with the majority of those being below 50 m (see Supplementary Table 1, Fig. 6). The deepest documented nursery sites are occupied by *B. trachura* (652–1069 m). In most instances, as depth increases, the current velocity decreases. Egg cases are not necessarily limited by current velocity alone; *Amblyraja hyperborea* egg cases are relatively small with non-rigid tapered horns and are found at depths of 750 m, where the current velocity reaches over 100 cm/s.

The egg capsules of many of the eastern Bering Sea and Aleutian species share similar macromorphology, having a short and stout streamlined mid-capsule, and a prominent U-shaped curvature between the anterior horns (Fig. 2). All species have a lateral keel along the edge of the case; this was particularly broad in *B. interrupta* and *B. trachura*. The egg cases of *B. aleutica* are longer and wider than the other Alaskan species, but *B. binoculata* is the largest in length, width, and height of all species in this study. The anterior horns are consistently shorter than posterior horns. Aside from case size and shape, the other primary variation between these egg cases is in the posterior horns; some are long and flexible (*B. parmifera*), others are rigid and highly curved inward (*B. aleutica, B. minispinosa, B. trachura*). The two posterior horn oddities of this dataset are *B. binoculata,* which lacks a posterior gap because the apron continues to the bottom of each horn, and *R. rhina,* in which the horns hook ventrally, versus medially as in other species (Fig. 2).

There is variation in the surface microstructure both within a single capsule and among species (Fig. 4). For example, *B. aleutica* has thorn-like projections which transition to paddle-like structures near the anterior horn, and the horn itself is smooth with a few ridges (Figs. 4I. A, B, and C). Also, *B. minispinosa* has lobular notches that make up the longitudinal ridges on the main body of the capsule, but the transitional zone (body to horn) exhibits thin and jagged longitudinal ridges, and the horns have short sharp ridges (Figs. 4III. A, B, and C). There is also variation between species, for example the two species that co-occur in the Salish Sea, *B. binoculata* and *R. rhina*, both lack longitudinal ridges, and while *B. binoculata* cases are smooth, *R. rhina* cases

have thin, string-like fibers (Figs. 4VII. A and C; 4VIII. A and C).

There is also variation in the performance measures—coefficient of static friction and break-away velocity—within a single capsule and among capsules from different species. But these relationships are not simple. For example, break-away velocity is predicted by the interaction of area and species, but not area or species alone. The coefficient of static friction is predicted by species, but not orientation. Our finding that break-away velocity is predicted by the interaction of area, species, and the coefficient of static friction (Tables 1 and 2, Figs. 5G, H, and I) indicates that microstructure does influence the ability to stay stuck, since friction is largely determined by microstructure. But friction alone does not account for how those species stay stuck on a similar substrate, as the coefficient of static friction was not significant for the posterior and lateral orientations (Table 1). Further, the computational estimated drag (20 cm/s) also determines whether the shape of a species will be significantly different from other species in variable nursery sites and experimental habitats (Table 1).

Discussion

Here we investigated the hydrodynamic properties of egg cases deposited by skates of the eastern North Pacific. Our results suggest that orientation and surface microstructure influence the ability of an egg case to adhere to the substrate, thus maintaining its position in favorable current velocity and conditions that favor circulation of oxygen flow through the egg case during their long developmental period.

The constant temperature and high nutrient load of submarine canyons, driven by coastal upwelling, provides an excellent environment for the long, slow development process of skates (Luchin et al. 1999; Hoff 2008). Skate egg cases need several things for successful development. These include exposure to a narrow range of temperatures over a multiple-year time frame, well-oxygenated water, and, for post-hatching nutrition, an abundance of small invertebrate prey. Upwelling sites provide all these resources. Egg cases can take 1–4 years to develop and for much of this time the embryo gets oxygen from water that flows through the capsule, driven by surrounding currents (Koob and Summers 1996; Long and Koob 1997; Hoff 2008). The complex topography at the heads of canyons ensures a current flow with well-oxygenated water from the mixing of the ocean thermocline (Sigler et al. 2015; Ropper et al. 2019). Eggs must be found in regions with moderate currents to create sufficient water flow across the egg surface to sustain metabolic processes (Leonard et al. 1999; Hoff 2007, 2008) and ensure eggs are not covered with sediments. When the embryo finally hatches it has a small amount of yolk, but it must start eating soon. Prey, usually small invertebrates like copepods and amphipods, are common on the nutrient-rich seafloor around an upwelling area (Springer et al. 1996; Stabeno et al. 1999; Whitledge and Luchin 1999). Similarly, mothers are more likely to deposit eggs in habitats where food is guaranteed, so that they can eat and replenish their own energy stores before the next reproductive cycle (Hoff 2008).

Although we regularly find egg cases for *B. binoculata* and *R. rhina* in the Puget Sound and Salish Sea, the abiotic factors relevant for a highly populated nursery site do not exist consistently enough in this location. Based on seafloor topography, slower current velocity, and depth range we propose that a nursery site for *R. rhina* is likely to occur off the coast of Victoria, Canada in the Juan de Fuca Canyon (Fig. 1, blue dot). Two alternative locations for nursery sites would be the Quinault Canyon and Austoria Canyon off the coast of northern Washington. The findings of Hitz (1964) and our study support the notion that *B. binoculata* should lay their eggs in regions with slower currents because their cases perform worse in high current systems than *R. rhina*. It is interesting to note a contradiction in morphology and performance (Figs. 5 and 6) for *B. binoculata*. The asymmetrical capsule, with dorsal keels (see Supplementary Fig. 1), suggests that this species would perform better in higher currents; instead, we found that *B. binoculata* has one of the lowest abilities to withstand high flow in both experimental and mathematical testing. These results support the one *in situ* encounter of a *B. binoculata* nursery site, where eggs were found relatively shallow at 65 m, in currents under 13 cm/s (see Supplementary Table 1, Fig. 6). The current velocity within and around the San Juan Archipelago are notoriously fast at 1–3 m/s (Yang et al. 2021), illustrating why we find solitary egg cases, not dozens to hundreds of cases in one location.

One thing to note is the apparent dichotomy between species that live in a shallower environment vs a deeper one (Fig. 6; Hoff 2009). Shallower species (*B. parmifera*, *B. interrupta*, *B. taranetzi*) all have a relatively similar morphology with distinct lateral keels, smooth surfaces, and shallow nursery sites (Figs. 2, 4, and 6). The other *Bathyraja* species (*B. aleutica*, *B. minispinosa*) found in deeper nursery sites tend to have narrow lateral keels and a complex surface microstructure. The one exception to this trend, between deep and shallow species, is *B. trachura* which is a deep-water species with egg cases that are morphologically similar to the shallow species. This dichotomy could be the basis for further

investigation into the relationship between case morphology and habitat preference.

We found that friction is not the only thing that determines case mobility or lack thereof (Figs. 5G, H, and I). Once deposited from the mother, the cases, are covered in a sticky thread-like material which functions to pick up particulates (shells, substrate, etc.) from the surrounding environment (Koob 1999). This allows the egg case to settle securely into the substrate and resist fast and fluctuating currents (Koob 1999; Compagno 2001; Rocha et al. 2010). The collection of particles may contribute to the case's ability to stay in place. The sticky attachment fibrils of *B. binoculata* are a mat-like pad atop the posterior apron (see Supplementary Fig. 1), we found that this fibrous-mat seemed to function as a weighted anchor to keep the case in contact with the substrate, as this case morphology lacks "true horns" that might otherwise attach to structures. In addition to the gross morphology and microstructures, these horns and fibrous tendrils, are additional systems used to anchor or attach the case to the substrate and allow the eggs to remain in unlikely high-current habitats (Love et al. 2008; Graiff et al. 2016). Unlike skates, mother catsharks (Scyliorhinidae) are known to intentionally wrap the tendrils of the candle-shaped egg cases around kelp stalks to keep them in place (Pretorius 2012; Hiscock et al. 2019). For species that lack tendrils, such as *A. hyperborea,* females may prioritize other secure substrates, such as tubeworm fields and other sessile invertebrates, that the cases can grip onto (see Supplementary Table 1; Sen et al. 2019). The egg cases of *A. hyperborea* are relatively small with non-rigid tapered horns and are found at depths of 750 m, where current velocity reaches over 100 cm/s (Fig. 6; Åström et al. 2020; Sen et al. 2019). These species are capable of remaining attached in such a high current system because the mothers prioritize sites with copious amounts of tubeworms and other structure-forming marine invertebrates to keep them anchored to the nursery area (see Supplementary Table 1; Graiff et al. 2016).

Further research incorporating the life-history of the taxa in question, their biology, and biomechanics would aid in fine-tuning the predictive models for future habitat protection plans. Cross-referencing, species ranges, canyons, and upwelling zones will optimize where to survey via submersible camera systems (ROV, Fernandez-Arcaya et al. 2017; Bernhardt and Schwanghart 2021). Pinpointing habitat hotspots, or essential fish habitats will supply the data needed to validate policy regulations as to where longline limitations should be imposed. These regions should be made the top priority in protective fisheries management proposals in the future.

Acknowledgments

We thank D. Stevenson and J. Hoff of the National Oceanic and Atmospheric Administration's Alaska Fisheries Science Center for the Alaskan species egg cases collected during the eastern Bering Sea bottom trawl survey. We thank Dr. Stacy Farina for leading the 2019 cohort of researchers. Lastly, we thank the Washington Department of Fish and Wildlife for Salish Sea species egg cases and the Friday Harbor Laboratories (FHL) Kittiwake.

Funding

This work was supported by the NSF-REU and FHL Blinks-Beacon for funding JNE. And the Stephen and Ruth Wainwright Endowed Fellowship, BEACON and Hoag Awards, Robert T. Paine Experimental and Field Ecology Award, FHL Award, FHL Marine Science Fund, FHL Student Fund (Kohn), Patricia L. Dudley Endowment for funding KCH.

Supplementary data

Supplementary data available at *ICB* online.

Conflicts of interest

None.

Data availability statement

All data will be housed/available for public viewing and downloading in this googlefolder: https://docs.google.com/spreadsheets/d/1TZHoU08erodYvWcSsmDpnFnvvGVMwnX4/edit?usp=sharing&ouid=112694120904919400715&rtpof=true&sd=true.

References

Åström EK, Sen A, Carroll ML, Carroll J. 2020. Cold Seeps in a warming Arctic: insights for benthic ecology. Front Mar Sci 7:244.

Atwood TB, Witt A, Mayorga J, Hammill E, Sala E. 2020. Global patterns in marine sediment carbon stocks. Front Mar Sci 7:165.

Bates D, Mächler M, Bolker B, Walker S. 2015. Fitting linear mixed-effects models using lme4. J Stat Softw 67:1–48.

Bernhardt A, Schwanghart W. 2021. Where and why do submarine canyons remain connected to the shore during sea-level rise? Insights from global topographic analysis and Bayesian regression. Geophys Res Lett 48:e2020GL092234.

Bowden FP, Tabor D. 1950. The friction and lubrication of solids. Oxford: Clarendon Press.

Chiquillo KL, Ebert DA, Slager CJ, Crow KD. 2014. The secret of the mermaid's purse: phylogenetic affinities within the Rajidae and the evolution of a novel reproductive strategy in skates. Mol Phylogenet Evol 75:245–51.

Compagno LJ. 2001. Sharks of the world: bullhead, mackerel, and carpet sharks (Heterodontiformes, Lamniformes, and Orectolobiformes). Vol. 4. New Delhi: Food and Agriculture Organization.

Core Team R. 2021. R: a language and environment for statistical computing. Vienna: R Foundation for Statistical Computing.

Ditsche P, Summers A. 2019. Learning from northern clingfish (*Gobiesox maeandricus*): bioinspired suction cups attach to rough surfaces. Philos Trans R Soc B: Biol Sci 374: 20190204.

Ebert DA, Winton MV. 2010. Chondrichthyans of high latitude seas. In: Carrier Jeffery C, Musick John A, Heithaus Michael R., editors. The biology of sharks and their relatives. Vol. 2. Boca Raton (FL): CRC Press.

Fernandez-Arcaya U, Ramirez-Llodra E, Aguzzi J, Allcock AL, Davies JS, Dissanayake A, Harris P, Howell K, Huvenne VA, Macmillan-Lawler M, et al. 2017. Ecological role of submarine canyons and need for canyon conservation: a review. Front Mar Sci 4:5.

Fox J, Weisberg S. 2019. An R companion to applied regression. 3rd ed. Thousand Oaks (CA): Sage.

Graiff K, Lipski DM, Etnoyer PJ, Cochrane GR, Williams GC, Salgado E. 2016. Benthic characterization of deep-water habitat in the newly expanded areas of Cordell Bank and Greater Farallones National Marine Sanctuaries. NOAA Institutional Repository ONMS-16-01.

Heiden TCK, Haines AN, Manire C, Lombardi J, Koob TJ. 2005. Structure and permeability of the egg capsule of the bonnethead shark, *Sphyrna tiburo*. J Exp Zool A Comp Exp Biol 303A:577–89.

Hiscock K, Christie H, Bekkby T. 2019. The ecology of the rocky subtidal habitats of the northeast Atlantic. In: Hawkins SJ, Bohn K, Firth LB, Williams GA, editors. Interactions in the marine benthos: global patterns and processes. Cambridge: Cambridge University Press.

Hitz CR. 1964. Observations on egg cases of the big skate (*Raja binoculata* Girard) found in Oregon coastal waters. J Fish Res Board Can 21:851–4.

Hoerner SF. 1965. Fluid-dynamic drag. Hoerner fluid dynamics. Published by the author.

Hoff GR. 2007. Reproductive biology of the Alaska skate Bathyraja parmifera, with regard to nursery sites, embryo development and predation [dissertation]. [Seattle (WA)]: University of Washington.

Hoff GR. 2008. A nursery site of the Alaska skate (*Bathyraja parmifera*) in the eastern Bering Sea. Fish Bull 106:233–44.

Hoff GR. 2009. Skate *Bathyraja spp.* egg predation in the eastern Bering Sea. J Fish Biol 74:250–69.

Hoff GR. 2010. Identification of skate nursery habitat in the eastern Bering Sea. Mar Ecol Prog Ser 403:243–54.

Hoff GR. 2016. Identification of multiple nursery habitats of skates in the eastern Bering Sea. J Fish Biol 88:1746–57.

Ishihara H, Treloar M, Bor PH, Senou H, Jeong C. 2012. The comparative morphology of skate egg capsules (Chondrichthyes: Elasmobranchii: Rajiformes). Bull Kanagawa Prefect Mus (Nat Sci) 41:9–25.

Koob TJ, Summers A. 1996. On the hydrodynamic shape of little skate (*Raja erinacea*) egg capsules. Bull Mt Desert Isl Biol Lab 35:108–11.

Koob TJ. 1999. Female reproductive system. Sharks, skates, and rays: the biology of elasmobranch fishes. JHU Press. p.398.

Laforsch C, Tollrian R. 2000. A new preparation technique of daphnids for scanning electron microscopy using hexamethyldisilazane. Archiv für Hydrobiologie 149:587–96.

Leonard JB, Summers AP, Koob TJ. 1999. Metabolic rate of embryonic little skate, *Raja erinacea* (Chondrichthyes: Batoidea): the cost of active pumping. J Exp Zool 283:13–8.

Long JH, Koob TJ. 1997. Ventilating the skate egg capsule: the transitory tail pump of embryonic little skates (*Raja erinacea*). Bull Mt Desert Is Biol Lab 36:117–9.

Love MS, Schroeder DM, Snook L, York A, Cochrane G. 2008. All their eggs in one basket: a rocky reef nursery for the longnose skate (Raja rhina Jordan & Gilbert, 1880) in the southern California Bight. Vol. 106. Fishery Bulletin, 471–5.

Luchin VA, Menovshchikov VA, Lavrentiev VM, Reed RK. 1999. Thermohaline structure and water masses in the Bering Sea. In: Loughlin TR, Ohtani K, editors. Dynamics of the Bering Sea, AK-SG-99-03, Fairbanks, AK: University of Alaska Sea Grant College Program. p. 61–91.

Melton S, Kelly SR, Witherell D, Eagleton M, Olson JV, Ellgen S, Hansen K, Hoff GR, Ormseth OA, Kenne AJ, et al. 2014. Final Environmental Assessment for Amendment 104 to the Fishery Management Plan for Groundfish of the Bering Sea and Aleutian Islands Management Area Habitat Areas of Particular Concern (HAPC) Areas of Skate Egg Concentration December 2014.

Pretorius CA. 2012. Factors influencing the development and mortality rate of shy and cat shark embryos in South African waters [dissertation]. [Cape Town]: University of Cape Town.

Reichert AN. 2020. Habitat associations of catshark egg cases (Chondrichthyes: Carcharhiniformes: Pentanchidae) from the US Pacific Coast. Master's Theses at Digital Commons @ CSUMB: California State University Monterey Bay.

Rocha F, Oddone MC, Gadig OB. 2010. Egg capsules of the little skate, *Psammobatis extenta* (Garman, 1913) (Chondrichthyes, Rajidae). Braz J Oceanogr 58:251–4.

Rooper CN, Hoff GR, Stevenson DE, Orr JW, Spies IB. 2019. Skate egg nursery habitat in the eastern Bering Sea: a predictive model. Mar Ecol Prog Ser 609:163–78.

RStudio Team. 2020. RStudio: integrated development for R. Boston (MA): RStudio, PBC.

Schindelin J, Arganda-Carreras I, Frise E, Kaynig V, Longair M, Pietzsch T, Preibisch S, Rueden C, Saalfeld S, Schmid B, et al. 2012. Fiji: an open-source platform for biological-image analysis. Nat Methods 9:676–82.

Sen A, Himmler T, Hong WL, Chitkara C, Lee RW, Ferré B, Lepland A, Knies J. 2019. Atypical biological features of a new cold seep site on the Lofoten-Vesterålen continental margin (northern Norway). Sci Rep 9:1–14.

Sigler MF, Rooper CN, Hoff GR, Stone RP, McConnaughey RA, Wilderbuer TK. 2015. Faunal features of submarine canyons on the eastern Bering Sea slope. Mar Ecol Prog Ser 526:21–40.

Springer AM, McROY CP, Flint MV. 1996. The Bering Sea Green Belt: shelf-edge processes and ecosystem production. Fish Oceanogr 5:205–23.

Stabeno PJ, Schumacher JD, Ohtani K. 1999. The physical oceanography of the Bering Sea. Dynamics of the Bering Sea 1–28.

Stevenson DE, Hoff GR, Orr JW, Spies IB, Rooper CN. 2019. Interactions between fisheries and early life stages of skates in nursery areas of the eastern Bering Sea. Fish Bull 117: 8–14.

Stevenson DE, Orr JW, Hoff GR, McEachran JD. 2007. Field guide to sharks, skates, and ratfish of Alaska. Anchorage (AK): Alaska Sea Grant College Program.

Vogel S.1994. Life in moving fluids: the physical biology of flow. Princeton (NJ): Princeton University Press.

Whitledge TE, Luchin VA. 1999. Summary of chemical distribution and dynamics in the Bering Sea. In Dynamics of the Bering Sea 217–49.

Wickham H. 2016. Ggplot2: elegant graphics for data analysis. New York (NY): Springer-Verlag.

Wourms JP. 1977. Reproduction and development in chondrichthyan fishes. Am Zool 17: 379–410.

Yang Z, Wang T, Branch R, Xiao Z, Deb M. 2021. Tidal stream energy resource characterization in the Salish Sea. Renew Energy 172:188–208.

Flappy, flouncy fins: swimming kinematics of the spotted ratfish (*Hydrolagus colliei*)

Kayla C. Hall[1], Adam P. Summers[1], Cassandra M. Donatelli[2]

1) Friday Harbor Labs, University of Washington. 620 University Rd., Friday Harbor, WA 98250

2) Fowler School of Engineering, Chapman University. One University Drive, Orange, CA 92866

*Author for Correspondence: kchall8@uw.edu

Keywords: chimaeras, hydrodynamics, locomotor mode, gait transition, appendicular skeleton

Abstract

Chimaeras are an ancient lineage of cartilaginous fishes distinguished by their large wing-like pectoral fins which they use to swim throughout the deep seas. Chimaeras are capable of oscillatory swimming: flapping flight through pelagic environments, and undulatory swimming: or fluttering of the fins when hovering or station holding in slow currents. Like their large pectoral fins, the pelvic fins of chimaeras are equally prominent, but have yet to be analyzed in a kinematic context. We characterized and quantified the relationship between these two sets of fins, and the reliance on the rest of the body to aid in swimming. To determine full-body swimming kinematics of the spotted ratfish (*Hydrolagus colliei*), we swam *H. colliei* (N = 3) in a flume with speeds ranging from 0-0.5 body lengths per second (BL/s). We point-tracked videos to determine pectoral fin, pelvic fin, tail beat frequencies and amplitudes. At low speeds, *H. colliei* uses both sets of fins to hover, where the pelvic fins flutter up and down, perhaps in response to vortices shed by the pectoral fins, while the dorsal fin and spine mimic a sailboat mast being upright. At high speeds, *H. colliei* transitions to pectoral flapping flight with no movement of the pelvic fins, quick bursts of body undulation, and the dorsal spine tucks down towards the body, becoming streamlined.

Introduction

Holocephalans (chimaeras) are thought to have originated some 420 million years ago, making them one of the oldest lineages of vertebrates or fish to still swim throughout the depths of the ocean today. Chimaeras are deep-water cartilaginous fishes and are the sister group to Elasmobranchs (sharks, skates, rays), although these two are sister lineages, chimaeras look dramatically different, almost archaic, compared to the more familiar cartilaginous fishes. Chimaeras get their name from the mythological Greek term, a hybrid monster, probably because of their large glowing eyes that allow them to see in the deep, and their fused rabbit-like teeth which allow them to crush hard prey. But chimaeras go by many common-names, one aptly attributed to them is "ratfish", due to their long gracile tail that follows behind them as they swim. Unlike sharks that primarily swim using full-body undulations to propel themselves forward, chimaeras or "ghost sharks" are not known to swim by using their tails, except as an escape/startle response (Kryvi and Totland 1978). Rather than using their tails, chimaeras are thought to move via pectoral fin-based swimming, generally seen gliding through the water column or flapping and fluttering their large fins in order to propel themselves through their deep dark world. While there have been many observations on how chimaeras move throughout their world (Kryvi and Totland 1978; Maia et al. 2012 and sources within), only a few studies have quantified the swimming kinematics of chimaeras (Combes and Daniel 2001; Higham et al. 2018), but we aim to characterize and quantify the full-body movements of these creatures.

Foundational swimming kinematic papers have categorized fish into groups based on which appendage (fin) they use to swim, and the functional kinematics of how they use that fin to swim (Breder 1926; Lighthill 1969; Lindsey 1978; Webb 1994). Some fishes use pectoral fin locomotion, while others, like sharks, exhibit full-body undulations. Some fish use a combination of fins or rely on a different form of locomotion with changes in current speed. Changes in locomotion or alterations to how something moves regarding its speed or pace are known as gaits. Gaits often change as a response to increasing or decreasing speed, generally activated when the energy required to maintain a motion surpasses the energy required to transition to the next natural pace (Andriacchi et al. 2000; Hoyt and Taylor 1981; Stolze et al. 1997). Gait changes have been described quite extensively for sharks and bony fish, especially reef fishes and freshwater fishes (Drucker et al. 2005). Gait shifts and swimming kinematics of chimaeras are currently limited to analyses based on how they swim via their pectoral fins. Pectoral fin swimming is quite prominent among cartilaginous fishes, primarily among chimaeras and rays,

and there is a swimming continuum that exists within these groups with the extremes being undulatory and oscillatory modes of swimming (Combes and Daniel 2001; Rosenberger 2001). Undulatory swimming is when multiple waves are simultaneously propagated along the pectoral fin margin at any one time and is a maneuverable gait that is mechanically efficient for hovering and swimming above the benthos at low speeds (Di Santo et al. 2017; Rosenberger 2001; Walker and Westneat 2000; Webb 1994). Oscillatory swimming resembles flight in birds, characterized by having less than half a wavelength along the pectoral fin margin which translates to the pectoral fins oscillating up and down (Heine 1992; Rosenberger 2001; Webb 1994). Relative to undulatory swimming, oscillatory swimming minimizes drag while increasing both lift and thrust, making it efficient for cruising in a pelagic environment (Fish et al. 2016; Lighthill 1969; Rosenberger 2001; Webb 1975).

Aside from comparing the swimming modes of chimaeras to other cartilaginous fishes, a parallel has been made between chimaeras and labriformes reef fishes (Drucker et al. 2005; Foster and Higham 2010). Fishes categorized within the Labriform swimming mode are those that implement dorsoventral oscillation or flapping of the pectoral fins (Drucker et al. 2005), examples being *Hydrolagus* (Combes and Daniel 2001), *Gomphosus* a genus of wrasse (Labridae, Labriformes. Walker and Westneat 1997, 2002), and *Scarus* a genus of parrotfish (Scaridae, Labriformes. Breder 1926). The distinct difference though is that chimaeras are capable of swimming via dorsoventral flapping and anteroposterior undulations of the fin in a horizontal plane. In contrast, labriform pectoral fins are oriented in the vertical plane and therefore their undulatory swimming mode is known as rowing (Walker and Westneat 1997, 2002). Further, labriforms do not have an intermediate swimming mode, they are tied to one of the swimming mode extremes and their pectoral fin morphology reflects the function. The "rowers" have broad paddle-like fins that move anteroposteriorly and this is thought to be the swimming mode in fishes in slower flow environments (Walker and Westneat 1997, 2002). The "flappers" fins flap up and down, generally recognized as oscillatory flight, and which is the faster swimming mode and on found in many labriforms in reef habitats. It is unclear if chimaeras should be categorized as labriform swimmers as this is based off of one swimming mode (flapping), not including undulatory swimming, and chimaeras do not row their fins in a fore-aft motion like labrids, chimaeras flutter them up and down sending small waves to the back of the fin.

Another major difference, based on observations, between chimaeras and other labriform swimmers is the reliance and usage of the large flexible pelvic fins that chimaeras have and use during swimming. Until recently, pelvic fins were thought to be held fairly still, acting as static trimming foils rather than dynamic moving structures (Standen 2008). But, similar to the pectoral fins, muscles of the pelvic fins control both movement and surface conformation (Lauder and Drucker 2004), so we should expect to see pelvic fins involved in underwater locomotion. In rainbow trout, pelvic fins help control speed and stabilize the body position during slow-speed locomotion (Standen 2010). Similarly, previous authors have hinted that the pelvic fins may play a role in steering, braking or gliding during chimaera locomotion (Higham et al. 2018). These authors found positive allometric growth of the *adductor superficialis* and *abductor proximalis* muscles in the pelvic fins, indicating that they do likely play a role in the active movement of fins, but the kinematic role of pelvic fins has yet to be tested. Here we investigate how locomotion and fin beats change with increasing speeds and determine whether the pelvic fins and tail are used to give the spotted ratfish an additional boost. The aims of this study are fourfold: (a) Characterize the spotted ratfish (*Hydrolagus colliei*) full-body swimming kinematics; (b) Describe the different gaits of the spotted ratfish; (c) Compare spotted ratfish gaits with other pectoral fin swimmers; (d) Document the spotted ratfish's pelvic fin use over many speeds.

Methods

Chimaeras are extremely elusive deep-sea dwellers, leading to minimal literature regarding their life-history or how they move through their world. It is especially tricky to find them in the wild because they live so deep in the water column, let alone to then collect and bring them to the surface; even more difficult is getting them to acclimate in an experimental environment, that's dark and has a consistent temperature, long enough for them to become stable and then be able to run them through kinematic trials.

The spotted ratfish (*Hydrolagus colliei*) collected for this study were caught via otter trawl off of Point Caution San Juan Island, WA; with a maximum trawl depth of 365 meters. After letting the fish acclimate in the holding tanks for a week, we used a flume with a 152.4 × 38.1 × 50.8 cm working area (Rolling Hills Research Corporation, Model 1520 Water Tunnel) to

gather lateral-view swimming kinematics of 3 individuals; their total lengths were 19 inches, 17.5 in. and 13 in (or 48.26 cm, 44.45 cm, and 33.02 cm).

Kinematic Swimming Trials

A GoPro Hero4 camera (Gopro.com 2017) was placed at mid-height of the flume viewing tank to record the lateral view of the kinematics at 60 frames per second. Each individual fish was moved from the holding tank to the saltwater flume and allotted a 30 minute adjustment period in the flume to decrease stress and encourage natural swimming (Figure 1). During that time, their body length was measured and recorded to calculate flow rates in inches per second (ips). To encourage fixed swimming, fish were blocked in the flume tank using fitted wire mesh gates to produce a swimming area of roughly four times the body length.

The first bout was 0.0 times each body length to simulate low flow zones that chimaeras regularly encounter in the deep sea, the second bout or flow rate was equivalent to 0.1 of the body length of the fish, the third bout was 0.2 BL/s. We did this same setup for each fish, where the flow rate was increased sequentially by 0.1 BL/s, up to 0.5 times the body length, for each fish. Each flow rate was maintained for 2-4 minutes, until consistent swimming was recorded (at least five pectoral fin flaps at max amplitude). The flume flow rate was reduced to 0.1 BL/s when the fish was no longer able to maintain the given swim speed, this generally occurred at 0.6 BL/s, those data was not included in this study.

Calculations and Statistics

The videos from the six bouts (0-0.5 BL/s) of each individual were first segmented into bouts of 5-10 trackable pectoral beats for each flow regime (Bout 1-6). Each individual video was then digitized using MATLAB (MathWorks, Natick, MA, USA). Digitization software was used to quantify swimming movements and to aid in the identification of gait changes. Using DLTdv8 digitizing tool (Hedrick 2008) we tracked a total of seven landmarks on each chimaera: 1. nose, 2. tail, 3. pectoral fin, 4. pelvic fin, 5. cloaca, 6. base of dorsal fin, 7. tip of dorsal spine (Figure 2). All points were tracked via semi-automation with manual edits at each frame of the individual GoPro clips. Fin and tail beat frequencies were also calculated using the coordinates and MATLAB code. We then used R (version 4.2.1 R Core Team 2021), a free coding language

for statistics and modeling, and RStudio (R Team 2021) to analyze the data, perform multiple one-way ANOVAs, and to create figures (3-7 and S1-8).

Results

We found clear transitions in pectoral and pelvic fin use across each bout 1-6 (equivalent to 0-0.5 BL/s). Throughout bout 1 (0 BL/s) we see the distinct undulations of the pectoral fins and interestingly the pelvic fins as well (Figure 4). Individuals exhibit distinct shifts in swimming modes, at low speeds they use undulations while at higher swimming speeds, at 0.4 BL/s we see a clear transition to the distinct flapping behavior, up and down strokes of the entire fin acting as a singular plane. At increased BL/s we see that the pelvic fins are now uncoupled in their mimicry of the pectoral fin swimming behavior, where they seem to remain relatively stable in the y-axis (i.e. not "bouncing/flouncing" up and down with each stroke). At 0.5 BL/s we see the same distinct flapping behavior, up and down strokes, but even more extreme than the 0.4 BL/s kinematics, and again, the pelvic fins are even more constrained in their flouncing behavior of movement in the y-axis (Figure 3 & 4, S1-6). In figure 4, comparing 0.0 BL/s to 0.5 BL/s, we can see the distinct decoupling of the pelvic fins from the pectoral fins when swimming at faster speeds. At faster swimming speeds the amplitude of the pelvic fins is vastly decreased, and the frequency of fin movement is also limited. At low speeds, *H. colliei* uses both sets of fins to hover, where the pelvic fins flutter up and down, while the dorsal fin and spine are upright, mimicking a sailing mast on a windy day, (Figure S1-S8). At high speeds, *H. colliei* transitions to pectoral flapping flight with no movement of the pelvic fins, quick bursts of body undulation, and the dorsal spine tucks down, streamlined. Generally, when the tail does fluctuate it is in quick burst movements, similar to an escape response (Figure S1, S3, S5).

The pectoral fin kinematics exhibit similar trends across all individuals (TL: 48.26, 44.45 and 33.02 centimeters), where at slow speeds the pectoral fins undulate and at fast speeds the pectoral fins oscillate up and down to propel the fish forward. The scale of the trends are similar for all individuals when swimming slow, but at faster speeds we can see individual variation between the amplitudes of the pectoral fins flaps (Figure 5, S2, S4, S6); smaller individuals must flap more to their maximum amplitude, while the larger individual is capable of swimming at these faster speeds with smaller amplitude oscillations (likely with less effort and energy

expenditure). Similarly, when looking at pelvic fin kinematics we see that there is a consistent trend across individuals in the use of pelvic fins and the undulations produced at slow speeds. When comparing the individual's pelvic fin use at high speeds we see that they are much more constrained in their amplitude and therefore overall movement (Figure 5, S2, S4, S6). There is also less variation between the individuals and their use of the pelvic fins at high speeds (Figure S7, S8). The last major takeaway from comparing the swimming speed extremes is that at 0.0 BL/s the pectoral and pelvic fins are out of phase with one another. When comparing the fin movements at fast speeds we see that the pectoral and pelvic fins movements are now decoupled, i.e. the pectoral fins are flapping and the pelvic fins do not flounce up and down. At these faster speeds, we see the pelvic fins held relatively stable and close to the body wall. These trends were found to be consistent across individuals (Figure 5, S7, S8). In slower flow, chimaeras flutter both sets of fins, and in faster flow, they flap their pectoral fins with streamlined bursts.

By point tracking the full-body swimming kinematics of *H. colliei* we were able to determine gait changes across the varying speeds. Specifically, by comparing the fin beat frequency and amplitude of pectoral fins versus the pelvic fins we were able to identify transitions between undulatory to oscillatory fin movements and when they occur (Figure 6 and 7). The gait change from undulation to oscillations was roughly at 0.3 BL/s across the individuals analyzed, as there is a distinct jump in pectoral fin frequency at this phase. The pectoral and pelvic fin beat frequencies increase in synch until about 0.4 BL/s where pelvic fin usage drops. By 0.5 BL/s this can be characterized as consistent oscillatory swimming, as there is minimal movement in both frequency of use and the amplitude of the pelvic fins; again an indication that the pelvic fins are being held close to the body wall when swimming at faster speeds. Overall, the frequency of appendage use (including the tail) increases with increasing speeds, until it hits a threshold, and the amplitudes of all appendages decrease with increasing speeds.

Discussion

Chimaeras are capable of full-body swimming, using all appendages to move through the water column and propel themselves through their deep, dark world. When swimming slowly chimaeras rely on both sets of appendages to maneuver and stabilize themselves. When hovering above the substrate or station-holding chimaeras can be seen flapping their pelvic fins beyond 45

degrees from the midline. When moving through faster-flow environments chimaeras switch to oscillatory flapping of their pectoral fins and rely less on their pelvic fins for maneuvering, but more for stabilizing (Figure S7). Chimaeras stabilize themselves by holding their pelvic fins close to the body wall when swimming through fast currents, in order to become more streamlined and minimize drag (Figure S8). The usage of the dorsal spine, during swimming kinematics, needs to be untangled further but, this study determined that with increasing speeds the amplitude and frequency of the spine movement decreases (Figure S1, S3, S5); suggesting that the spine is being tucked in towards the body to streamline its effect during fast swimming chimaeras are primarily using pectoral fin propulsion, and in slower-moving environments, all of their fins, dorsal fin and spine included, tend to flap with the flow.

We find it best not to categorize chimaeras as labriform swimmers because chimaeras are capable of swimming within the continuum of pectoral undulatory (rowing) and oscillatory (flapping). Unlike labriformes which are constrained to rowing or flapping by their anatomy, chimaeras can switch between these swimming modes, at their convenience, and in response to changing environments. Although chimaeras have previously been grouped into the kinematic category of labriform swimming (dorsoventral oscillation), we find that if you consider both sets of appendages (pectoral and pelvic), chimaeras fins move more similarly to those of coelacanths than they do to labriformes. Interestingly, coelacanths also swim via dorsoventral oscillation of the fins (Drucker et al. 2005), and they exhibit a lateral insertion of the pectorals on the trunk, like what we see in Chondrichthyes (Fricke et al. 1987; Fricke and Hissmann 1992). Because of this lateral insertion, the rotational axis with which chimaeras move their pectoral fins more closely resembles the mechanics of those seen in coelacanths, where the pectoral fin can be moved in the dorso-ventral and anteroposterior directions up to 120° (Fricke and Hissmann, 1992); compared to other labriform swimmers, *Gomphosus varius* with ~115º figure-of-eight dorso-ventral rotation (Walker and Westneat 1997). If we consider the use and reliance on pelvic fins, chimaeras swimming more closely resembles that of coelacanths as well. Fricke et al. (1987) found that when coelacanths got close to the substrate they either tucked the fins against the body and swim up, or they stabilize the body by sculling of the pelvic fins; this is exactly what we see in chimaeras, especially when braking or turning (Figure 1, S7, S8. Fricke and Hissmann, 1992; McKenzie 2007; Uyeno 1991). Pelvic fins are critical for locomotion in fishes (Harris 1936; Harris 1938; Standen 2008; Standen 2010), further work needs to be done to

validate if the pelvic fin muscles of chimaeras are playing an active role in holding these fins stable. We can say that these fins are not just moving via passive actions because if that were the case then we would expect that pelvic fins would move around freely, as a result of the vortices produced from the pectoral fins (Wilga and Lauder 1999; Wilga and Lauder 2001). If the pelvic fins move passively we should see much greater movement and oscillations at faster speeds as the pectoral fins are producing more thrust and therefore larger vortices at faster swimming speeds, but we do not see this (Figure S7, S8).

Last, we consider the effects that species-specific morphology may have on the study and the variation in kinematics that could be produced across all holocephalans in future comparative studies. The pectoral and pelvic fins of chimaeras are composed of basal and radial pterygiophores which support the base of the fin, the remainder of the fin is composed of ceratotrichia which are unsegmented collagen fibrils that are flexible enough to allow the fin to fold in all axes (Figure S9). We see this flexibility to move the pectoral fin in 3D space not only at the fin base, similar to the rotation seen in coelacanths, but also of the ceratotrichia themselves (Figure 1, 2, S7, S8, S9). It would be interesting to do a study using histological or µCT data, with all families within the Holocephali, to quantify the ceratotrichia in a comparative context (diameter, total count, distribution, and area). There are many ways to vary the physical properties of collagen, just by changing the morphology, whether it be on the micro or macro level (Tomita et al. 2014), thereby directly determining the kinematic limitations of these types of fins. For example, on the macro-level, the fin morphology of *Callorhinchus callorhynchus* vs *Hydrolagus colliei* are quite dramatically different (Figure S9), and just based on observations their swimming kinematics are as well. *Callorhinchus callorhynchus* has a pronounced leading edge and round-broad tip to its pectoral fin, which would provide it with an exceptional advantage in oscillatory flight, with less energy expenditure, compared to the small-pointed fin tip found in *Hydrolagus.* We might find then that *Callorhinchus* relies less on their pelvic fins, because of these efficient pectoral fins. Even more interesting would be to compare the full-body swimming kinematics between these two species, especially because *Callorhinchus* have more of a heterocercal caudal fin (resembling sharks); the reliance on this fin as an additional source for propulsion has not been studied, but the gait changes and relationships/reliance on the pectoral and pelvic fins are likely very different than that of *Hydrolagus colliei* studied here. Future

kinematic studies using morphologically relevant models to distinguish the variation in swimming parameters across holocephalans are in the works with a past student of mine, and I look forward to what we publish when the time comes.

Acknowledgements

Anna Mehlhorn (College of William & Mary), Sarah Handy (Arizona State University), Olivia Hawkins (University of Louisiana at Lafayette), Amani Webber-Schultz (New Jersey Institute of Technology), Lauren Simonitis (Florida Atlantic University), Duncan Kennedy (University of Calgary), Aaron Vliet (Friday Harbor Labs). Funding from FHL Fellowship Award, UW Biology BEACON Award, UW Biology Hoag Award supported this work.

FIGURES

Figure 1. Kinematic repertoire of *Hydrolagus colliei* pectoral fins: steady swimming, the swimming continuum: undulatory to oscillatory, other behaviors such as braking to slow down or stabilize.

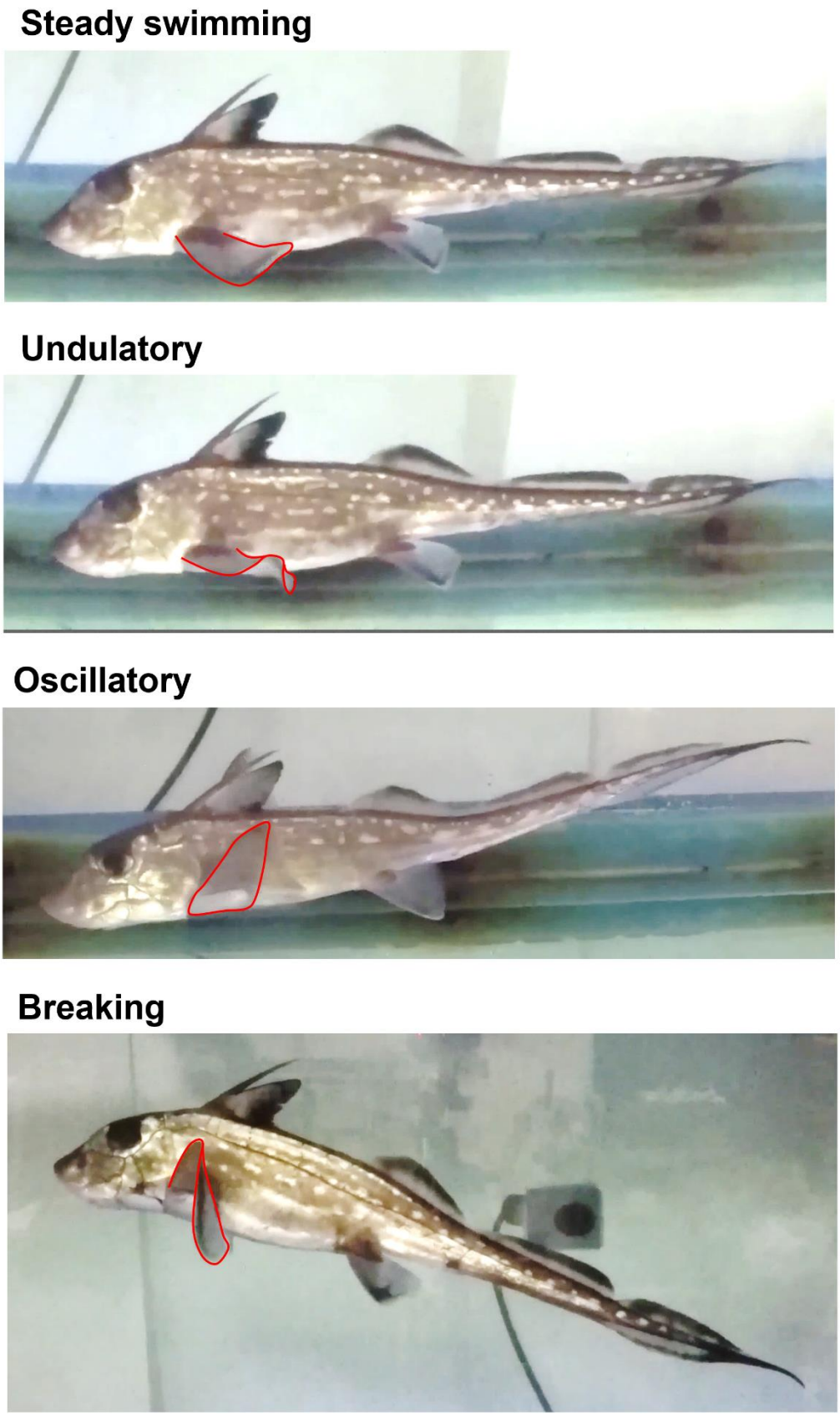

Figure 2. Point tracking of *Hydrolagus colliei* for swimming full-body swimming kinematics. 1- Nose, 2- Tail, 3- Pectoral, 4- Pelvic, 5- Cloaca, 6- Dorsal (base), 7- Spine (tip).

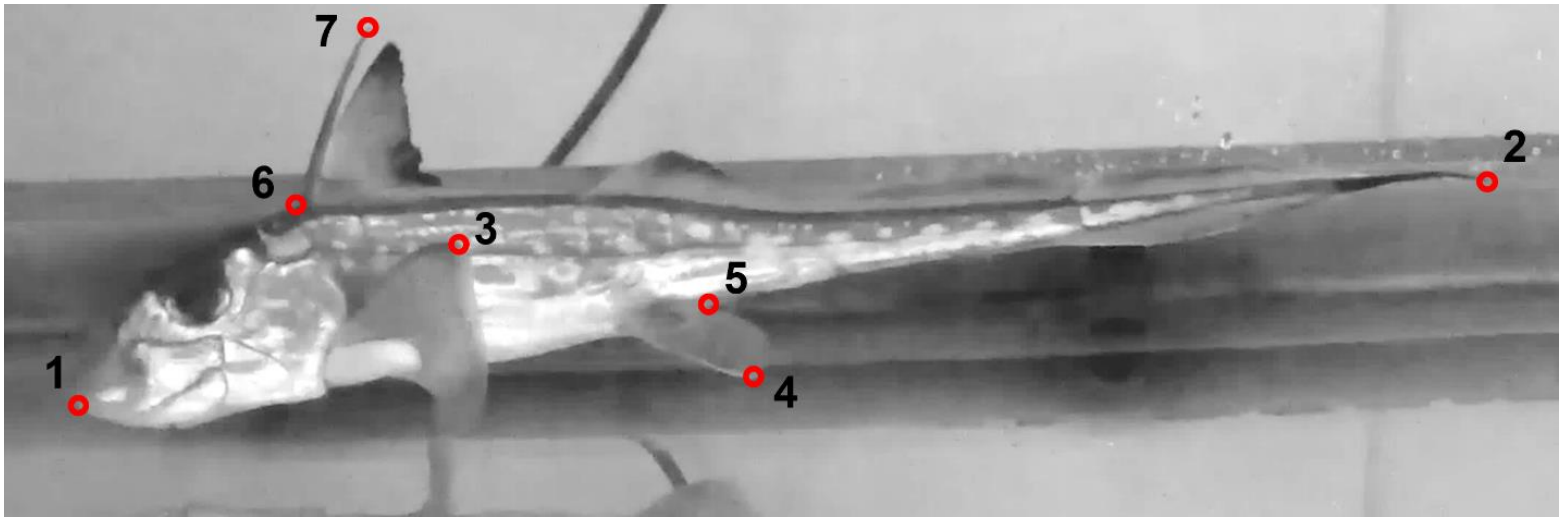

Figure 3. Pectoral vs. pelvic fin kinematics of individual Hco1, across each bout 1-5 (0-0.5 BL/s). Bout 1 is orange, Bout 2 is aqua, Bout 3 is purple, Bout 4 is magenta, Bout 5 is lime, Bout 6 is blue.

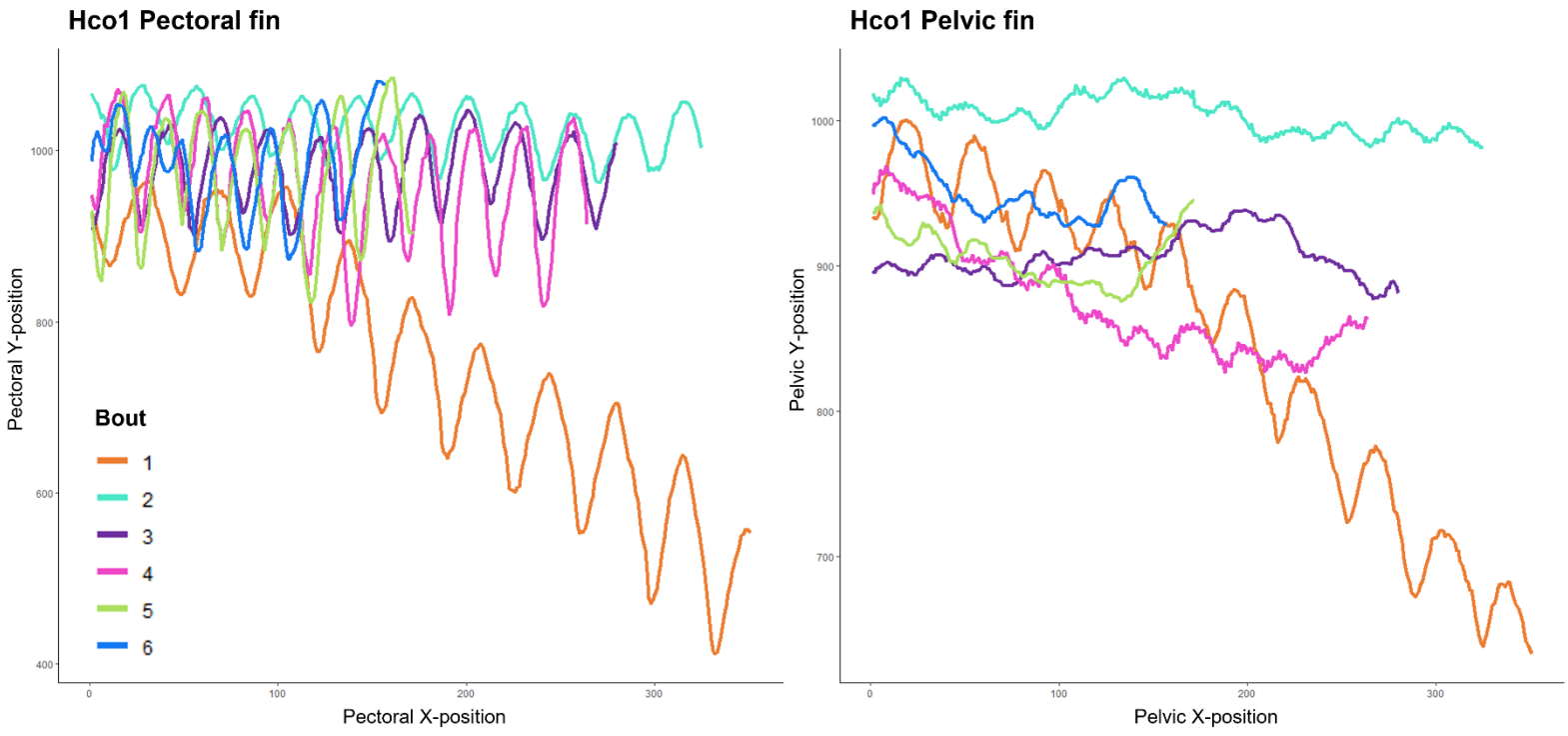

Figure 4. Pectoral vs. pelvic fin kinematics of individual Hco1, comparing bout 1 vs bout 5. Bout 1 is in orange and bout 5 in blue. The pectoral and pelvic fin in bout 1 undulate at about the same frequency, where in bout 5 we can see the movement and frequency of use between the pectoral and pelvic fin is decoupled.

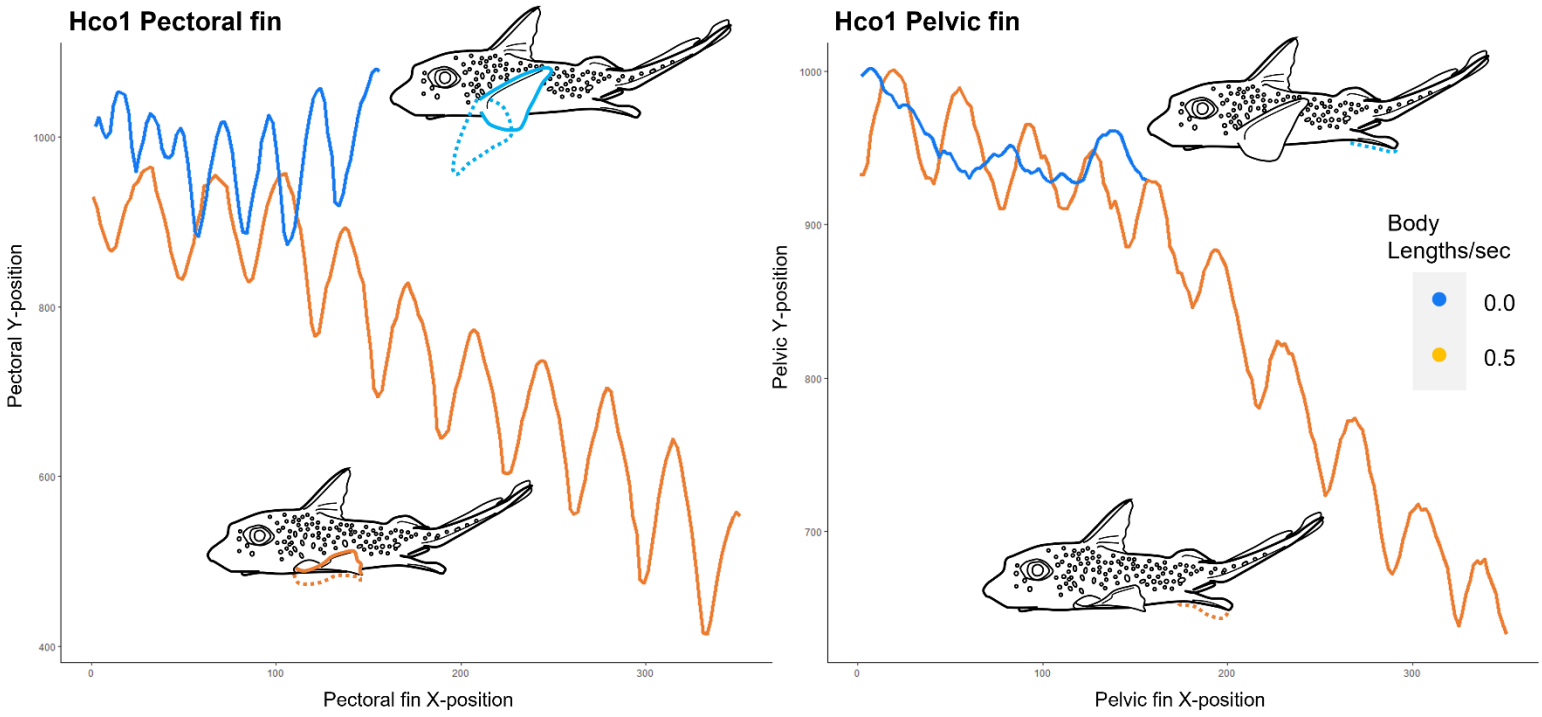

Figure 5. The progression from Undulatory to Oscillatory swimming in *Hydrolagus colliei.* Pectoral and pelvic fin kinematics across individuals, across each bout 1-5 (0-0.5 BL/s). Raspberry circles indicate the largest specimen Hco1, TL = 48.26 centimeters. The Lavender triangles indicate the medium specimen Hco2, TL = 44.45 cm. Lastly the peach squares indicate the data for the smallest specimen Hco3, TL = 33.02 cm. The first and third row show the data of each individuals pectoral fins strokes during that bout. Similarly, the second and fourth row show

the individuals pelvic fin data during the same bout A) pectoral and pelvic fin strokes during bout 1 = 0 BL/s, B) pectoral and pelvic fin strokes during bout 2 = 0.1 BL/s, C) pectoral and pelvic fin strokes during bout 3 = 0.2 BL/s, D) pectoral and pelvic fin strokes during bout 4 = 0.3 BL/s, E) pectoral and pelvic fin strokes during bout 5 = 0.4 BL/s, F) pectoral and pelvic fin strokes during bout 6 = 0.5 BL/s.

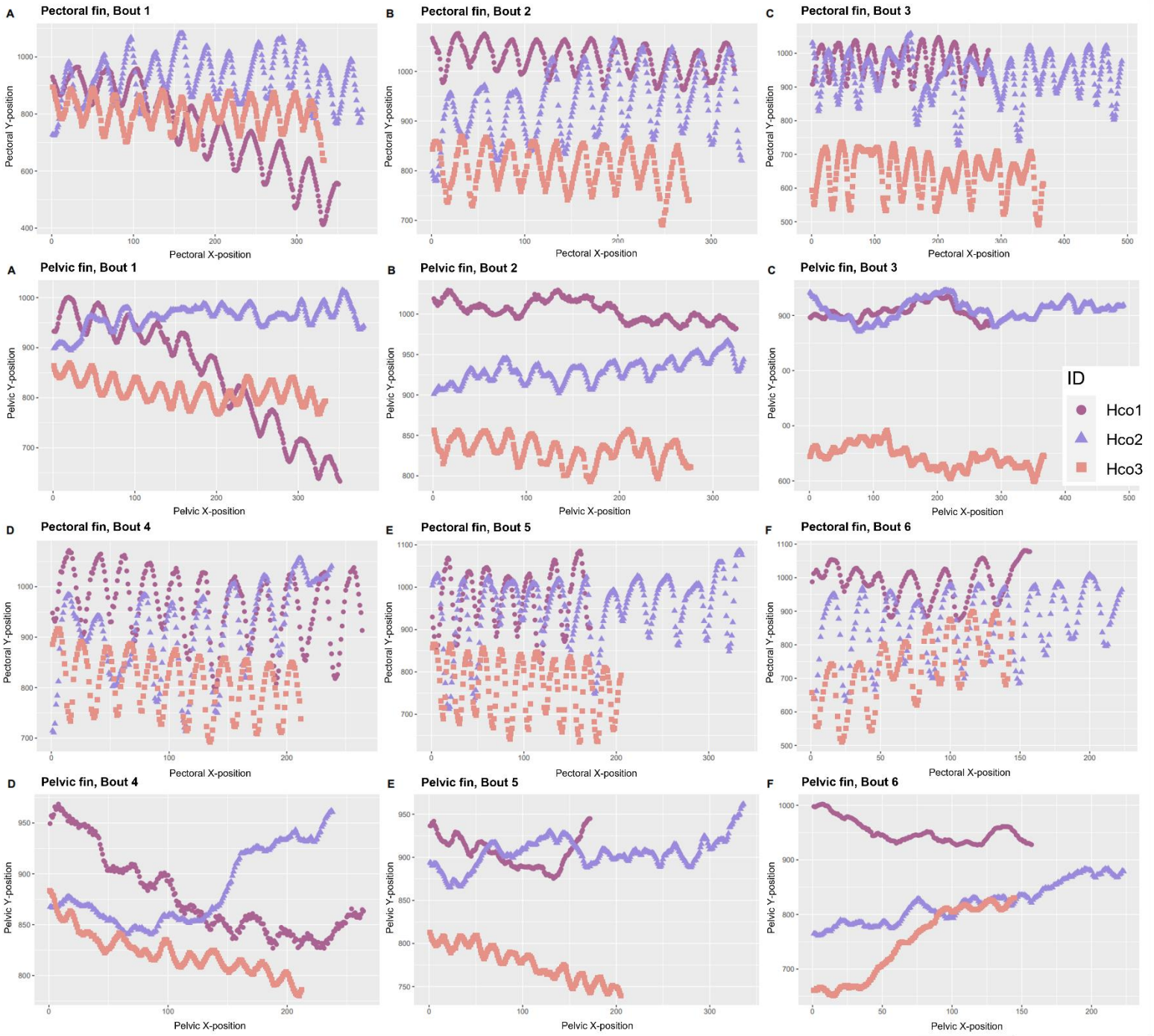

Figure 6. Frequency of appendage usage with increasing swimming speeds. Average frequency of pectoral fin, pelvic fin, and tail across each bout 1-5 (0-0.5 BL/s). Pectoral data shown with red triangles, pelvic fins with turquoise squares, and the tail with oranges circles. The trendlines of each appendage have been imposed upon the stacked boxplots to show average change in usage across each bout/increase in swimming speed.

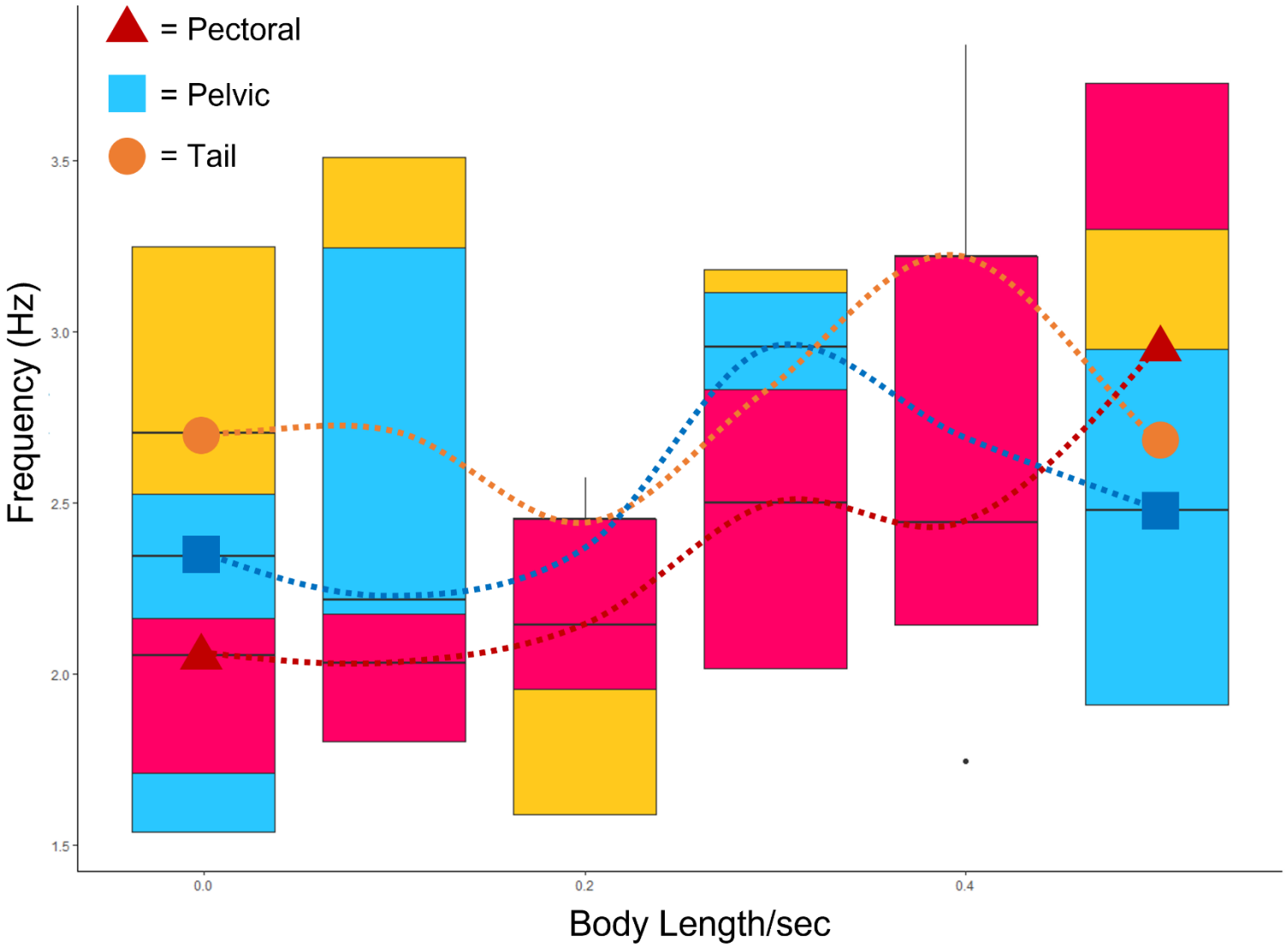

Figure 7. Amplitude of appendage usage with increasing swimming speeds. Average amplitude of pectoral fin, pelvic fin, and tail across each bout 1-5 (0-0.5 BL/s). Pectoral data shown with red triangles, pelvic fins with turquoise squares, and the tail with oranges circles. The trendlines of each appendage have been imposed upon the stacked boxplots to show average change in usage across each bout/increase in swimming speed.

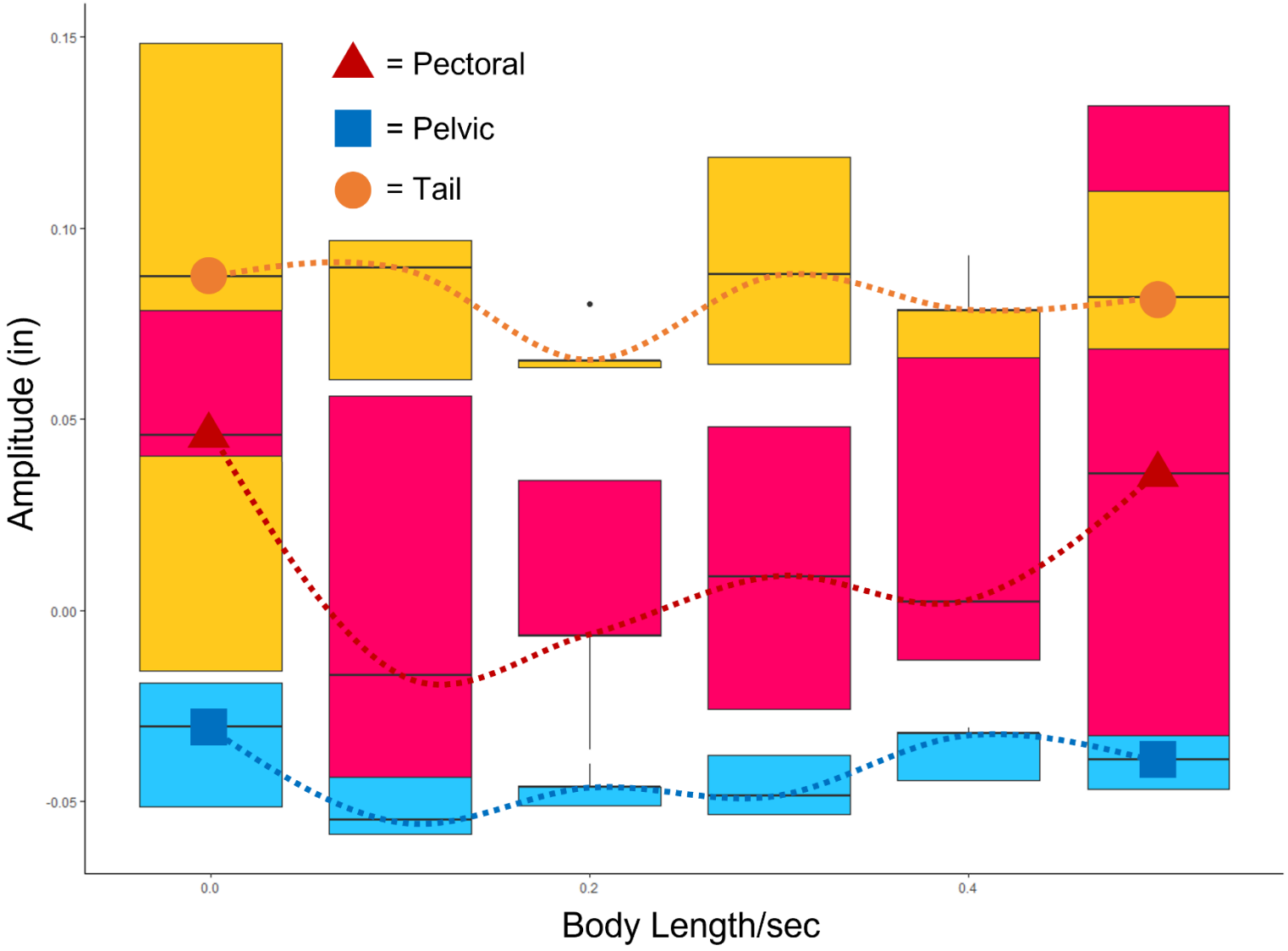

Supplemental Figures

Figure S1. All tracking-point movements from the largest individual Hco1. Data from each anatomical point, throughout the 5-10 flaps, per bout visualized. Graphs follow order from Figure 3: 1- Nose, 2- Tail, 3- Pectoral, 4- Pelvic, 5- Cloaca, 6- Dorsal (base), 7- Spine (tip). Line color is indicative of bout number but also is the swimming speed scale (BL/s = 0-0.5), Bout 1 is orange, Bout 2 is aqua, Bout 3 is purple, Bout 4 is magenta, Bout 5 is lime, Bout 6 is blue.

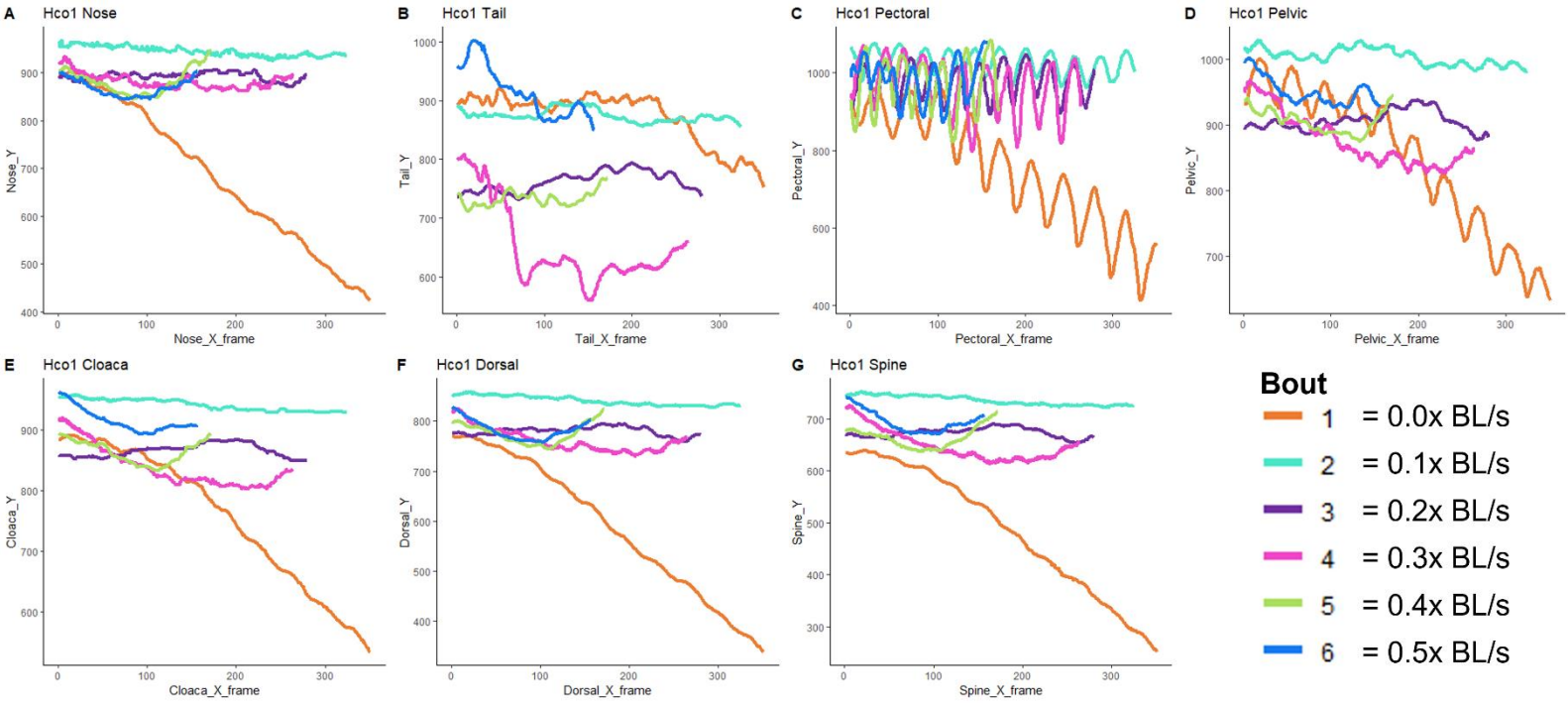

Figure S2. Pectoral and Pelvic fin kinematics of Hco1 with increasing swimming speeds. The first and third row show the data of the pectoral fin strokes during that bout. Similarly, the second and fourth row show the individuals pelvic fin data during the same bout A) pectoral and pelvic fin strokes during bout 1 = 0 BL/s, B) pectoral and pelvic fin strokes during bout 2 = 0.1 BL/s, C) pectoral and pelvic fin strokes during bout 3 = 0.2 BL/s, D) pectoral and pelvic fin strokes during bout 4 = 0.3 BL/s, E) pectoral and pelvic fin strokes during bout 5 = 0.4 BL/s, F) pectoral and pelvic fin strokes during bout 6 = 0.5 BL/s. Line color is indicative of bout number

but also is the swimming speed scale (BL/s = 0-0.5), Bout 1 is orange, Bout 2 is aqua, Bout 3 is purple, Bout 4 is magenta, Bout 5 is lime, Bout 6 is blue.

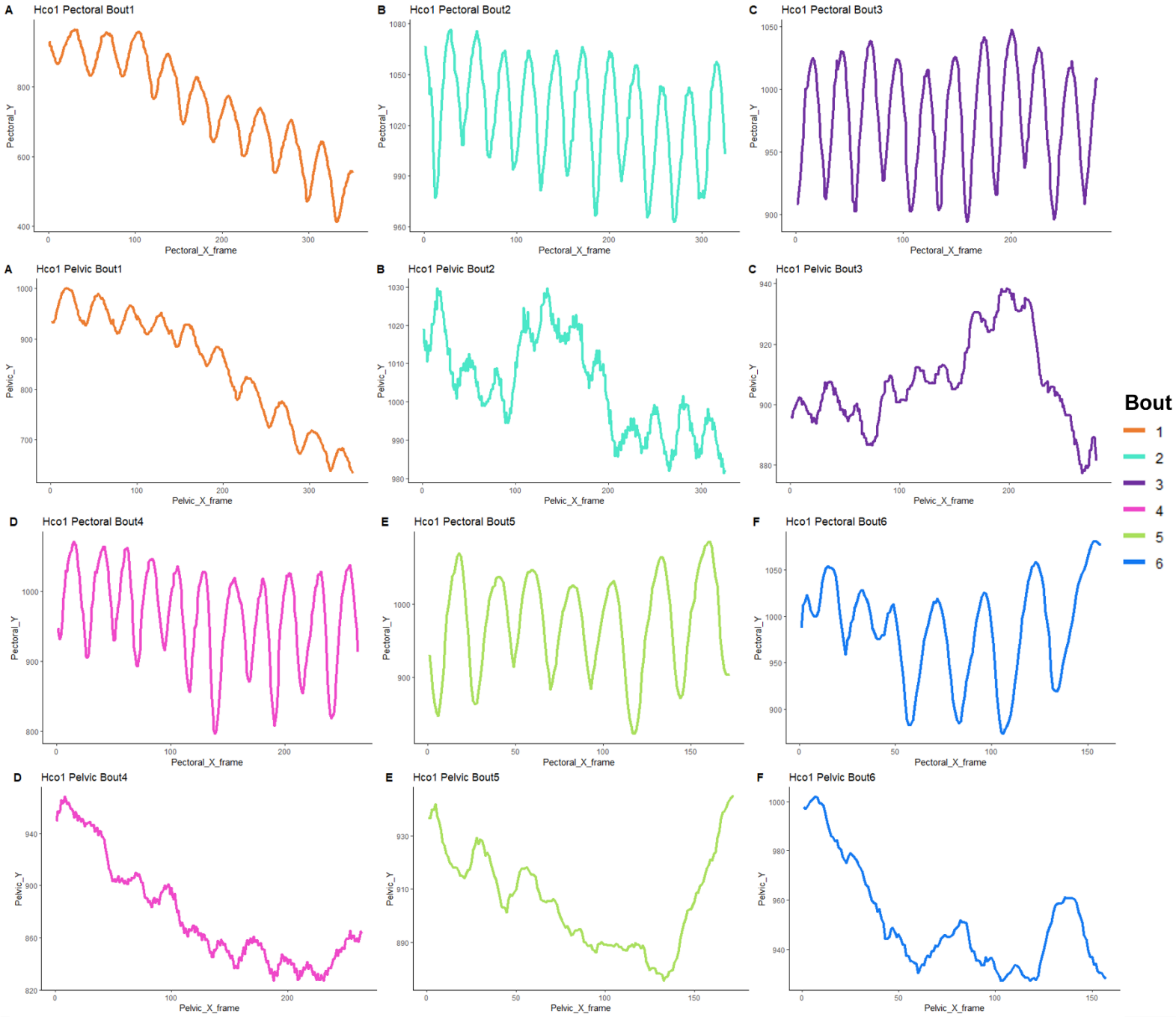

Figure S3. All tracking-point movements from the medium individual Hco2.

Data from each anatomical point, throughout the 5-10 flaps, per bout visualized. Graphs follow order from Figure 3: 1- Nose, 2- Tail, 3- Pectoral, 4- Pelvic, 5- Cloaca, 6- Dorsal (base), 7- Spine (tip). Line color is indicative of bout number but also is the swimming speed scale (BL/s = 0-0.5), Bout 1 is orange, Bout 2 is aqua, Bout 3 is purple, Bout 4 is magenta, Bout 5 is lime, Bout 6 is blue.

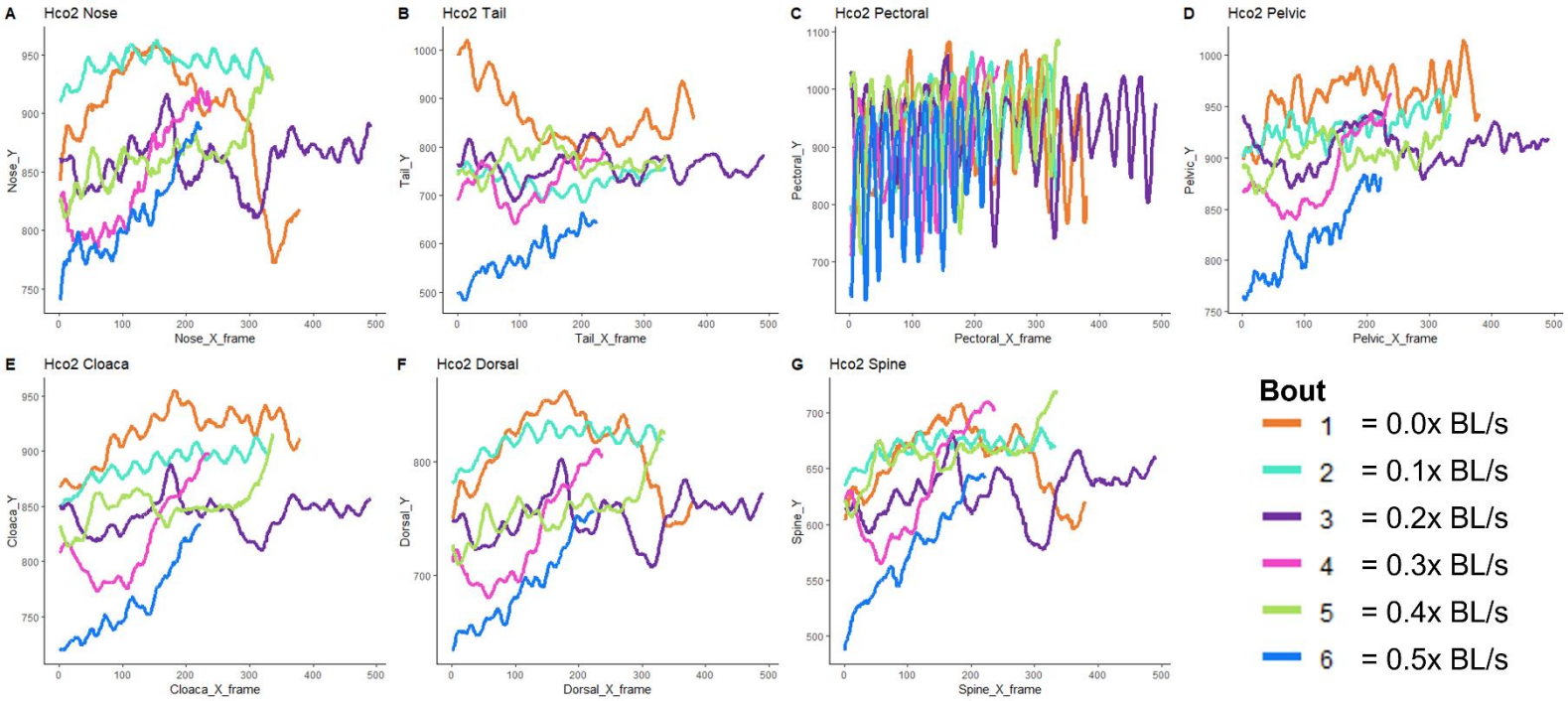

Figure S4. Pectoral and Pelvic fin kinematics of Hco2 with increasing swimming speeds. The first and third row show the data of the pectoral fin strokes during that bout. Similarly, the second and fourth row show the individuals pelvic fin data during the same bout A) pectoral and pelvic fin strokes during bout 1 = 0 BL/s, B) pectoral and pelvic fin strokes during bout 2 = 0.1 BL/s, C) pectoral and pelvic fin strokes during bout 3 = 0.2 BL/s, D) pectoral and pelvic fin strokes during bout 4 = 0.3 BL/s, E) pectoral and pelvic fin strokes during bout 5 = 0.4 BL/s, F) pectoral and pelvic fin strokes during bout 6 = 0.5 BL/s. Line color is indicative of bout number

but also is the swimming speed scale (BL/s = 0-0.5), Bout 1 is orange, Bout 2 is aqua, Bout 3 is purple, Bout 4 is magenta, Bout 5 is lime, Bout 6 is blue.

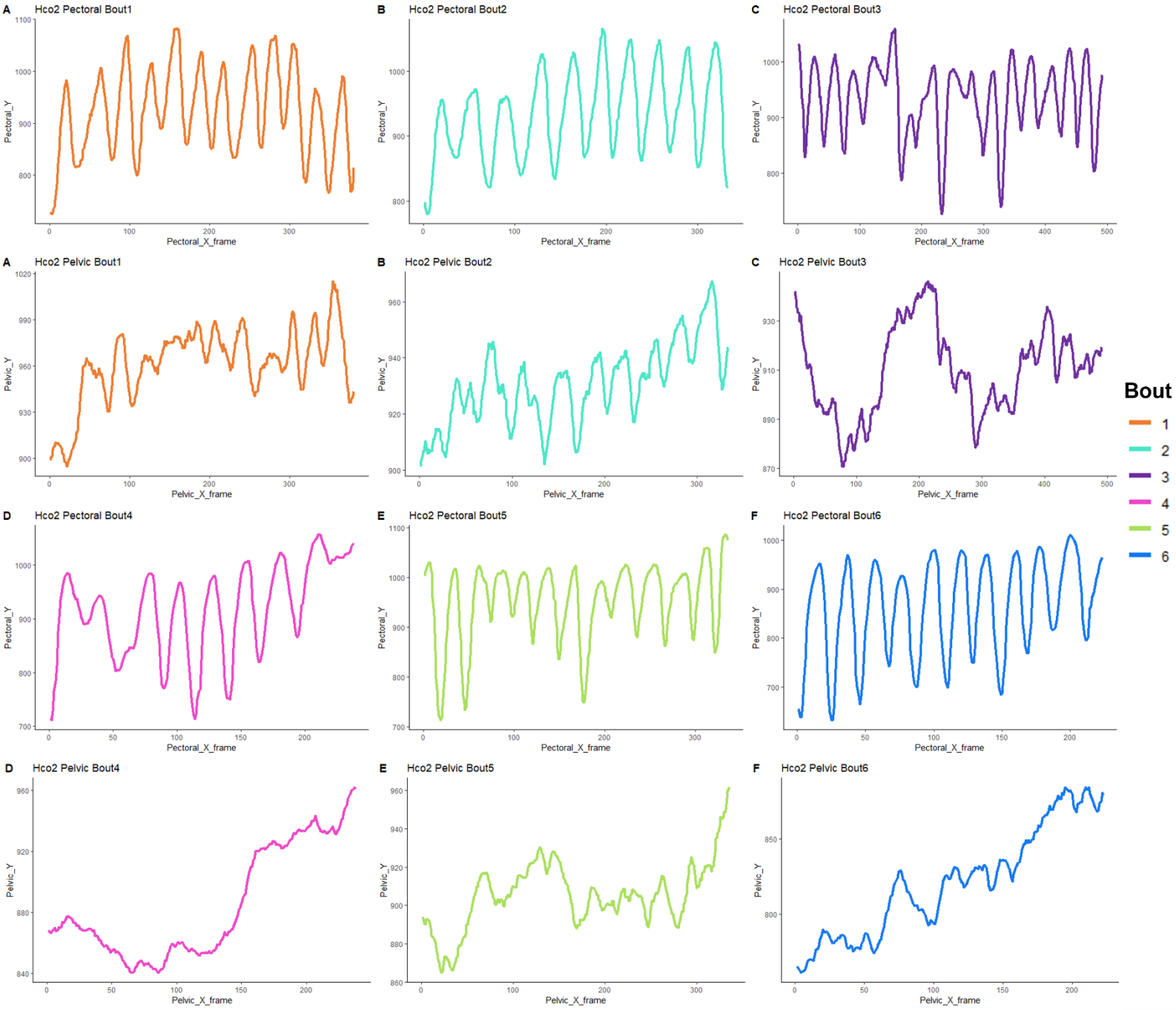

Figure S5. All tracking-point movements from the smallest individual Hco3.

Data from each anatomical point, throughout the 5-10 flaps, per bout visualized. Graphs follow order from Figure 3: 1- Nose, 2- Tail, 3- Pectoral, 4- Pelvic, 5- Cloaca, 6- Dorsal (base), 7- Spine (tip). Line color is indicative of bout number but also is the swimming speed scale (BL/s = 0-0.5), Bout 1 is orange, Bout 2 is aqua, Bout 3 is purple, Bout 4 is magenta, Bout 5 is lime, Bout 6 is blue.

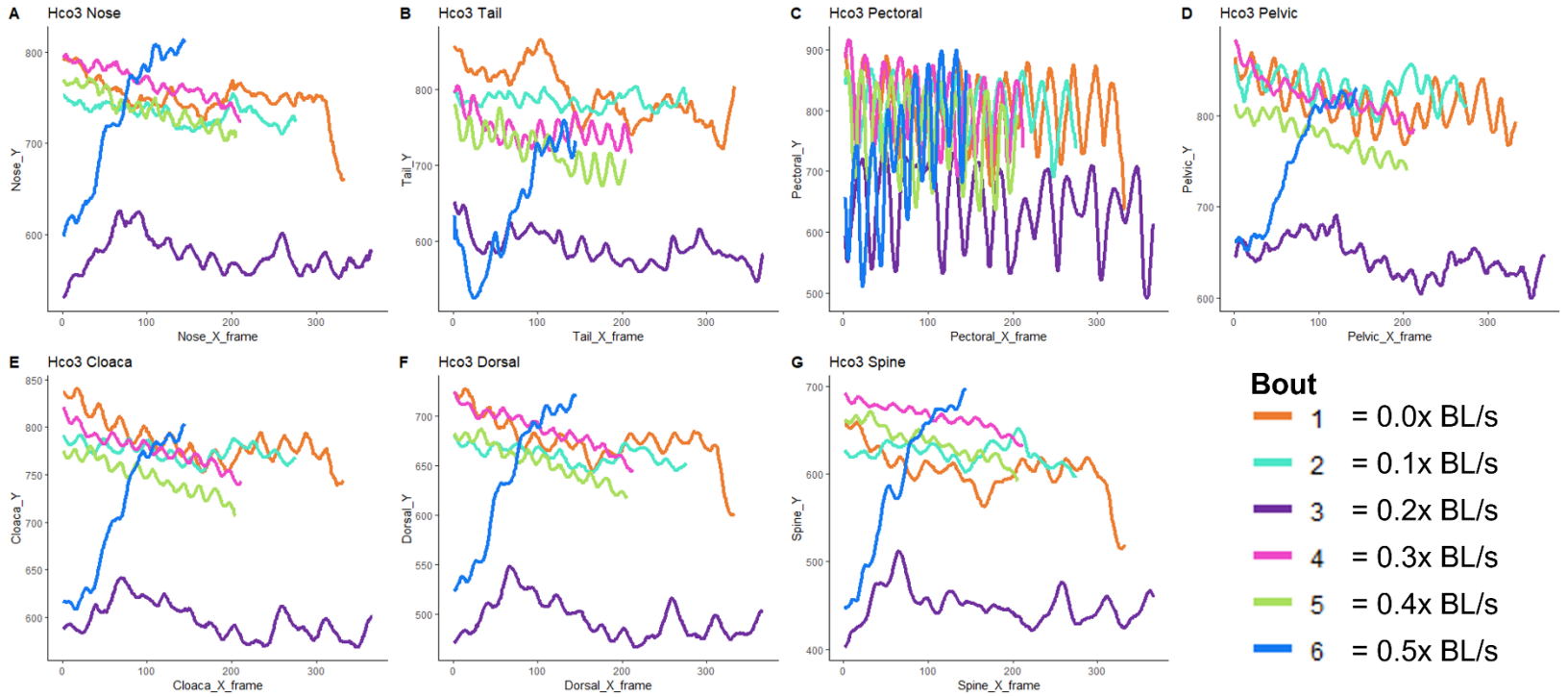

Figure S6. Pectoral and Pelvic fin kinematics of Hco3 with increasing swimming speeds. The first and third row show the data of the pectoral fin strokes during that bout. Similarly, the second and fourth row show the individuals pelvic fin data during the same bout A) pectoral and pelvic fin strokes during bout 1 = 0 BL/s, B) pectoral and pelvic fin strokes during bout 2 = 0.1 BL/s, C) pectoral and pelvic fin strokes during bout 3 = 0.2 BL/s, D) pectoral and pelvic fin strokes during bout 4 = 0.3 BL/s, E) pectoral and pelvic fin strokes during bout 5 = 0.4 BL/s, F) pectoral and pelvic fin strokes during bout 6 = 0.5 BL/s. Line color is indicative of bout number

but also is the swimming speed scale (BL/s = 0-0.5), Bout 1 is orange, Bout 2 is aqua, Bout 3 is purple, Bout 4 is magenta, Bout 5 is lime, Bout 6 is blue.

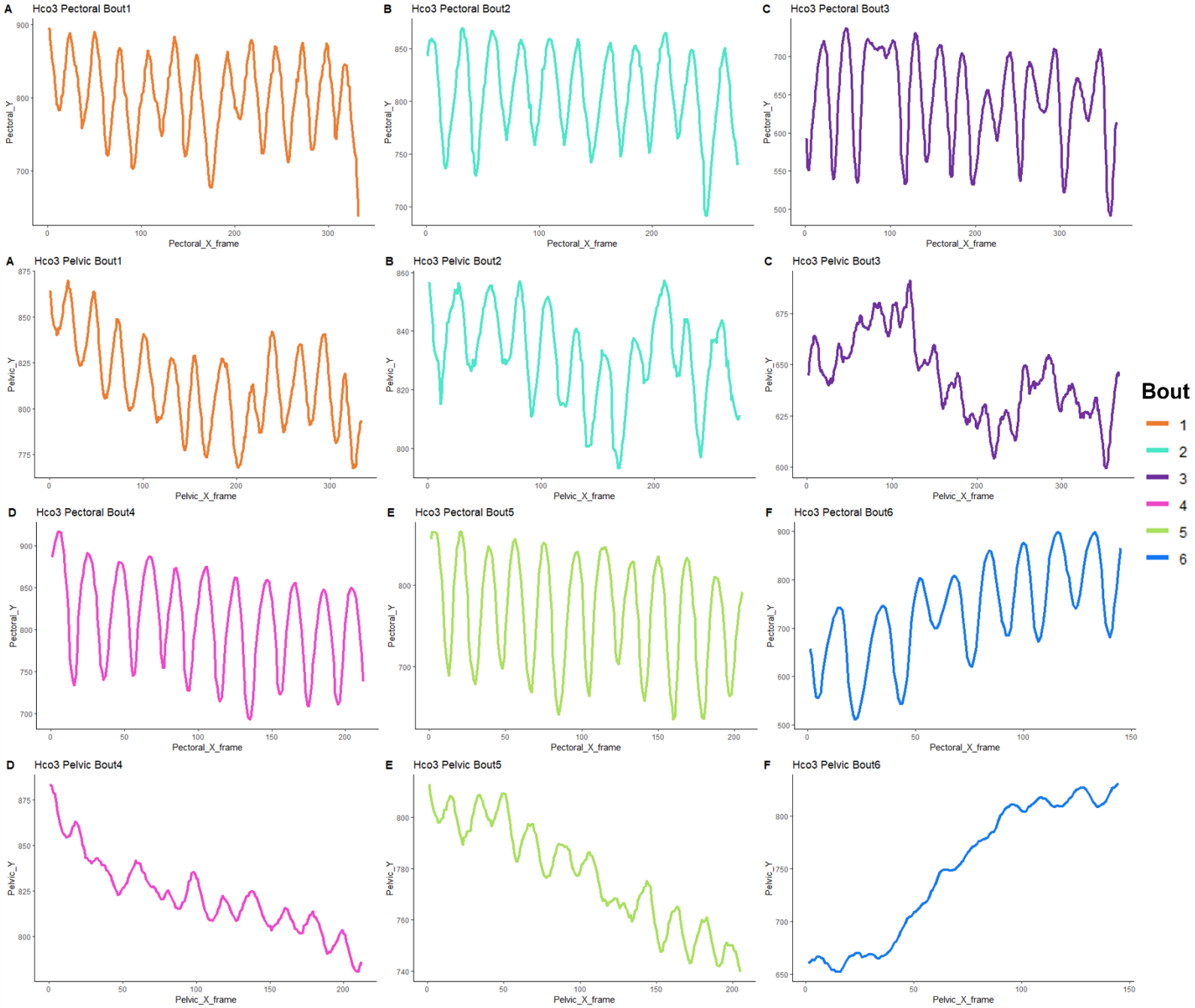

Figure S7. Pectoral fin kinematics across individuals of varying sizes. Pectoral fin displacement during bout 1 vs bout 5, undulatory or slower swimming shown with an orange outline, and faster oscillatory movement of the fin shown with a blue line.

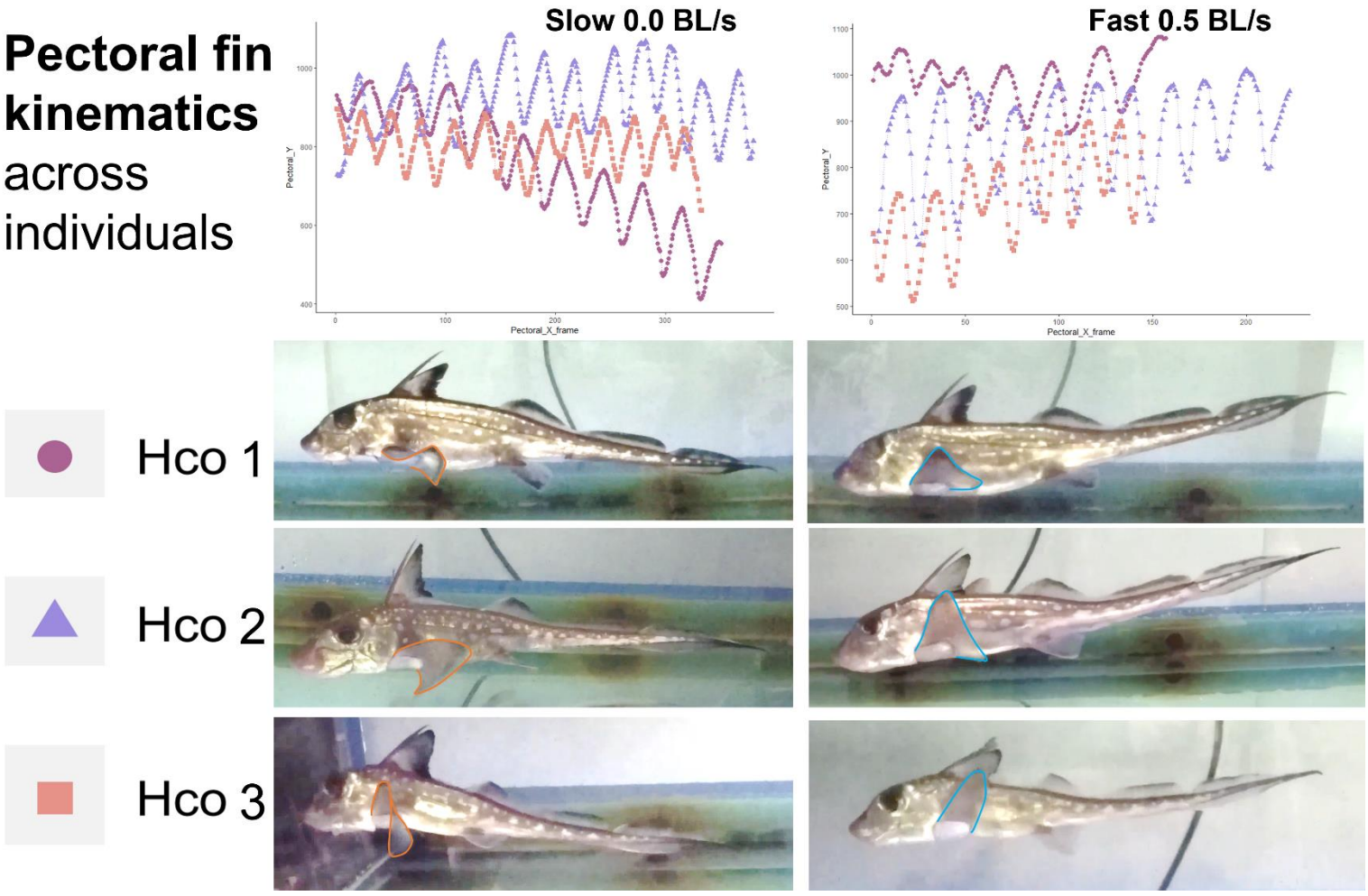

Figure S8. Pelvic fin kinematics across individuals of varying sizes. Pelvic fin displacement during bout 1 vs bout 5, undulatory or slower swimming shown with an orange outline, and faster oscillatory movement of the fin shown with a blue line.

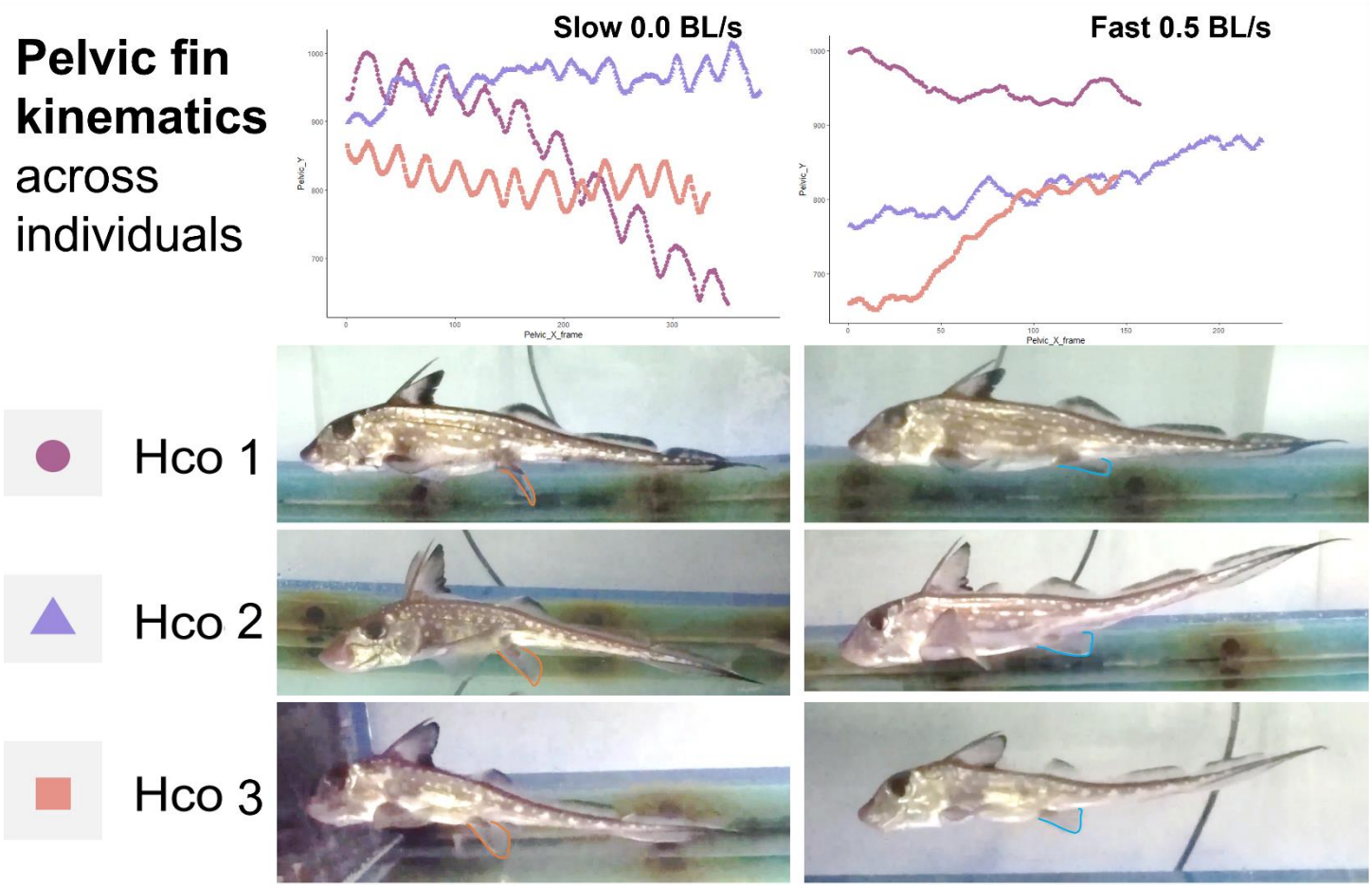

Figure S9. The anatomy and morphology of holocephalan pectoral and pelvic fins. Basal and radial pterygiophores, with the black space being filled by ceratotrichia which fan out towards fin tip. The dashed line reflects the gross morphology of each fin respectively across all families of chimaeriformes: *Callorhinchus callorhynchus* (Challorhinchidae), *Rhinochimaera pacifica* (Rhinochimaeridae), *Chimaera monstrosa* (Chimaeridae). Redrawn them from the original dissection illustrations from Garman (1904), and for *Chimaera monstrosa*, i've supported a portion of the pelvic fin illustration from a µCT scan I took while at FHL; the original illustration wasnt very conclusive about all of the radial pterygiophores, so I scaled and aligned both images and then drew the illustration. I then scaled the illustrations to a lateral full-body image of *C. monstrosa* so that the pectoral and pelvic fin would be in the correct proportion to each other. I then made all other illustrations the same size to compare the morphology of the fins to each other across families.

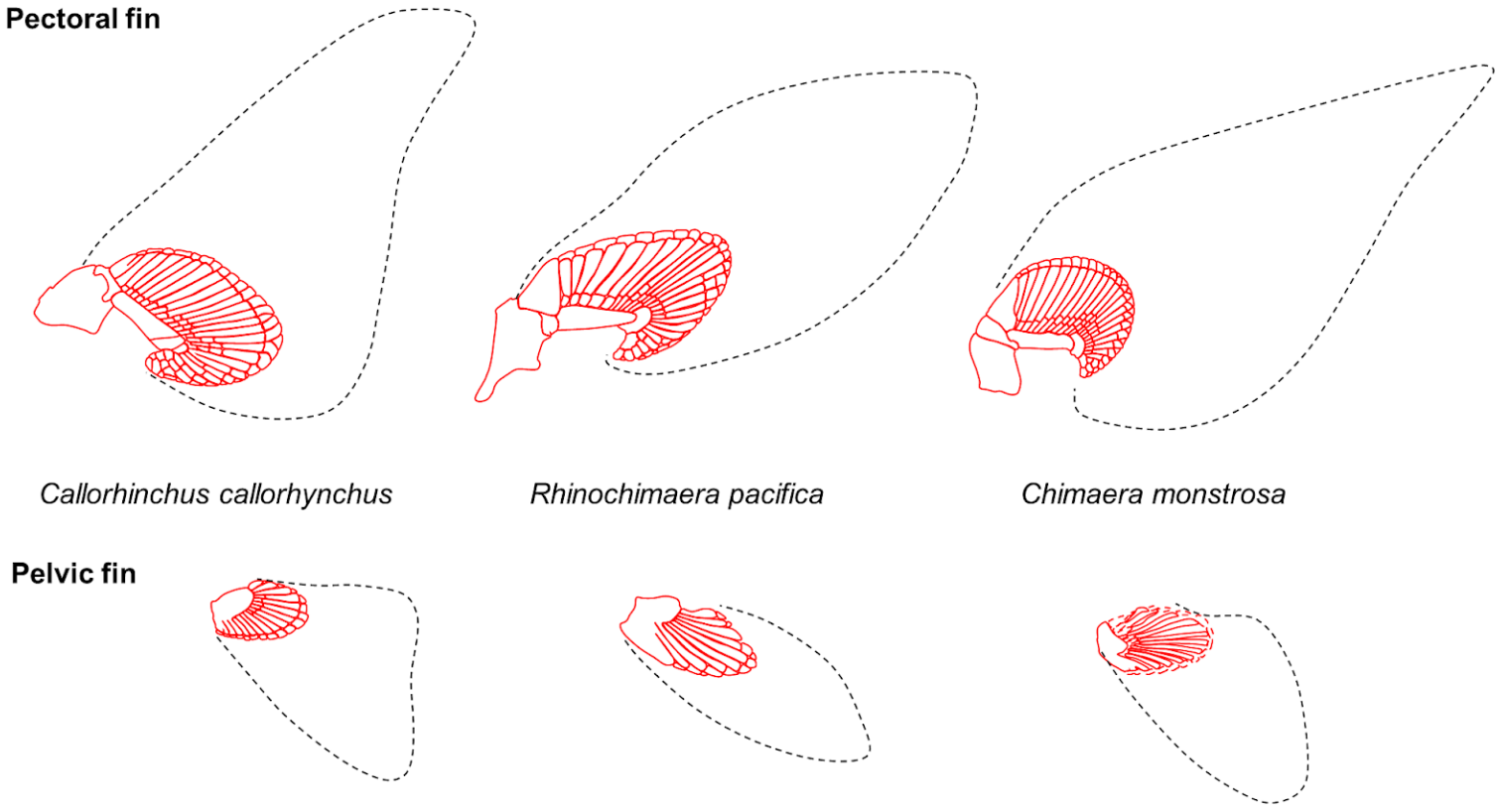

References

Andriacchi, T.P., and Alexander, E.J. 2000. Studies of human locomotion: past, present and future. Journal of biomechanics, 33(10), pp.1217-1224.

Breder, C.M. 1926. The locomotion of fishes. Zoologica, 4, pp.159-297.

Combes, S.A., and Daniel, T.L. 2001. Shape, flapping and flexion: wing and fin design for forward flight. Journal of experimental biology, 204(12), pp.2073-2085.

Di Santo, V., Blevins, E.L., and Lauder, G.V. 2017. Batoid locomotion: effects of speed on pectoral fin deformation in the little skate, *Leucoraja erinacea*. Journal of Experimental Biology, 220(4), pp.705-712.

Drucker, E.G., Walker, J.A., and Westneat, M.W. 2005. Mechanics of pectoral fin swimming in fishes. Fish Physiology, 23, pp.369-423.

Drucker, E.G., and Jensen, J.S. 1996. Pectoral fin locomotion in the striped surfperch: I. Kinematic effects of swimming speed and body size. Journal of Experimental Biology, 199(10), pp.2235-2242.

Fish, F.E., Schreiber, C.M., Moored, K.W., Liu, G., Dong, H., and Bart-Smith, H. 2016. Hydrodynamic performance of aquatic flapping: efficiency of underwater flight in the manta. Aerospace, 3(3), p.20.

Foster, K.L., and Higham, T.E. 2010. How to build a pectoral fin: functional morphology and steady swimming kinematics of the spotted ratfish (*Hydrolagus colliei*). Canadian journal of zoology, 88(8), pp.774-780.

Fricke, H., and Hissmann, K. 1992. Locomotion, fin coordination and body form of the living coelacanth *Latimeria chalumnae*. Environmental Biology of Fishes, 34, pp.329-356.

Fricke, H., Reinicke, O., Hofer, H., and Nachtigall, W. 1987. Locomotion of the coelacanth *Latimeria chalumnae* in its natural environment. Nature, 329(6137), pp.331-333.

Garman, S. 1904. The chimaeroids (Chismopnea Raf., 1815; Holocephala Mull., 1834), especially *Rhinochimaera* and its allies. Bull. Mus. Comp. Zool., Harvard, 41, pp.243-271.

Gopro.com. 2017. GoPro Official Website - Capture + share your world - About Us. [online] Available at: <https://gopro.com/about-us> [Accessed 3 May 2017].

Hedrick, T.L. 2008. Software techniques for two-and three-dimensional kinematic measurements of biological and biomimetic systems. Bioinspiration & biomimetics, 3(3), p.034001.

Heine, C.E. 1992. *Mechanics of flapping fin locomotion in the cownose ray, Rhinoptera bonasus (Elasmobranchii: Myliobatidae)*. Duke University.

Higham, T.E., Seamone, S.G., Arnold, A., Toews, D., Janmohamed, Z., Smith, S.J., and Rogers, S.M. 2018. The ontogenetic scaling of form and function in the spotted ratfish, *Hydrolagus colliei* (Chondrichthyes: Chimaeriformes): fins, muscles, and locomotion. Journal of Morphology, 279(10), pp.1408-1418.

Hoffmann, S.L., Donatelli, C.M., Leigh, S.C., Brainerd, E.L., and Porter, M.E. 2019. Three-dimensional movements of the pectoral fin during yaw turns in the Pacific spiny dogfish, *Squalus suckleyi*. Biology Open, 8(1), p.bio037291.

Hoyt, D.F., and Taylor, C.R. 1981. Gait and the energetics of locomotion in horses. Nature, 292(5820), pp.239-240.

Kryvi, H., and Totland, G.K. 1978. Fibre types in locomotory muscles of the cartilaginous fish *Chimaera monstrosa*. Journal of Fish Biology, 12(3), pp.257-265.

Lindsey, C. 1978. Form, function and locomotory habits in fish. Fish physiology.

Lighthill, M.J. 1969. Hydromechanics of aquatic animal propulsion. *Annual review of fluid mechanics*, *1*(1), pp.413-446.

Maia, A.M., Wilga, C.A., and Lauder, G.V. 2012. Biomechanics of Locomotion in Sharks, Rays, and Chimaeras. Biology of Sharks and Their Relatives, p.125.

McKenzie, D.J., Hale, M.E. and Domenici, P. 2007. Locomotion in primitive fishes. Fish Physiology, 26, pp.319-380.

Rosenberger, L.J. 2001. Pectoral fin locomotion in batoid fishes: undulation versus oscillation. Journal of Experimental Biology, 204(2), pp.379-394.

Standen, E.M. 2008. Pelvic fin locomotor function in fishes: three-dimensional kinematics in rainbow trout (*Oncorhynchus mykiss*). Journal of Experimental Biology, 211(18), pp.2931-2942.

Standen, E.M. 2010. Muscle activity and hydrodynamic function of pelvic fins in trout (*Oncorhynchus mykiss*). Journal of Experimental Biology, 213(5), pp.831-841.

Stolze, H., Kuhtz-Buschbeck, J.P., Mondwurf, C., Boczek-Funcke, A., Jöhnk, K., Deuschl, G., and Illert, M. 1997. Gait analysis during treadmill and overground locomotion in children and adults. Electroencephalography and Clinical Neurophysiology/Electromyography and Motor Control, 105(6), pp.490-497.

Team, R.C. 2021. R: A language and environment for statistical computing. Published online

2020.

Team, R. 2021. RStudio: integrated development for R. RStudio, PBC, Boston, MA. 2020.

Tomita, T., Tanaka, S., Sato, K. and Nakaya, K. 2014. Pectoral fin of the megamouth shark: skeletal and muscular systems, skin histology, and functional morphology. PLoS One, 9(1), p.e86205.

The MathWorks Inc. 2022. MATLAB version: 9.13.0 (R2022b), Natick, Massachusetts: The MathWorks Inc. https://www.mathworks.com

Uyeno, T. 1991. Observations on locomotion and feeding of released coelacanths, *Latimeria chalumnae*. Environmental Biology of Fishes, 32, pp.267-273.

Walker, J.A., and Westneat, M.W. 1997. Labriform propulsion in fishes: kinematics of flapping aquatic flight in the bird wrasse *Gomphosus varius* (Labridae). Journal of Experimental Biology, 200(11), pp.1549-1569.

Walker, J.A., and Westneat, M.W. 2000. Mechanical performance of aquatic rowing and flying. Proceedings of the Royal Society of London. Series B: Biological Sciences, 267(1455), pp.1875-1881.

Walker, J.A., and Westneat, M.W. 2002. Performance limits of labriform propulsion and correlates with fin shape and motion. Journal of Experimental Biology, 205(2), pp.177-187.

Wilga, C.D. and Lauder, G.V. 1999. Locomotion in sturgeon: function of the pectoral fins. Journal of Experimental Biology, 202(18), pp.2413-2432.

Wilga, C.D. and Lauder, G.V. 2001. Functional morphology of the pectoral fins in bamboo sharks, *Chiloscyllium plagiosum*: Benthic vs. pelagic station-holding. Journal of

Morphology, 249(3), pp.195-209.

Webb, P.W. 1973. Kinematics of pectoral fin propulsion in *Cymatogaster aggregata.* Journal of Experimental Biology, 59(3), pp.697-710.

Webb, P.W. 1975. Efficiency of pectoral-fin propulsion of *Cymatogaster aggregata*. Swimming and Flying in Nature: Volume 2, pp.573-584.

Webb, P.W. 1994. The biology of fish swimming. *Mechanics and physiology of animal swimming*, 4562.

A dive into deep time: Literature review of chondrichthyan fossil assemblages and diversity throughout the Phanerozoic.

SILURIAN- Chondrichthyes represent an ancient group of fishes originating approximately 420 million years ago in the Silurian (Coates et al. 2017; Inoue et al., 2010, Johanson 2019). The basic chondrichthyan body plan has undergone two major modifications: one at the end of the Devonian Period, when modern holocephalans (chimaeras) first appeared, and another in the Jurassic Period, when the flattened batoid bauplan evolved. The first peak of chondrichthyan diversity came in the Middle Paleozoic, replacing the placoderms, they then had a second peak diversification event in the Mesozoic (Johanson 2019).

DEVONIAN- The extreme modification of bauplans to benthic life is not unique to batoids. This morphology is also seen in the squatinomorphs (angel sharks), as well as several Paleozoic sharks such as the petalodonts and squatinactids (Carroll, 1988). This suggests that the benthic body plan has evolved at least four times within Chondrichthyes (Maxwell et al. 2008)

Olive et al. (2016) looked at the palaeoecology of the Strud nursery and suggests that placoderms had a life history similar to other fossil and modern fishes, laying eggs or giving live birth in nearshore or in shallow continental environments. In those Devonian environments, shallow waters offered minimized flow velocity and protection against large predators. The structuring of Strud nursery implies partitioning of habitat usage between adults and young. Adult placoderms may have used the nursery of Strud only to lay eggs and/or give live birth and would have generally lived far from the nursery, in deeper waters. This is similar to the structuring we know of in extinct and extant chimaeras that lay eggs. While most chimaeras inhabit deep waters, some species are known to venture into shallow areas to feed or to breed (Bigelow and Schroeder 1953). There have also been fossils remains found in shallow water contexts (Kriwet and Gaździcki 2003; Takeuchi and Huddleston 2006; Kriwet and Klug 2011). Strud also represents the first occurrence of a placoderm nursery used at the same time by several placoderm taxa (Olive et al. 2016), while today in the north Alaskan seas we find most skate nursery sites are used by a single species.

PENNSYLVANIAN- A new group of holocephalans, Iniopterygia, bridged the morphological gap of holocephalans to the early elasmobranchs that diverged in pre-Pennsylvanian time. The iniopterygians are morphological intermediates between chimaeras and the elasmobranchs, though they are not phylogenetically intermediate. Iniopterygians and chimaeroids exhibit different structural and morphological solutions to similar problems, which suggests sister-group relation, not an ancestor-descendant relationship (Zangel 1973).

PERMIAN- The Permian and Triassic saw the extinction of most major chondrichthyan taxa. The modern fauna, which increased slowly during the Paleozoic Era, quickly rose in diversity and dominance after the Late Permian extinctions of other marine organisms (Compagno 1990).

TRIASSIC – The timeline of divergence and radiation for modern sharks and batoids (Neoselachii), based on taxonomic and phylogenetic interpretations, generally links to diversification during the Late Triassic and subsequent radiation event during the Jurassic (Kriwet et al. 2009).

Batoids are here estimated to have originated between about 200 and 230 MYA, followed by the derivation of their major lineages by about 140 MA. During this time, most of the planet's shallow continental seas were associated with the Tethys Ocean, a major tropical waterway extending from the opening Central Atlantic to what is today the Western Pacific. Most groups of extant batoids occur in similar habitats or are thought to have originated in shallow environments before being competitively displaced to the deep sea, as stingrays might have displaced skates (McEachran and Aschliman, 2004; Siverson and Cappetta, 2001).

JURASSIC- The origin of modern sharks and batoids occurred in the Early Jurassic (Maisey et al. 2004; Kriwet & Klug 2008). Modern groups that originated: Hexanchiformes, Heterodontiformes, Squatiniformes, Orectolobiformes, Carcharhiniformes, Batoidea (Kriwet et al. 2009, 2008; Musick et al. 2004).

Early Jurassic expansion of neoselachians was opportunistic in the aftermath of the end-Triassic mass extinction; this rapid diversification and radiation has been attributed to their small body size, short lifespans and oviparity, enabling faster ecological reorganizations and innovations in body plans for adapting to changing environmental conditions (Kriwet et al. 2009).

A nectobenthic lifestyle, one in which organisms swim freely on or near the bottom of the sea, has been also suggested for Jurassic batomorphs (Thies and Reif 1985, Underwood 2004, Klug and Kriwet 2013), in particular for taxa known from complete skeletons such as *Belemnobatis* and *Spathobatis,* which are generally characterized by sharing a bauplan similar to extant rhinobatids, with an elongated rostrum, dorso-ventrally flattened body with enlarged pectoral fins and a muscular tail (Stumpf and Kriwet 2019).

Batoids are indicated to have diverged from neoselachian sharks in the Late Triassic, between 203.3 and 228.8 MYA (Aschliman et al. 2012). The major groups of batoids are estimated to have diverged throughout the Jurassic and possibly into the Cretaceous, with subsequent crown radiations of each group arising from the Late Cretaceous to the Cenozoic (Aschliman et al. 2012).

Fossil evidence of both Orectolobiformes and Batoidea from late Pliensbachian marginal marine, near-shore facies provide some support for the hypothesis by Underwood (2004, 2006) that most neoselachian crown-group representatives were initially linked to marginal marine, near-shore environments, before moving into open marine, offshore habitats by the Toarcian, thus providing promising clues for better understanding Early Jurassic chondrichthyan diversity and distributional patterns (Stumpf and Kriwet 2019).

During the latest Jurassic and beginning of the Cretaceous, neoselachians rapidly diversified and in the late Early Cretaceous. The colonization of pelagic environments during the Cretaceous presumably represented one of the major steps in the evolution of modern sharks.

CRETACEOUS- Despite their initial success, the hybodonts declined during the Cretaceous in marine habitats but were still abundant in freshwater and brackish settings.

The most speciouse group of rays, the Myliobatiformes, first appeared in the Late Cretaceous and rapidly diversified during the early Cenozoic (Johanson 2019).

End-Cretaceous niche-filling by benthic Mesozoic survivors resulted in a prominent

increase of durophagous families, these being rays capable of crushing hard invertebrate prey. This resulted in the appearance of the earliest representatives of several extant lineages, including the pelagic myliobatids, characterized by a derived swimming mode and feeding habits (Marrama 2019).

PALEOCENE- Divergence time estimates place the origin and radiation of the pelagic durophagous stingrays around or slightly before the K-Pg boundary, coincident with the immediate niches filling scenario of the benthic K-Pg survivors and their exploitation by durophagous stingrays (Aschliman et al. 2012). After the appearance and initial radiation of planktivorous taxa during late Paleocene-early Eocene (Underwood et al. 2017), a second wave of radiation occurred at the Oligocene-Miocene boundary within pelagic stingrays when the filter-feeding devil rays Mobulidae possibly separated from the Rhinopteridae (Aschliman et al. 2012, Marrama et al. 2019).

EOCENE- End of the Eocene went from warm waters to colder-nutrient rich waters, allowing skates and rays to radiate and colonize new habitats allowing for modern body plans and forms (Marrama 2019). Fossil remains of Myliobatiformes are known from many localities in marine and freshwater deposits (de Carvalho et al. 2004). By examining the global Eocene fossil record, Engelbrecht et al. (2017) showed that batoids were more abundant in the Northern than in the Southern Hemisphere.

References

Aschliman, N.C., Nishida, M., Miya, M., Inoue, J.G., Rosana, K.M., and Naylor, G.J.P. 2012. Body plan convergence in the evolution of skates and rays (Chondrichthyes: Batoidea). Molecular Phylogenetics and Evolution, 63(1), 28–42.

Bigelow, H.B., and Schroeder, W.C. 1953. *Fishes of the Gulf of Maine* (No. 592). US Government Printing Office.

Carroll, R.L. 1988. *Vertebrate paleontology and evolution.* Freeman.

Coates, M.I., Gess, R.W., Finarelli, J.A., Criswell, K.E., and Tietjen, K. 2017. A symmoriiform chondrichthyan braincase and the origin of chimaeroid fishes. Nature, 541(7636), pp.208-211.

Compagno, L.J. 1990. Alternative life-history styles of cartilaginous fishes in time and space. Environmental Biology of Fishes, 28, pp.33-75.

De Carvalho, M.R., Maisey, J.G., and Grande, L. 2004. Freshwater stingrays of the Green River Formation of Wyoming (Early Eocene), with the description of a new genus and species and an analysis of its phylogenetic relationships (Chondrichthyes: Myliobatiformes). *Bulletin of the American Museum of Natural History*, *2004*(284), pp.1-136.

Engelbrecht, A., Mörs, T., Reguero, M.A., and Kriwet, J. 2017. New carcharhiniform sharks (Chondrichthyes, Elasmobranchii) from the early to middle Eocene of Seymour Island, Antarctic Peninsula. *Journal of vertebrate paleontology*, *37*(6), p.e1371724.

Inoue, J.G., Miya, M., Lam, K., Tay, B.H., Danks, J.A., Bell, J., Walker, T.I., and Venkatesh, B. 2010. Evolutionary origin and phylogeny of the modern holocephalans (Chondrichthyes: Chimaeriformes): a mitogenomic perspective. *Molecular biology and evolution*, *27*(11), pp.2576-2586.

Johanson, Z., Underwood, C., and Richter, M. 2019. *Evolution and development of fishes*. Cambridge University Press.

Kriwet, J., and Gazdzicki, A. 2003. A new chimeroid fish (Chondrichthyes, Holocephali) from the Eocene La Meseta Fm of Seymour Island. *Polish Polar Research, 24*, pp.29-51.

Kriwet, J., Kiessling. W., and Klug, S. 2009. Diversification trajectories and evolutionary life-history traits in early sharks and batoids. Proceedings of the Royal Society B: Biological

Sciences, 276(1658), pp.945-951.

Kriwet, J., and Klug, S. 2008. Diversity and biogeography patterns of Late Jurassic neoselachians (Chondrichthyes: Elasmobranchii). *Geological Society, London, Special Publications*, *295*(1), pp.55-70.

Kriwet, J., and Klug, S. 2011. A new Jurassic cow shark (Chondrichthyes, Hexanchiformes) with comments on Jurassic hexanchiform systematics. *Swiss Journal of Geosciences*, *104*(1), pp.107-114.

Klug, S., and Kriwet, J. 2013. An offshore fish assemblage (Elasmobranchii, Actinopterygii) from the Late Jurassic of NE Spain. *Paläontologische Zeitschrift*, *87*, pp.235-257.

Maisey, J.G., Naylor, G.J., and Ward, D.J. 2004. Mesozoic elasmobranchs, neoselachian phylogeny and the rise of modern elasmobranch diversity. *Mesozoic fishes*, *3*, pp.17-56.

Marramà, G., Carnevale, G., Naylor, G.J., and Kriwet, J. 2019. Mosaic of plesiomorphic and derived characters in an Eocene myliobatiform batomorph (Chondrichthyes, Elasmobranchii) from Italy defines a new, basal body plan in pelagic stingrays. *Zoological Letters*, *5*(1), pp.1-18.

Maxwell, E.E., Fröbisch, N.B., and Heppleston, A.C. 2008. Variability and conservation in late chondrichthyan development: ontogeny of the winter skate (Leucoraja ocellata). *The Anatomical Record: Advances in Integrative Anatomy and Evolutionary Biology*, *291*(9), pp.1079-1087.

McEachran, J.D., and Aschliman, N. 2004. Phylogeny of batoidea. Biology of sharks and their relatives, (Boca Raton (FL), pp.79-113.

Musick, J.A., Harbin, M.M., and Compagno, L.J. 2004. Historical zoogeography of the Selachii. *Biology of sharks and their relatives*, *20043354*.

Olive, S., Clément, G., Daeschler, E.B., and Dupret, V. 2016. Placoderm assemblage from the tetrapod-bearing locality of Strud (Belgium, Upper Famennian) provides evidence for a fish nursery. Plos One, 11(8), p.e0161540.

Siverson, M., and Cappetta, H. 2001. A skate in the lowermost Maastrichtian of southern Sweden. Palaeontology, 44(3), pp.431-445.

Stumpf, S., and Kriwet, J. 2019. A new Pliensbachian elasmobranch (Vertebrata, Chondrichthyes) assemblage from Europe, and its contribution to the understanding of late Early Jurassic elasmobranch diversity and distributional patterns. *PalZ*, *93*(4), pp.637-658.

Takeuchi, G.T., and Huddleston, R.W. 2006. A Miocene chimaeroid fin spine from Kern County, California. *Bulletin, Southern California Academy of Sciences*, *105*(2), pp.85-90.

Thies, D., and Reif, W.E. 1985. Konstruktionsmorphologie, Nr. 173: Phylogeny and evolutionary ecology of Mesozoic Neoselachii. *Neues Jahrbuch für Geologie und Paläontologie. Abhandlungen*, *169*(3), pp.333-361.

Underwood, C.J. 2004. Environmental controls on the distribution of neoselachian sharks and rays within the British Bathonian (Middle Jurassic). Palaeogeography, Palaeoclimatology, Palaeoecology 203: 107–126.

Underwood, C.J. 2006. Diversification of the Neoselachii (Chondrichthyes) during the Jurassic and Cretaceous. Paleobiology 32: 215–235.

Underwood, C.J., Kolmann, M.A., and Ward, D.J. 2017. Paleogene origin of planktivory in the Batoidea. *Journal of Vertebrate Paleontology*, *37*(3), p.e1293068.

Zangerl, R. 1973. Interrelationships of early chondrichthyans. *Interrelationships of fishes*, pp.1-14.